A CONSTITUTIVE EQUATION FOR PARALLEL-FIBERED ELASTIC TISSUE

Thesis for the Degree of Ph. D.
MICHIGAN STATE UNIVERSITY
ROLFE B. JENKINS
1973

This is to certify that the

thesis entitled

A CONSTITUTIVE EQUATION FOR

PARALLEL-FIBERED ELASTIC TISSUE.

presented by

Rolfe B. Jenkins

has been accepted towards fulfillment
of the requirements for

Ph.D. degree in Mechanics

Major professor

Date Feb 15, 1973

O-7639

ABSTRACT

A CONSTITUTIVE EQUATION FOR
PARALLEL-FIBERED ELASTIC TISSUE

By

Rolfe B. Jenkins

The intent of this research is to develop a constitutive equation for the elastic fiber-dominant ligamentum nuchae and to determine the contributions of its two fibrous components to the parameters forming that constitutive equation. Tests specimens for the ligamentum nuchae were obtained from gross bovine specimens. Three types of mechanical tests were conducted on specially prepared test pieces. The first series of tests were stress relaxation tests at various strain levels, strain rates, and temperatures. The second series were loading and unloading cycles conducted at strain levels, strain rates, and temperatures comparable with those of the relaxation tests. The third test series were cyclic sinusoidally-varying strain tests conducted at various strain amplitudes, frequencies, and at temperatures just below and above the physiological range of the specimens considered. Tissue degradation and histologic analysis were employed to determine specifically the contribution of elastic and collagen fibers to the mechanical properties of the ligamentum nuchae as shown in the tests described.

A "a

upon a su

certain ma

as to esta

was then e

loading cu

Rolfe B. Jenkins

A "quasi-linear" viscoelasticity law has been formulated based upon a suggestion forwarded by Y. C. Fung. Using this development, certain material constants were determined from relaxation tests so as to establish a constitutive equation. The constitutive equation was then employed to predict the results of constant strain rate loading curves, hysteresis loops, and sinusoidal input tests.

A CONSTITUTIVE EQUATION FOR PARALLEL-FIBERED ELASTIC TISSUE

By

Rolfe Brian Jenkins

A THESIS

Submitted to
Michigan State University
in partial fulfillment of the requirements
for the degree of

DOCTOR OF PHILOSOPHY

Department of Metallurgy, Mechanics and Materials Science

1973

ACKNOWLEDGEMENTS

I wish to thank Dr. R. W. Little for acting as my thesis director and for patiently awaiting the development of this thesis. Also I express my appreciation to Dr. W. A. Bradley, Dr. G. E. Mase, and Dr. R. Echt for their helpful suggestions.

I wish to express my gratitude to Dr. Echt, Dr. A. W. Stinson, Dr. K. Keahey, and Mrs. Alice Middleton for their attention to details with which I was not particularly familiar.

I also appreciate the financial support of the Division of Engineering Research and the technical assistance of Tony.

TABLE OF CONTENTS

LIST OF TABLES

LIST OF FIGURES

LIST OF FIGURES (Cont.)

LIST OF FIGURES (Cont.)

The ce

group of ce

a particula

body organs

its tissues

ful in char

There

structural

1) E

free a

lines

2) M

to st

3) N

of ex

4) C

funct

I. INTRODUCTION

The cell is the basic unit of a living organism. A tissue is a group of cells and cell products specialized in some manner to perform a particular function. Tissues are the binding materials from which body organs are formed. Since organ activities are actually those of its tissues, a knowledge of tissue response to various stimuli is useful in characterizing organ activities.

There are four basic types of tissues which are functionally and structurally distinct.

1) Epithelial Tissue

This tissue forms sheet-like coverings with one surface free and the other attached to other tissues. Epithelial tissue lines most body cavities and forms the skin.

2) Muscle Tissue

This tissue is a group of elongated cells which respond to stimulation to provide oriented contractile movements.

3) Nervous Tissue

This is irritable tissue capable of conducting waves of excitation in the form of nerve impulses.

4) Connective Tissue

This tissue provides connecting, supporting, and binding functions (1).

This p

Corrective

pairs int

tissue, a

are not c

ical fun

organize

vary in

mechanics

of connec

physiolog

to perform

general su

Connec

brous comp

substance

It is gene

substance

ration of

influence.

The c

defense, s

exchange,

storage, a

tissue.

The c

which sur

This particular research is concerned with connective tissue. Connective tissue differs from the other three types in that it contains intercellular material as its primary constituent. Epithelial, muscle, and nervous tissues are essentially cellular and thus they are not capable of withstanding mechanical loads or performing mechanical functions independently. Connective tissue is composed of an organized network of cellular and intercellular substances which may vary in proportion and in structure with anatomic location. The mechanics involved in the formation, maintenance, and degeneration of connective tissue are not completely understood. However, the physiology of connective tissue is well documented in that it is known to perform the functions of transport, defense, storage, repair, and general support (2).

Connective tissue is composed of a sparse array of cells, a fibrous component lying between these cells, and an amorphous ground substance which may vary from fluid to semi-solid in its consistency. It is generally believed that connective tissue cells secrete ground substance from which connective tissue fibers are formed. The formation of fibers from ground substance is controlled by some cellular influence.

The cells of connective tissue perform the functions of transport, defense, storage, and repair. They perform these functions by oxygen exchange, phagocytosis and antibody production, fat and serum protein storage, and by cell secretion which aids in the repair of injured tissue.

The connective tissue fibers along with the ground substance which surrounds them provide connective tissue with its support

apability.

lastic, an

ysiologis

ar in var

ascular wa

ey combi

support in

re subject

of interes

be used to

hich thes

tissue fib

of body ch

nert.

Of th

is the bes

lagen whic

Microscopy

rofibrils

in paralle

he fiber,

fibers to

to form th

appear in

membranes

flat bands

and diges

capability. Three types of connective tissue fibers; collagenous, elastic, and reticular, have interested anatomists, histologists, physiologists and others for years. These types of fibers are present in varying proportions in bone, cartilage, tendon, ligament, skin, vascular walls, and in most body organs providing mechanical functions. They combine with smooth and striated muscle to provide motion or support in or around all body organs. Since connective tissue fibers are subject to mechanical loadings, their mechanical properties are of interest. Properties of these fibers determined from testing may be used to define the mechanical characteristics of the organs with which these fibers are associated. Mechanical testing of connective tissue fibers is facilitated by the fact that, by normal standards of body chemical activity, these fibers are almost metabolically inert.

Of the three types of connective tissue fibers, the collagen fiber is the best understood. It is composed primarily of the protein collagen which is an arrangement of a large number of amino acid chains. Microscopy reveals the collagen fiber to be composed of very thin microfibrils which combine in parallel to form a fibril. Fibrils combine in parallel to form fibers which are from 1 to 15 microns in diameter. The fiber, barely visible to the naked eye, may combine with other fibers to form a membranous network or they may combine in parallel to form thick bundles. On a macroscopic level, collagen fibers appear in parallel bundles as in ligament and tendon, in sheet-like membranes as in fascia or as in parts of the vascular system, or in flat bands or rings as in the walls of the circulatory, respiratory, and digestive tracts (3).

Retic

ue fibers.

ner paral

ic fiber b

eral physi

fibrils.

ary regar

Of pr

primary co

as a much

lagen fiber

with the c

anatomical

Elastic fi

collagen f

anatomic a

cult to is

teristics

Reticular fibers are, embryologically, the first connective tissue fibers. They usually occur as two-dimensional networks rather than parallel fiber bundles and are usually holding collagen and elastic fiber bundles together. Reticular microfibrils have the same general physical structure and chemical composition as collagen microfibrils. So, despite some marked differences in staining reactions, many regard reticular fibers as immature collagen fibers.

Of primary interest here is the elastic fiber. It has as its primary component the protein albuminoid elastin. An elastic fiber has a much greater extensibility and a much lower modulus than a collagen fiber of the same size. The elastic fiber is usually compared with the collagen fiber because the two are very closely associated anatomically, morphologically, chemically, and physiologically. Elastic fibers are always found in close anatomic association with collagen fibers and are usually dominated by collagen fibers. This anatomic association is the reason why elastic fibers are very difficult to isolate and test mechanically. Thus, the mechanical characteristics of elastic fibers are not well defined.

II.

2.1 Nomen

composed
posed of
a charact
croscopy.
to 10 mic
tein elas
with the
elastic f
such as t
of elasti

Elas
fibers as
collageno
tissue or
reference

2.2 Phys

2.2.

or m

II. THE ELASTIC FIBER

2.1 Nomenclature

Elastic fibers are thin thread-like strands which are composed of smaller sub-units. These sub-units are themselves composed of smaller sub-units until this progression of sub-units reaches a characteristic filament which can only be observed by electron microscopy. The elastic fiber will be defined as a strand of about 1 to 10 microns in diameter which has as its primary component the protein elastin. The elastic fiber may have collagen fibrils interwoven with the elastic fibrils which are the principal components of the elastic fiber. By this definition of fiber size, elastic membranes such as those in the vascular walls and in the lung are also composed of elastic fibers.

Elastic tissue may refer to a connective tissue which has elastic fibers as its principal component. Elastic tissue totally devoid of collagenous tissue and other tissues is called elastica. Thus, elastic tissue or elastic fiber has a structural connotation while elastin references the chemical character of elastic fibers.

2.2 Physicochemical Properties

2.2.A Physical Properties

Elastic fibers arranged in parallel bundles, flat bands, or membranes always form a continuous network with no free ends.

In t
almo
or s
ane
elec

cros
cros
chol
The t
combi
trate
Colla
incid
cellu

diges
meter
the e
fish
ligam
in pa
strom
threa
stanc
tic f
Subst

In the state of relaxation, elastic fibers are highly refractile, almost isotropic, and somewhat kinked in appearance. The drying or stretching of these fibers is a birefringence inducing, volume reducing process. Elastic fibers are paramagnetic and show electrical and magnetic anisotropy.

A fine structure description of an elastic fiber on a microscopic level is one offered by Gross (6,7). By electron microscopy, he was able to define two distinct chemical and morphological components; threads and an amorphous ground substance. The threads are arranged in long, generally parallel bundles which combine in great numbers to form a fiber. The fibers are infiltrated by and imbedded in a trypsin-sensitive ground substance. Collagen filaments are present within the elastic fiber as an incidental component probably incorporated into the fiber extracellularly during its formation.

Gross was able to fragment the elastic fiber by trypsin digestion and observe a filament of about 70 angstroms in diameter. He regarded the filament as the characteristic unit of the elastic fiber because it appeared in elastic fibers from the fish swim bladder, rabbit, rat, and human aortas, and in the ligamentum nuchae of the ox. Filaments wind around one another in pairs to form threads which have a width of about 120 angstroms. The exact nature of the ground substance surrounding the threads is not completely understood. However, the ground substance is apparently responsible for the heat resistance of elastic fibers because when trypsin disperses the matrix of ground substance, the elastic fiber becomes heat labile (7).

of (

cer

sub

sin

enz

tic

2.2

fit

cha

kal

is

to

(1)

are

by

cha

int

pep

and

In

Vul

bei

In

Spr

Later work by Stack does not confirm all the observations of Gross. Stack (8) defined a different characteristic unit and denies the existence of a structural periodicity of elastic fiber sub-units which Gross suggests. Other authors suggest that trypsin does not disperse the matrix of ground substance but the enzyme pepsin does (9). These contradicitons imply that the elastic fiber microscopic morphology warrants further investigation.

2.2.B Chemical Properties

The protein elastin, the principal protein of the elastic fiber, is the most resistant of all body proteins to chemical change (10). It resists boiling water and dilute acids and alkalis. Elastin consists of thirty amino acids only one of which is polar. This nonpolar nature of elastin probably contributes to the great extensibility of the elastic fiber. Meyer and Ferri (11) described elastin as made up of long polymeric chains which are highly contorted and bound together in the lateral direction by only a few cross-links. Stretching a fiber orients these chains in an axial direction reducing entropy and increasing the internal energy of the fiber. There is enough polarity in the peptide linkages of the elastin polymeric chains to cross-link and thus maintain an extended state when the fiber is dried (12). In this last property, the elastic fiber differs from lightly vulcanized rubber with which it is so often compared. Rubber, being completely apolar, will not lock in an extended state (7). In the dry, extended state, water imbibition is necessary to spread polymeric chains of the elastic fiber apart and permit

thermal

Tr

from ar

a and

weight

of app

amino-

their

The pr

and pr

acids

mino a

ophili

S

elasti

was mo

while

powers

for e

hemato

these

the re

attrac

and ch

hanced

thermal contraction.

The molecular nature of elastin does not vary significantly from animal to animal (13). There are two molecular chains noted α and β wound around one another. The α chain has a molecular weight of between 60,000 to 84,000 while the β chain has a weight of approximately 6,000. Both the α and β chains have similar amino-acid compositions. Their hydroxyproline content is low and their proline and valine content is high compared with collagen. The principal acids of elastin are amino-acetic, leucine, alanine, and phenyalanine. These acids are less neutralized by basic amino acids than those of collagen. Elastin contains few of the diamino acids which are basic. Thus elastin is not strongly acidophilic (4).

Staining did not become an important means of differentiating elastic from collagen fibers until it was learned that elastin was more acid than collagen, that collagen swelled in dilute acids while elastin did not, and that elastin possessed certain reducing powers that collagen did not (4). Four common stains developed for elastic fibers are orcein, resorcinol-iron-basic fuchsin, iron-hematoxylin, and aldehyde-fuchsin(14). The most consistent of these stains, orcein and resorcin-fuchsin, utilize the effect of the reducing power of elastin. By this reducing power, elastin attracts and reduces highly oxidized metallic acids such as osmic and chromic acids. This means that the acidity of elastin is enhanced, thus increasing its affinity for basic dyes (4).

2.3 Anatom

The el

uman body.

tissue the

exhibits gr

adipose tis

are intimat

tongue. In

uscle that

%.

Almost

have elasti

erally spea

llagen fiber

in thick ne

scanty. If

ial skin), t

many elastic

pleura conta

eye has very

From ar

tions for el

stresses aim

the coordina

fiber networ

relaxation o

brous networ

2.3 Anatomic and Structural Distribution

The elastic fiber-collagen fiber ratio varies greatly over the human body. In general, the looser the texture of the connective tissue the less abundant the elastic fibers. Thus cartilage, which exhibits great flexibility, contains a great many elastic fibers while adipose tissue has few and bone almost none at all. Elastic fibers are intimately associated with the voluntary muscle in the eye and tongue. In the circulatory system, they are so associated with smooth muscle that the combination has been referred to as myoelastic tissue (4).

Almost all vessels in the cardiovascular and lymphatic systems have elastic fibers present in their walls in some arrangement. Generally speaking, the larger the vessel the larger the elastic to collagen fiber ratio. In the skin and beneath it, elastic fibers exist in thick networks. If skin folds over easily, elastic fibers are scanty. If the skin is bound lightly to the underlying structure (facial skin), the fibers are abundant (15). The respiratory tract has many elastic fibers while the alimentary tract has few. The visceral pleura contains many fiber networks of various orientations while the eye has very delicate networks in the sclera and cornea.

From an anatomic point of view, there appears to be five functions for elastic fiber networks. First, fiber networks disseminate stresses aimed at isolated points. Second, networks are designed for the coordination of the rhythmic motions of the body parts. Third, fiber networks conserve energy by the maintenance of tone during the relaxation of muscle elements. Fourth, the continuous nature of fibrous networks provides a defense against excessive forces. Fifth,

fiber exter

their under

An ex

lationship

ic fiber

ulse pres

capillarie

sustaining

have the r

fiber extensibility and retractility assist organs in returning to their undeformed configuration once all forces have been removed.

An example of some of the above anatomic-physiological relationships might be the arterial walls. The more abundant the elastic fiber bands and membranes in the arterial wall, the lower the pulse pressure and the more uniform the blood flow all the way to the capillaries. It has also been observed that the parts of the lung sustaining the greatest amount of fluctuation in normal respiration have the richest supply of elastic fibers (4).

....

3.1 Mecha

anisms wh
the point
whether or
the injury
of the bod
Some have
ture of el
be related
fibers hav
action of
integrity
tional cap
accompany
the only m
fiber and
ment. Such
devices for

The hu
nuchae are
The aortas

III. LITERATURE SURVEY

3.1 Mechanical Properties

The mechanical properties of elastic fibers and the mechanisms which effect changes in them have long been of interest from the point of view of pathology. Workers have tried to determine whether or not there exists a cause and effect relationship between the injury or degeneration of elastic fibers and the susceptibility of the body to arteriosclerosis, emphysema, or aneurytic conditions. Some have suggested that an aneurysm may be the result of the rupture of elastic fibers. Others feel that ruptured elastic fibers may be related to arteriosclerosis and emphysema because ruptured elastic fibers have been shown to bind iron and calcium thus inhibiting the motion of associated tissues. Changes in the chemical or structural integrity of an elastic fiber does not always imply a change in functional capacity. Neither does a change in functional capacity always accompany a change in staining reaction or structural integrity. Thus the only means of determining the mechanical properties of the elastic fiber and subsequent changes in those properties is by direct measurement. Such determinations can also assist in the design of prosthetic devices for replacing or repairing damaged connective tissue.

The human aorta, the bovine aorta, and the bovine ligamentum nuchae are the most common specimens used in elastic fiber testing. The aortas are about 35% to 40 % elastin by dry weight and the bovine

ligament
weight mea
seem to be
In 18
mat may b
fiber-dom
data with
calculate
strips.
dynes/cm^2
afterward
variables
to remove
exposure
(elastica
strain ar
stress ne
In 1
tum mucha
order to
used data
determine
load-elo
ments. T
separate
collagen

ligamentum nuchae is 78% to 83% elastin by the same measure. Dry weight measurements are used in specifying percentages because they seem to be the most consistent (4).

In 1880, C. S. Roy (16) tested human aortic strips and provided what may be the first accurate force-extension curves for an elastic fiber-dominant tissue. For about fifty years, his work provided the data with which others compared their results. In 1937, J. Krafka (17) calculated the average Young's moduli for aortic and ligamentum nuchae strips. He calculated moduli of $.238 \cdot 10^6$ dynes/cm^2 and $3.06 \cdot 10^6$ dynes/cm^2 for the aorta and ligamentum nuchae respectively. Shortly afterward, Hass (18,19) tested human aortic rings and introduced the variables of age and degree of purification of the tissue. He attempted to remove non-elastic fiber components from the specimens by prolonged exposure to warm formic acid. He defined the rings as purified fibers (elastica) at seventy-two hours exposure. Elastica showed 32% greater strain and 170% greater retractility than untreated rings at a given stress near the maximum stress the material would sustain.

In 1954, G. C. Wood (20) conducted several tests on the ligamentum nuchae in small strain. He considered only strains up to 20% in order to avoid any time or hysteresis effects in the material. He used data obtained from the native ligament to serve as a control to determine the relative weakening or strengthening effects upon the load-elongation curve of various enzymes, acids, and testing environments. The chemical treatments employed by Wood were designed to separate the effects upon the load-elongation curve of elastic fibers, collagen fibers, and ground substances. He concluded that the collagen

fibers of th

strain) natu

the load-elo

absence of

by the char

relative st

change in w

ible to def

In 195

nature of t

view. They

effects had

sient effec

one may app

dynes/cm^2.

or Burton (

llagen fiber

only at str

In 196

curve fit f

were teased

of collagen

fibers had

effects wer

of the liga

stance, per

represented

fibers of the ligamentum nuchae were of a highly extensible (70% strain) nature and did not participate to any significant extent in the load-elongation curve up to a 20% strain level. The presence or absence of ground substance, on the other hand, was very much evidenced by the character of the load-elongation curve. Wood interpreted the relative strengthening or weakening of a test strip in terms of the change in work required to perform a 20% extension. It is not possible to define a stress-strain law for loading from his data.

In 1959, Hoeve and Flory (21) analyzed the thermal-mechanical nature of the ligamentum nuchae from a statistical mechanics point of view. They measured load at various elongations after all transient effects had died out but they made no note of how great these transient effects were. From their linear load-elongation graph at 50.5°C one may approximate a lower limit of Young's modulus as $2.65 \cdot 10^6$ dynes/cm^2. This value is somewhat lower than that obtained by Krafka or Burton (22) from Hass' work. Hoeve and Flory concluded that collagen fibers had a significant effect upon the load-elongation curve only at strains greater than 70%.

In 1962, Carton, Dainauskas, and Clark (23) proposed the first curve fit for single elastic fibers in uniaxial tension. These fibers were teased from fresh ligamentum nuchae and had a negligible quantity of collagen fibers surrounding them. Over a 60% strain range the fibers had an average Young's modulus of $8.8 \cdot 10^6$ dynes/cm^2. No time effects were observed in the loadings up to 130% strain. Larger strips of the ligamentum nuchae containing some collagen fibers, ground substance, perhaps some reticular fibers, as well as many elastic fibers represented a lower modulus material of a much different load-strain

haracter.

bers inc

id not se

The r

by Mead (2

aw of Lap

ers and o

The f

btained d

mall stra

o elastic

o the str

ay be att

o rubber

erms of t

ordan and

very signi

The t

composites

tractility

and Ayer e

thermal sh

rather con

and probab

phase, occ

related to

thermal pro

character. The authors agreed with Wood's conclusion that collagen fibers included in the predominantly elastic fiber ligamentum nuchae did not seem to retard the extensibility of that ligament.

The mechanical properties of the lung have recently been reviewed by Mead (24). He emphasized the need for the implementation of the Law of Laplace in evaluating the mechanical properties of elastic fibers and of the entire lung from pressure-volume curves.

The few works from which quantitative stress-strain data may be obtained depict a curve of two distinct regions. There appears, at small strain, a reversible straight line region which is attributed to elastic fibers. At higher strains there appears a region convex to the stress axis which, according to Krafka (25) and Hoeve and Flory, may be attributed to collagen fibers. The resemblance of this curve to rubber led to a thermodynamic analysis of elastin-rich tissue in terms of the well-documented thermodynmaics of rubber. The work of Jordan and Garrod (12), King and Lawton (26), and Hoeve and Flory are very significant with regard to this approach.

The thermal character of the elastic fiber or of elastin-rich composites has been investigated with more interest in thermal contractility than in thermal elasticity. McCartney (27), Lennox (28), and Ayer et al (29) indicate that in the case of aortic tissue, hydrothermal shrinkage is a two-phase reaction. The first phase is a rather continuous contraction up to about 65°C which is reversible and probable attributable to elastic fiber properties. The second phase, occuring at or near 65°C, is mostly irreversible and can be related to the presence of collagen fibers in the aorta. If the thermal properties of elastic fibers are anything like those of

collager

part (30

tance to

In

of elast

elastic

suitable

is the

exist.

of anoth

and ever

very dif

3.2 Mat

The

for body

stress-s

provide

of all c

mechanic

necessar

the bio

system,

strain

material

of any m

stress f

collagen fibers, this hydrothermal shrinkage is probably time dependent (30). It does appear that elastic fibers offer greater resistance to straining at higher temperatures (21).

In general, the literature documenting the mechanical properties of elastic fibers is rather sparse. One reason for this is that the elastic fiber is very difficult to isolate in any kind of a pure form suitable for testing. Another reason for this incomplete documentation is the lack of continuity or consistency in the literature that does exist. The work of one author is often difficult to interpret in terms of another. Variation in experimental methods, data representation, and even nomenclature render critical interpretation of existing data very difficult.

3.2 Mathematical Models

The need for a mathematical description of the stress-strain law for body tissues has long been recognized. A properly formulated stress-strain law with a certain number of suitable parameters can provide for the unification of all experiments and the normalization of all data obtained from them. The mathematical description of the mechanical properties of tissues and their essential components is necessary before a theoretical approach can be taken with respect to the biomechanics of tendons, ligaments, lung, heart, the circulatory system, or of other organs. A constitutive equation, as the stress-strain law may be called, is not completely known for any biological material. One reason for this is that the experimental verification of any model is very difficult to perform in two or three-dimensional stress fields (31).

Most

rly in

as been

est. Oth

certain a

all, tiss

tative ec

The

for the e

lationshi

where e i

inverted

where A

centimet

tin-rich

statisti

for an e

functior

ferromag

And

of prima

(32). .

frictio

Most mathematical models attempt to describe biological materials only in uniaxial tension. Some curve fitting and mathematical modeling has been done with the elastic fiber as the material of primary interest. Other constitutive equations have been formulated to provide a certain amount of universality among body tissues so that most, if not all, tissues may be classified as special cases of the general constitutive equation.

The principal work in mathematically modeling the loading curve for the elastic fiber is that of Clark et al. They proposed the relationship

$$\varepsilon = 1.3(1 - e^{-.17T})$$

where ε is strain and T is load in dynes. This relationship can be inverted to yield

$$\sigma = \frac{5.89}{A} \ln\left(\frac{1.3}{1.3-\varepsilon}\right)$$

where A is area in square centimeters and stress is in dynes per square centimeters. King and Lawton modeled the mechanical behavior of elastin-rich tissues in terms of a general elastomer theory derived from statistical mechanics. They derived the pressure-volume relationship for an elastomeric sphere and closed cylinder in terms of the Langevin function which is well documented due to its role in the theory of ferromagnetism.

Another method of modeling tissues with elastic fibers not being of primary concern was proposed by Frisén, Mägi, Sunnerup, and Viidik (32). They proposed combinations of linear springs. dashpots, and dry friction elements to model the behavior of parallel fibered collagen-

ror tiss

f collag

viscoelas

he rate

tudered

ed para

The

tive la

continuu

his rat

form of

sufficie

elastici

tropic,

adapted

muscle,

to latex

data eve

were onl

dissipat

The

Y. C. Fu

the fact

An analo

introduc

sidered

Much mor

rich tissue. The necessity of accounting for the nonlinear response of collagen fibers to strain resulted in the introduction of linear viscoelastic dashpots into the mechanical system at different times. The mathematical model of the resulting mechanical system became encumbered with many step functions which made mathematical analysis and parameter quantification very difficult.

There are two other methods of mathematically modeling a constitutive law for biological materials. One of these is the macroscropic continuum theory based upon the existence of a strain energy function. This method usually employs certain postulates which constrain the form of the strain energy function so as to lead to necessary and sufficient conditions for the existence of a specific number of finite elasticity parameters (33). These postulates usually imply an isotropic, incompressible, and elastic material. This approach was adapted by Blatz, Chu, and Wayland (34) and applied to frog striated muscle, human papillary muscle, cat and rabbit mesentery, as well as to latex rubber. Their theory was in good agreement with experimental data even with respect to the two-dimensional problem. Their results were only applicable to the loading problem as theirs' was a non-dissipative or elastic theory.

The other method of modeling biological material was proposed by Y. C. Fung (35) in 1967. This method was introduced to account for the fact that biological materials exhibit time and history dependence. An analog of the conventional linear theory of viscoelasticity was introduced. The history dependence of stress upon strain has been considered in the theories of plasticity but biological materials are much more complex. The stress-strain relation in both loading and

unloading in almost all biological materials is highly nonlinear. Also, biological materials exhibit stress relaxation and creep. The time dependence of biological materials, indicated by stress relaxation and creep, has not been incorporated into any statistical mechanics or continuum mechanics formulation of a constitutive equation until just recently (31).

The implication that some viscoelastic theory might be applied to body tissues prompted the use of discrete linear viscoelastic models (32,36). However, these models were not entirely successful in describing the nonlinear stress-strain behavior of these tissues. Fung attempted to resolve this problem by postulating the existence of a relaxation function $K(\lambda,t)$ assumed to be of the form

$$K(\lambda,t) = G(t)T^{e}(\lambda) \qquad , \quad G(o) = 1$$

where λ is the extension ratio and $T^{e}(\lambda)$ is called the "elastic" response (31). Assuming the separable nature of the relaxation function along with the principle of superposition of infinitisimal responses, Fung described the stress at any time as

$$\sigma(t) = \int_0^t G(t-\zeta)\frac{d\sigma^{e}[\varepsilon(\zeta)]}{d\varepsilon(\zeta)}\frac{d\varepsilon(\zeta)}{d\zeta}\,d\zeta \qquad .$$

$G(t)$ is called the "reduced" relaxation function the form of which is not specified. Because $\sigma^{e}(\varepsilon)$ is not linear in strain, the above theory is called "quasi-linear". The equation is linear in σ^{e}.

Although the form of the "reduced" relaxation function was not specified in Fung's integral, the works of others (37,38,39) indicate that it may be taken as logarithmic in form for some tissues. The hereditary integral has been employed to determine the stress response

of collagen fibers to constant strain rate loading and unloading and to sinusoidal strain input (38). An adaptation of Fung's hereditary integral will be employed to determine the response of the elastin-rich ligamentum nuchae to different strain inputs.

IV. EXPERIMENTAL METHODS

4.1 Mechanical Testing Procedures

In order to determine a uniaxial stress-strain law for the ligamentum nuchae, three different forms of loading were employed. Stress relaxation tests were conducted at different strain levels, strain rates, and temperatures. By loading and unloading specimen strips at constant strain rates, hysteresis loops were obtained. Sinusoidal tests at different strain levels, frequencies, and temperatures were also performed. The results of these tests were designed to determine and verify a constitutive equation for the ligamentum nuchae which will closely resemble that of the elastic fiber itself.

Specimens for testing were obtained from available cattle at a diagnostic laboratory. Holstein cattle of different ages were considered. Ligamentum nuchae specimens were obtained within about 8 hours after death. Large sections of the specimen of 12 to 15 inches in length and varying cross-sections were easily obtained. Such specimens were immediately washed in cold tap water and cut with scissors into smaller sections which were more suitable for further slicing into thin strips to be used in the testing apparatus. The smaller sections cut with scissors were generally about 2 inches long (along the long axis of fiber bundles), 2 inches in height, and of varying thickness. These sections possessed a cross-section similar in contour to that of an airplane wing. The scissor-cut sections were

again cut i

with the as

wire around

aluminum fr

a 3 x 2 inc

.0625" in d

formed fro

screws of

along the l

were placed

grating was

to hold the

razor blade

cut strips

and grating

strips fai

ligamentum

which is a

thus of su

cutting in

4-6°C in a

temperatur

utes after

the first

tissue cut

60 or more

their leng

again cut in two perpendicular planes. These latter cuts were achieved with the assistance of two piano wire gratings formed by winding piano wire around small regularly-spaced screws which were embedded in an aluminum frame (Figures 4.5, 4.6). The first grating was formed from a 3 x 2 inch frame with wire of .01" diameter wound around screws of .0625" in diameter spaced about .0625" apart. The second grating was formed from a 3 x 1 inch frame with wire of .005" diameter wound around screws of .0312" in diameter spaced about .0312" apart. The wire ran along the long axis of each frame. The scissor-cut thicker sections were placed on paraffin blocks in Lock's saline solution. The larger grating was placed on the tissue section and some pressure was exerted to hold the tissue snugly between the wires and paraffin. Commercial razor blades were then used, with the grating wires as guide wires, to cut strips of a fairly uniform thickness but variable width. The second grating was then employed in the same manner to make the tissue strips fairly uniform in width as well as in thickness. The resulting ligamentum strip was very similar in size to a office size rubber band which is about .75 mm by 1.5 mm or about 1.15 mm^2 in cross-section and thus of suitable dimensions for testing. Strips were placed soon after cutting in a closed container of Lock's saline solution and stored at 4-6°C in a refrigerator. Although tissue cutting was done at room temperature, tissue strips were refrigerated in saline within 20 minutes after cutting. Strips were stored in different containers and the first strips cut were generally the first tested. The process of tissue cutting usually took from 10 to 15 hours in order to achieve 60 or more testing strips which were uniform in cross-section along their lengths and with respect to one another.

All tests were conducted with tissue strips immersed in a temperature controlled saline bath. Strips were tested in the same type of solution in which they were refrigerated. The Lock's saline solution contained 3.78 grams KCl, 1.35 grams $NaHCO_3$, 2.16 grams $CaCl_2$, and 82.75 grams of NaCl per 9 liters of distilled water. The temperature of the saline bath in the 5 cubic inch plexiglas bath (Fig. 4.3) was controlled by circulating water from a constant temperature source through a copper heat exchanger coil placed in the bottom of the saline bath. The source temperature was monitored by a Bronwill Model 20 constant temperature circulator. The relationship between the temperature of the source and that of the saline bath was linear over a large temperature range. The temperature of the saline bath was measured with a iron-constantan thermocouple. One terminal of the thermocouple was submerged in a Rosemount Engineering Co. Model 911 constant termperature ice bath which was full of crushed ice and some distilled water. The temperature difference between the circulating ice bath and saline bath was monitored by voltage reading on a Keithley 160 Digital Multimeter which was capable of resolving a microvolt (Fig. 4.1).

The grips used to hold specimens were of the clamping type (4.7). Specimens were thin enough that severe squashing of the specimens was avoided. The gauge length of test specimens was measured at the points of insertion of the specimens in the grips. The gauge length varied somewhat but was usually from 15 to 18 millimeters. In order to check for possible specimen slippage in the grips, a red-colored paste, Microstop, was used to stain some non-control specimens near the grip insertion. Very high strains did not reveal any of the yellow unstained

portion

trat sli

All spec

for vert

dial ga

grits.

zontal

measure

the tes

the ent

cross-s

taken a

section

men of

used fo

Tw

The fi

rates,

machin

thread

into t

Statha

load c

sal Tr

unit c

placem

sertec

portion of the specimen beyond the clamps. Thus, it was determined that slippage was minimized by using specimens of the size indicated. All specimen dimensions were measured with a traveling microscope. For vertical measurements (gauge lengths) an Ames and a Scherr Tumico dial gauge were employed. Each dial gauge was graduated in .001 inch units. The cross-sections of the specimens were measured by the horizontal motion of the traveling microscope lens. Horizontal motion was measured by a micrometer graduated in .002 millimeter units. Because the test specimens were approximately rectangular in cross-section, the entire grip assembly had to be rotated 90 degrees to make complete cross-sectional measurements. Five measurements of cross-section were taken along the gauge length of the specimen. The specimen cross-section was taken to be the average of these five readings. No specimen of cross-section less than .75 mm^2 or greater than 1.5 mm^2 was used for data taking in any experiment.

Two separate testing fixtures were used for conducting the tests. The first fixture (Fig. 4.3), used for generating constant strain rates, is similar to many screw driven tensile testing machines. This machine operates by driving a crosshead by the turning of two finely threaded screws mounted in stainless steel ball bearings. Inserted into the stationary upper plate of the tensile testing fixture is a Statham Model UC3 Universal Transducing Cell along with a Statham UL4-0.5 load cell accessory. This cell is powered by a Statham SC1001 Universal Transducer Readout unit. This load cell, accessory, and readout unit can accommodate slightly over 100 grams load in tension. Displacements of the crosshead were measured with a steel clip gage inserted between the crosshead and load cell plate. The clip gage was

constructed from steel shim stock .01 inches in thickness, .20 inches in width, and about 6.0 inches in length. Attached to the convex side of the clip gauge was a Budd Metalfilm Strain Gauge Type C15-624. The strain gauge was balanced in the bridge circuit by a Heath Decade Box Resistance. The clip gauge and variable resistor were used in conjunction with a Ellis Associates Model BAM-1 Bridge Amplifier Meter. Another testing device was a variable amplitude scotch yoke used for sinusoidal tests. This fixture was used to induce displacements up to 15 millimeters (Fig. 4.4). Both testing fixtures were powered by a 1/70 horsepower Bodine Model NSR-12R shunt wound motor. The speed of the motor was controlled by a Minarik Model W-14 speed control unit. In order to obtain both high and low rates of crossbar displacement without radically changing motor speeds, a gearbox was used to achieve 5 to 1, 3 to 1, and 1 to 1 speed reduction ratios.

The loads and displacements of all specimens were recorded on a Sanborn 322 Dual Channel DC Amplifier Recorder. Occasionally, constant strain rate loading and unloading tests were monitored on a Varian F-80 X-Y Recorder. At times, both recorders were engaged in parallel. Because the testing of all specimens was done at high strain, the fixed upper grip and part of the universal joint attaching the grip to the load cell were submerged in the saline bath in order to insure that the entire test specimen remained in solution during straining. This immersion of grip and universal joint required that a slight adjustment be made in the load zeroing to account for the bouyant effect of the saline solution. Once a very small strain was introduced to fix the specimen in the grips, the initial gage length of the specimen was judged to be that length at which the specimen

just began to record load.

In the stress relaxation tests, specimens were loaded to a given level of strain and all motion of the crossbar ceased by manually turning the Minarik power unit dial to the zero speed setting. Stress relaxation was usually measured for six minutes. In constant strain rate loading and unloading tests, the strain rate reversal was achieved by manually flipping a switch on the power unit. In the case of sinusoidal testing, specimens were subjected to a sinusoidal input for about 25 to 30 minutes.

All tests run on specimens from a given animal were run during a 4 day or 96 hour period. Literature concerning the effects of time and manner of post-mortal storage on connective tissue mechanical properties (16,17,40,41) is contradictory. However, preliminary testing done on the ligamentum nuchae specimens stored in the refrigerator in preparation for this work implied that the mechanical character of specimens was not significantly altered within 96 hours after the gross ligament was taken from the cow. From 4 to 7 days storage, specimens lost their ability to dissipate load while retaining their general "elastic" or stiffness character. After 7 days storage, specimens began to putrify very noticeably. In order to preserve the specimens as best as one could, the saline solution in which they were stored in the refrigerator was changed and the specimens rinsed twice daily.

4.2 Hi

of that

rational

The pro

also si

fibers

mation

strongl

is felt

closely

fibers

fibers,

arentu

determi

nuchae

erally

are in

the co

matical

Th

ponents

physica

physica

infeas

results

termine

4.2 Histologic Methods

The mechanical character and the mathematical description of that character of any tissue depends on three factors. The deformational characteristics of the tissue fibers is certainly important. The proportion of the tissue fibers within the composite tissue is also significant. Finally, the geometrical relationship of the tissue fibers with each other and with other components must effect the deformation nature of the gross tissue (33). Since the elastic fibers very strongly dominates all other components of the ligamentum nuchae, it is felt that the mechanical nature of the ligamentum nuchae is very closely related to that of the mechanical properties of the elastic fibers composing it. However, the effect of collagen fiber, reticular fibers, and ground sustance upon the mechanical properties of the ligamentum nuchae cannot be ignored. Some work has been directed toward determining the effects which various components of the ligamentum nuchae have on its mechanical properties (20,21,42). There is generally little disagreement among these works as to what these effects are in a qualitative sense. An effort will be made to determine how the components of the ligamentum nuchae affect the quantitative mathematical model of the composite tissue.

The most certain way of determining the properties of the components of any tissue is to isolate the various components by some physical or chemical means. In the case of the ligamentum nuchae, physical isolation of components for mechanical testing has proved infeasible. Chemical methods have proved more successful but the results of chemical treatments must be studied histologically to determine their effectiveness. Elastic fibers have been removed from

tre li

tre gr

but re

diffic

rove n

tivere

provid

ligare

deter-

some o

P

nonela

given

ground

exposu

the mo

The bo

T

rate s

prescr

for go

from a

refrig

tic ac

refrig

all.

of piec

the ligament by various methods which have different effects upon the ground substance. No treatments are available for removing all but reticular fibers or all but ground substance. In view of the difficulties of removing elastic fibers, only methods designed to remove nonelastic fiber components were considered here. The effectiveness of these methods was studied by prepared slides which also provided information concerning the structural arrangement of the ligamentum nuchae in different stages of purification. In order to determine the relative proportion of elastic and collagen fibers, some of the very basic methods of stereology were applied (Appendix C).

Perhaps the best analysis of the various methods for removing nonelastic fibers from a predominantly elastic-fiber tissue is that given by Ayer (14). Boiling water removes young collagen fibers and ground substance from the ligamentum nuchae very effectively. Prolonged exposure to concentrated (88%) formic acid at 45°C to 50°C is probably the most effective means of removing collagen and ground substance. The boiling water and formic acid methods were employed in this study.

The ligamentum nuchae of a certain animal was cut into four separate sections. All four sections were cut and prepared for testing as prescribed. The pieces from one section were heated in distilled water for 90 minutes at 58°C and then stored in a refrigerator. The pieces from a second section were boiled in distilled water for 7.5 hours and refrigerated. The pieces from a third section were heated in 88% formic acid for 24 hours in a temperature controlled oven at 48°C and refrigerated. The pieces from the fourth section were not treated at all. The refrigeration times for all sections were similar. A number of pieces from all four sections were tested in the same testing

environment. Only stress relaxation tests were conducted.

Pieces from the untreated, boiled, and formic acid treated specimens were placed in a 10% formalin solution at room temperature as soon as they were available. These pieces were fixed in formalin for 36 to 48 hours (43). A number of slides were made of each of these three types of tissues. These slides were made on the Technicon Tissue Processor according to the prescribed methods for that machine (44). All tissue was rinsed in mixes of alcohol, cleared with xylene, embedded in paraffin, cut in 6 micron sections, and fixed to the slides with albumin. Three stains were employed to stain each of the three types of tissue pieces three different ways. Hematoxylin and Eosin served to give the slides contrast and to display the connective tissue cells. Gomori's One Step Trichrome stain was used to stain collagen specifically. Verhoeff's stain was used to stain elastic fibers specifically. An analysis of these nine slides was intended to show any changes in the structural integrity or chemical composition of the ligamentum nuchae as affected by means of chemical purification. Thus, an attempt was made to see how such changes affected the mechanical characteristics of the ligamentum nuchae and how the mathematical model established reflected an alteration in these mechanical characteristics.

Fig. 4

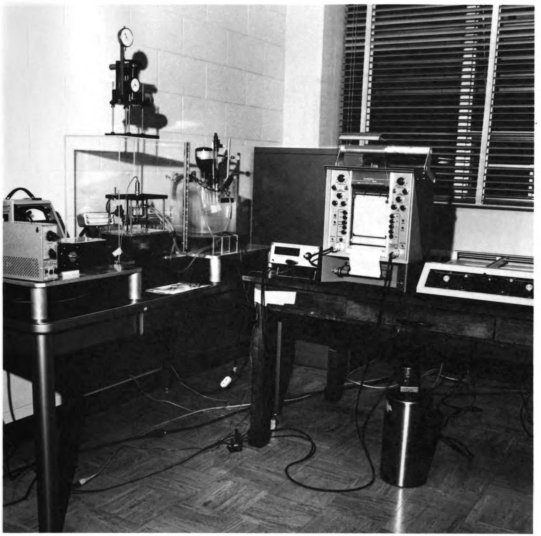

Fig. 4.1 Complete Recording and Testing Apparatus.

Fig. 4.

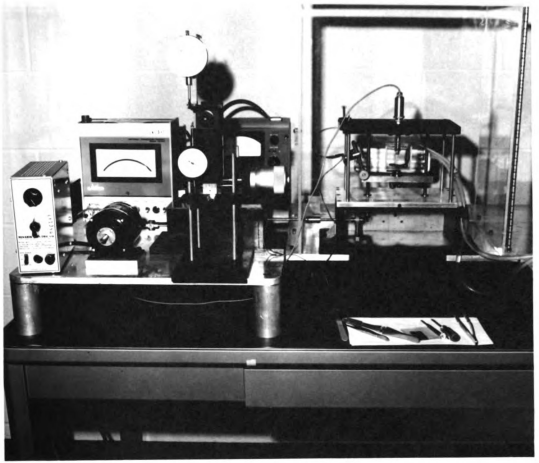

Fig. 4.2 Testing Apparatus.

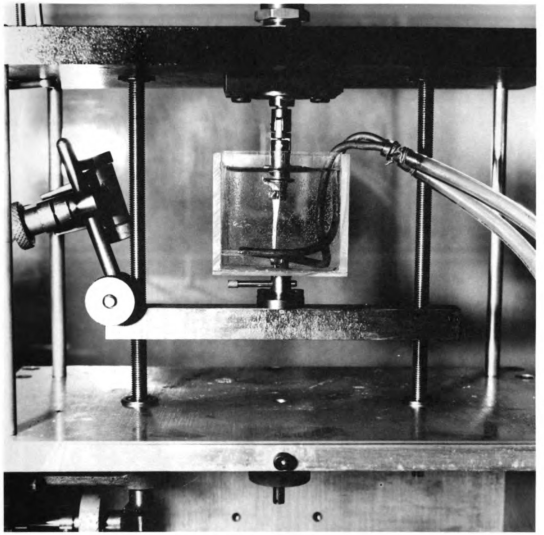

Fig. 4.3 Constant Strain Rate Fixture.

Fig. 4.4

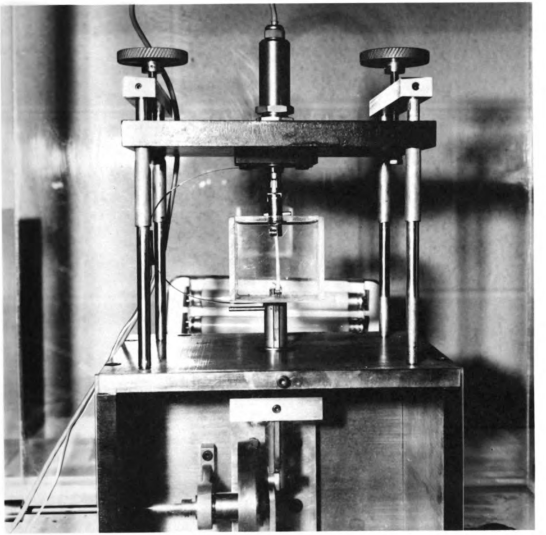

Fig. 4.4 Sinusoidal Strain Input Fixture.

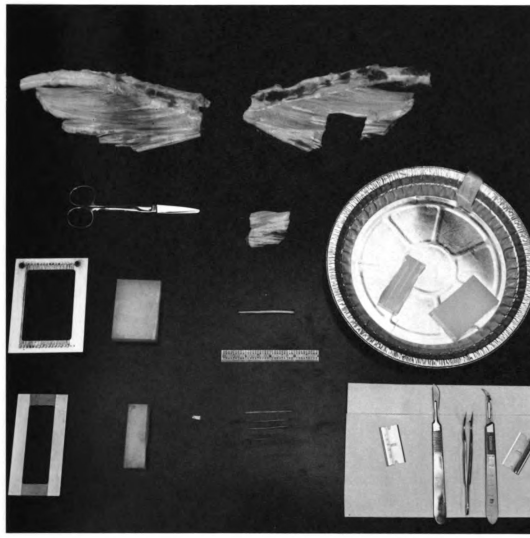

Fig. 4.5 Complete Specimen Preparation Equipment.

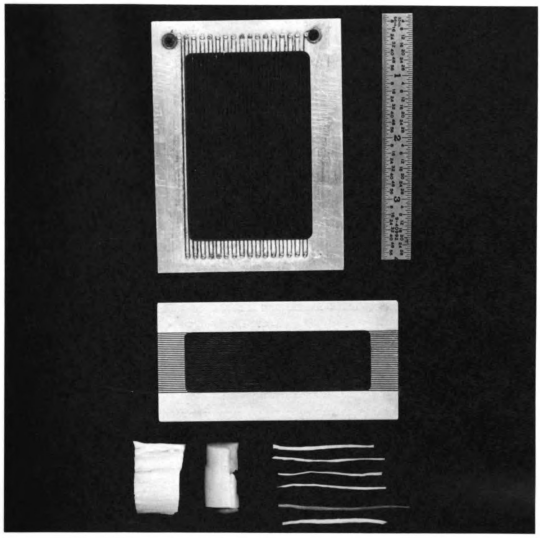

Fig. 4.6 Cutters and Sample Test Strips.

Fig. 4.7 Specimen Grips and Plexiglas Cube.

5.1 Determi

Be

response to

tion must be

time may be

here. This

mon to all

$F^e(s)$ may

sponse and

function.

defined pre

Fung (

character a

which is a

He describe

V. MATHEMATICAL FORMULATION

5.1 Determination of a Relaxation Function

Before the hereditary integral can be used to determine the response to any kind of strain input, the form of the relaxation function must be known. The assumption that the variables of strain and time may be separated in the relaxation function will not be employed here. This is to say, there is no "reduced" relaxation function common to all strain levels. Thus the relaxation function may be written

$$\kappa(\varepsilon,t) = F(\varepsilon,t)\ \sigma^{e}(\varepsilon) \quad . \qquad 5.1$$

$\sigma^{e}(\varepsilon)$ may be referred to as the "elastic" stress or "elastic" response and $F(\varepsilon,t)$ may be called a "normalized" or "modified" relaxation function. $F(\varepsilon,t)$ will replace the "reduced" relaxation function as defined previously (31,38).

Fung (45) has described the "elastic" response as exponential in character and modified by a nonlinear function of the stretch ratio which is a zero factor resulting from finite elasticity considerations. He described the "elastic" response as

$$\sigma^{e}(\lambda) = A[\lambda - \frac{1}{\lambda^{2}}]e^{a\lambda} \qquad 5.2$$

were A and

terms of the

Equation 5.

By expandin

be written

$$e^{(}$$

It is reas

Equation 5

in describ

been shown

the stress

nuchae, th

There are

er than th

where A and a are constants. If one writes the Lagrangian strain in terms of the extension ratio λ as

$$\varepsilon = \frac{L - Lo}{L} = \lambda - 1 \quad ,$$

Equation 5.2 may be written as

$$\sigma^e(\varepsilon) = B[\varepsilon - \varepsilon^2 + \frac{4\varepsilon^3}{3} + \frac{5\varepsilon^4}{3} + \ldots]e^{a\varepsilon} \quad . \qquad 5.3$$

By expanding the exponential term in a power series, Equation 5.3 may be written

$$\sigma^e(\varepsilon) = B[\varepsilon + (b-1)\varepsilon^2 + (\frac{b^2}{2} - b + \frac{4}{3})\varepsilon^3 + \ldots] \quad . \qquad 5.4$$

It is reasonable to assume that in a power series expansion such as Equation 5.4, certain terms will be much more important than others in describing the "elastic" response of different tissues. It has been shown (37,46) that the second term of Equation 5.4 approximates the stress-strain relation of collagen fibers. For the ligamentum nuchae, the first and second terms will be used to say that

$$\sigma^e(\varepsilon) = C\varepsilon + D\varepsilon^2 \quad . \qquad 5.5$$

There are many reasons for using the polynomial in Equation 5.5 rather than the expressions

$$\sigma^e(\varepsilon) = F\varepsilon^{\alpha}$$

or

where C, D,
all three e
accurately,
for curve f
constants i
tion means
with the ot
in their pa
it makes ma

The wo
biological
37,38,39).
work, this
the tendenc
be strongly
for if one

Equation 5.
logarithm c
of Equation
laxation fu

or

$$\sigma^e(\varepsilon) = G(e^{\beta\varepsilon} - 1)$$

where C, D, F, G, α, and β are constants. One reason is that, although all three expressions may be made to fit the "elastic" curve fairly accurately, the polynomial is linear in the constant parameters used for curve fitting. This linearity implies no correlation between the constants in a statistical manner of speaking. This lack of correlation means that a more accurate data curve fit is possible compared with the other two "elastic" response expressions which are nonlinear in their parameters. Another reason for picking a polynomial is that it makes mathematical analysis simpler.

The work of others has shown that in stress relaxation tests on biological tissues the stress relaxes with the logarithm of time (36, 37,38,39). In preliminary tests run on the ligamentum nuchae for this work, this was true for tests run at a given level of strain. However, the tendency of a given specimen to dissipate stress was determined to be strongly strain dependent. This strain dependency may be accounted for if one writes

$$F(\varepsilon,t) = 1 + \mu\varepsilon^2(t) \ln t \quad . \qquad 5.6$$

Equation 5.6 implies that relaxation is linearly dependent upon the logarithm of time only at a specified strain. The strain dependence of Equation 5.6 precludes the separation of variables in the total relaxation function.

With t

nderstandi

ay write t

$\sigma(t)$ =

5.2 Relaxa

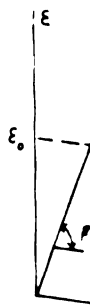

Fig.

where H(t)

function.

integral i

With the form of the stress relaxation determined and with the understanding that $F(\varepsilon,t)$ now replaces the $G(t)$ of Equation 3.1, one may write the generalized nonlinear hereditary integral as

$$\sigma(t) = \int_0^t [1 + \mu\varepsilon^2(t - \zeta) \ln (t - \zeta)] [C + 2D\varepsilon(\zeta)] \frac{d\varepsilon(\zeta)}{d\zeta} d\zeta \quad . \quad 5.7$$

5.2 Relaxation Test

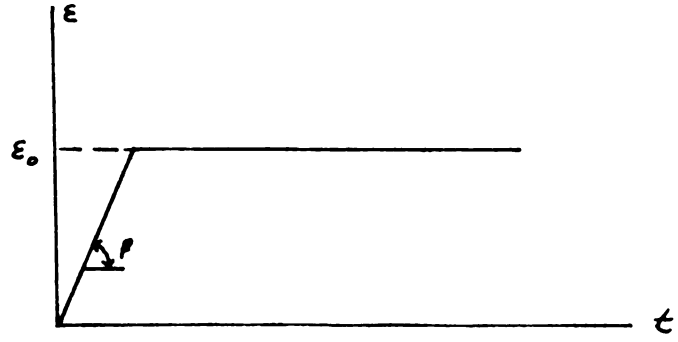

Fig. 5.1 Experimental Stress Relaxation Test.

In the stress relaxation test,

$$\varepsilon = \varepsilon_0 H(t) \quad \text{and} \quad \frac{d\varepsilon}{dt} = \varepsilon_0 \delta(t)$$

where $H(t)$ is the unit step function and $\delta(t)$ is the Dirac Delta function. The substitution of these expressions into the hereditary integral in Equation 5.7 yields

$$\varepsilon(t) = \int_0^t$$

By definit

evaluated

that

Equation 5

which is t

5.3 Consta

Fig.

$$\sigma(t) = \int_0^t [1 + \mu\varepsilon_0{}^2 H^2(t - \zeta) \ln (t - \zeta)] [C + 2D\varepsilon_0 H(\zeta)]\varepsilon_0 \delta(\zeta)\, d\zeta \quad . \quad 5.8$$

By definition of the Dirac Delta function $\sigma(t)$ is simply the integrand evaluated at $\zeta = 0$. In performing this evaluation it might be noted that

$$H(\alpha) = \begin{cases} 0 & \text{if } \alpha > 0 \\ 1 & \text{if } \alpha < 0 \\ 1/2 & \text{if } \alpha = 0 \quad \text{by Dirichlet condition} \end{cases} .$$

Equation 5.8 now becomes

$$\sigma(t) = [C\varepsilon_0 + D\varepsilon_0^2] [1 + \mu\varepsilon_0^2 \ln t] \qquad 5.9$$

which is the response to stress relaxation.

5.3 Constant Strain Rate Test

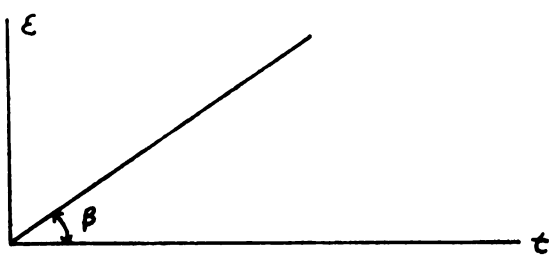

Fig. 5.2 Constant Strain Rate Test.

For a constant strain rate loading,

$$\varepsilon = \beta t \quad \text{and} \quad \frac{d\varepsilon}{dt} = \beta \quad .$$

Substituting the above expressions for loading into the hereditary integral of Equation 5.7 yields

$$\sigma(t) = \int_0^t [1 + \mu\beta^2(t - \zeta)^2 \ln (t - \zeta)] [C + 2D\beta\zeta]\beta d\zeta \quad ,$$

or

$$\sigma(t) = \int_0^t [C + 2D\beta\zeta]\beta d\zeta + \mu\beta^3 \int_0^t [C + 2D\beta\zeta] (t - \zeta)^2 \ln (t - \zeta)\, d\zeta$$

$$= C\beta t + D\beta^2 t^2 \qquad + \mu\beta^3 \int_0^t [C + 2D\beta\zeta] (t - \zeta)^2 \ln (t - \zeta)\, d\zeta \quad . \qquad 5.10$$

The integral in Equation 5.10 is best evaluated with the change of variables $t - \zeta = x$ which implies $x = 0$ when $\zeta = t$, $x = t$ when $\zeta = 0$, and $dx = -d\zeta$. Thus,

$$I_1 = \int_0^t [C + 2D\beta\zeta](t - \zeta)^2 \ln(t - \zeta)d\zeta = \int_0^t [C + 2D\beta(t - x)]\, x^2 \ln x\, dx$$

$$= (C + 2D\beta t) \int_0^t x^2 \ln x\, dx \qquad - 2D\beta \int_0^t x^3 \ln x\, dx$$

$$= (C + 2D\beta t)\left[\frac{x^3}{3}(\ln x - \frac{1}{3})\right]_0^t \qquad - 2D\beta \left[\frac{x^4}{4}(\ln x - \frac{1}{4})\right]_0^t \quad . \qquad 5.11$$

Each of the expressions in Equation 5.11 is zero at the lower limit of zero by a single application of L'Hospital's rule. Thus, Equation 5.11 becomes

$$I_1 = (C + 2D\beta t)\frac{t^3}{3}(\ln t - \frac{1}{3}) - 2D\beta\frac{t^4}{4}(\ln t - \frac{1}{4})$$

$$= t^3\left[(\frac{C}{3} + \frac{2}{3}D\beta t - \frac{1}{2}D\beta t)\ln t - (\frac{C}{9} + \frac{2}{9}D\beta t - \frac{1}{8}D\beta t)\right]$$

$$I_1 = \frac{t^3}{3}\left[(C + \frac{D\beta t}{2})\ln t - \frac{1}{3}(C + \frac{7}{8}D\beta t)\right] \quad . \qquad 5.12$$

Substituting Equation 5.12 for the evaluation of the integral in Equation 5.10 yields

$$\sigma(t) = C\beta t + D\beta^2 t^2 + \frac{\beta^3 t^3}{3}\left[(C + \frac{D\beta t}{2})\ln t - \frac{1}{3}(C + \frac{7}{8}D\beta t)\right]$$

which in terms of strain becomes

$$\sigma(t) = C\varepsilon + D\varepsilon^2 + \frac{\mu\varepsilon^3}{3}\left[(C + \frac{D\varepsilon}{2})\ln\frac{\varepsilon}{\beta} - \frac{1}{3}(C + \frac{7}{8}D)\right] \qquad 5.13$$

which is the response to a constant strain loading.

5.4 Constant Strain Rate Loading and Unloading Test

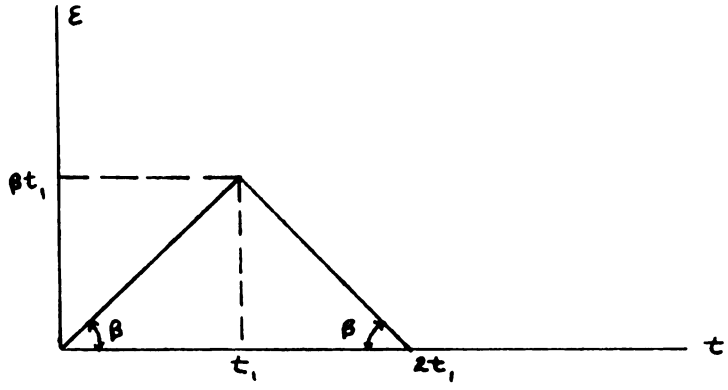

Fig. 5.3 Constant Strain Rate Cyclic Test.

For a constant strain rate loading and unloading, the strain at any time may be described as

$$\varepsilon(t) = \begin{cases} \beta t & \text{for } 0 \leq t \leq t_1 \\ 2\beta t_1 - \beta t & \text{for } t_1 \leq t \leq 2t_1 \end{cases} .$$

Substitution of this description of strain into the hereditary integral yields

$$\sigma(t) = \int_0^{t_1} [1 + \mu\beta^2(t - \zeta)^2 \ln(t - \zeta)][C + 2D\beta\zeta]\, \beta d\zeta$$

$$+ \int_{t_1}^{t} [1 + \mu\beta^2(2t_1 - t + \zeta)^2 \ln(t - \zeta)][C + 2D\beta(2t_1 - \zeta)]$$

$$(-\beta)\, d\zeta \quad . \qquad 5.14$$

Equation 5.14 can be rewritten as

$$\sigma(t) = \int_0^{t_1} \beta[C + 2D\beta\zeta]\, d\zeta \; - \int_{t_1}^{t} [C + 2D\beta(2t_1 - \zeta)]\, d\zeta$$

$$+ \mu\beta^3 \{\int_0^{t} (t - \zeta)^2 \ln(t - \zeta)[C + 2D\beta\zeta]\, d\zeta \; - \int_{t_1}^{t} (t - \zeta)^2 \ln(t - \zeta)$$

$$[C + 2D\beta\zeta]\, d\zeta \; - \int_{t_1}^{t} (2t_1 - t + \zeta)^2 \ln(t - \zeta)[C + 2D\beta(2t_1 - \zeta)]\, d\zeta\}.$$

This equation is valid for time greater than t_1 since for time less than t_1, Equation 5.13 applies. This equation can be rewritten as

$$\sigma(t) = \int_0^{t_1} \beta[C + 2D\beta\zeta]\, d\zeta \; - \beta\int_{t_1}^{t} [C + 2D\beta(2t_1 - \zeta)]\, d\zeta$$

$$+ \mu\beta^3 \{\int_0^{t} (t - \zeta)^2 \ln(t - \zeta)[C + 2D\beta\zeta]\, d\zeta\} - \mu\beta^3 \int_{t_1}^{t} \{(C + 2D\beta\zeta)(t - \zeta)^2$$

$$+ (2t_1 - t + \zeta)^2[C + 2D\beta(2t_1 - \zeta)]\} \ln(t - \zeta)d\zeta \quad .$$

5.15

The first two integrals in Equation 5.15 represent the strictly strain dependent portion of the stress response. They will be written in terms of strain. The rest of the response is left in separate "elastic" and "time dependent" parts of the stress response. With this idea in mind one may write

$$I_2 = \int_0^{t_1} \beta[C + 2D\beta\zeta]\, d\zeta - \int_{t_1}^{t} \beta[C + 2D\beta(2t_1 - \zeta)]\, d\zeta$$

$$= C\beta t_1 + D\beta^2 t_1^2 - C\beta t + C\beta t_1 - 4D\beta^2 t_1 t + 4D\beta^2 t_1^2 - D\beta^2 t_1^2 + D\beta^2 t^2$$

$$= C\beta(2t_1 - t) - D\beta^2(4tt_1 - 4t_1^2 - t^2)$$

$$= C\beta(2t_1 - t) + D\beta^2(2t_1 - t)^2$$

$$= C\varepsilon + D\varepsilon^2 \quad . \qquad 5.16$$

The first integral in the braces in Equation 5.15 is simply I_1 of Equation 5.11 which is evaluated in Equation 5.12. With this knowledge and with the result Equation 5.16, Equation 5.15 becomes

$$\sigma(t) = C\varepsilon + D\varepsilon^2 + \frac{\mu\beta^3 t^3}{3}\left[(C + \frac{D\beta t}{2})\ln t - \frac{1}{3}(C + \frac{7}{8} D\beta t)\right]$$

$$-\mu\beta^3 \int_{t_1}^{t} \{(C + 2D\beta\zeta)(t - \zeta)^2 + (2t_1 - t + \zeta)^2[C + 2D\beta(2t_1 - \zeta)]\}$$

$$\ln (t - \zeta)\, d\zeta \quad . \qquad 5.17$$

Now let

$$I_3 = \int_{t_1}^{t} \{(C + 2D\beta\zeta)(t - \zeta)^2 + (2t_1 - t + \zeta)^2[C + 2D\beta(2t_1 - \zeta)]\}\ln(t - \zeta)d\zeta \ .$$

Using the change of variables $x = t - \zeta$ and defining $\bar{t} = t - t_1$,

$$I_3 = \int_0^{\bar{t}} \{[C + 2D\beta(t - x)]\, x^2 + (2t_1 - x)^2[C + 2D\beta(2t_1 - t + x)]\}\ln x \, dx$$

which upon expanding the integrand becomes

$$I_3 = \int_0^{\bar{t}} \{[4t_1^2 C + 8D\beta t_1^2(2t_1 - t)] + (-4t_1 C + 3D\beta t_1 \bar{t})\, x + (2C - 4D\beta t_1)\, x^2\}$$

$$\ln x \, dx$$

or integrating

$$I_3 = \left[[4t_1^2 C + 8D\beta t_1^2(2t_1 - t)]\, x\, (\ln x - 1) + [-4t_1 C + 8D\beta t_1 \bar{t}]\, \frac{x^2}{2}(\ln x - \frac{1}{2}) \right.$$

$$\left. + [2C - 4D\beta t_1]\, \frac{x^3}{3}\, (\ln x - \frac{1}{3})\right]_0^{\bar{t}} \quad . \qquad 5.18$$

In evaluating this integral, it should be noted that, by L'Hospital's rule, the whole expression in Equation 5.18 is zero at the lower limit of zero. Thus, the integration becomes, after sorting terms,

$$I_3 = 2\bar{t}[C(2t_1^2 - t_1\bar{t} + \frac{\bar{t}^2}{3}) + 4D\beta t_1(2t_1^2 - t_1 t + \frac{\bar{t}^2}{3})] \ln \bar{t}$$

$$- 2\bar{t}[+ C(2t_1^2 - t_1\frac{\bar{t}}{2} + \frac{\bar{t}^2}{9}) + 4D\beta t_1(2t_1^2 - t_1 t + \frac{7}{36}\bar{t}^2)] \quad .$$

Since I_3 is the evaluation of the integral in braces in Equation 5.17, the substitution of I_3 from the above into Equation 5.17 yields

$$\sigma(t) = C\varepsilon + D\varepsilon^2 + \frac{\mu\beta^3 t^3}{3}\left[\left(C + \frac{D\beta t}{2}\right) \ln t - \frac{1}{3}\left(C + \frac{7}{8} D\beta t\right)\right]$$

$$- 2\mu\beta^3\bar{t}\left\{\left[C\left(2t_1^2 - t_1\bar{t} + \frac{\bar{t}^2}{3}\right) + 4D\beta t_1\left(2t_1^2 - t_1 t + \frac{\bar{t}^2}{3}\right)\right] \ln \bar{t}\right.$$

$$\left. - \left[C\left(2t_1^2 - t_1\frac{\bar{t}}{2} + \frac{\bar{t}^2}{9}\right) + 4D\beta t_1\left(2t_1^2 - t_1 t + \frac{7}{36}\bar{t}^2\right)\right]\right\} \quad 5.19$$

which is the response to unloading in the single cycle constant strain rate test.

5.5 Sinusoidal Test

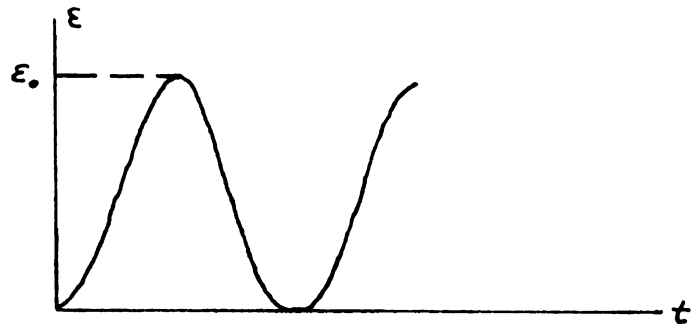

Fig. 5.4 Sinusoidal Strain Test.

For the sinusoidal input, the strain is defined as

$$\varepsilon = \frac{\varepsilon_0}{2}(1 - \cos \omega t)$$

and the derivative of strain with respect to time is written as

$$\frac{d\varepsilon}{dt} = \frac{\omega\varepsilon_o}{2} \sin \omega t \quad .$$

The substitution of these expressions into the hereditary integral of Equation 5.7 yields

$$\sigma(t) = \int_0^t \{1 + \frac{\mu\varepsilon_o^2}{4}[1 - \cos \quad (t - \zeta)]^2 \ln (t - \zeta)][C + D\varepsilon_o(1 - \cos \omega\zeta)]\}$$

$$\frac{\omega\varepsilon_o}{2} \sin \omega\zeta \, d\zeta \quad .$$

This expression can be separated into the time-dependent and time-independent parts to give

$$\sigma(t) = \int_0^t \frac{\omega\varepsilon_o}{2} [C + D\varepsilon_o(1 - \cos \omega\zeta)] \sin \omega\zeta \, d\zeta$$

$$+ \frac{\mu\varepsilon_o^3\omega}{8} \int_0^t [1 - \cos\omega(t - \zeta)]^2 \ln (t - \zeta)[C + D\varepsilon_o(1 - \cos\omega\zeta)]$$

$$\sin \omega\zeta \, d \, \zeta \quad . \qquad 5.20$$

The first integral is integrated to give

$$\frac{\omega\varepsilon_o}{2} \int_0^t [C + D\varepsilon_o(1 - \cos\omega\zeta)] \sin\omega\zeta \, d\zeta = \frac{C\varepsilon_o}{2}(1 - \cos\omega t) + \frac{d\varepsilon_o}{4}(1 - \cos\omega t)^2$$

$$= C\varepsilon + D\varepsilon^2 \quad .$$

Substituting this back into Equation 5.20 yields

$$\sigma(t) = C\varepsilon + D\varepsilon^2 + \frac{\mu\varepsilon_o{}^3\omega}{8} I_4 \qquad 5.21$$

where $I_4 = \int_0^t [1 - \cos\omega(t - \zeta)]^2 \ln(t-\zeta)[C + D\varepsilon_o(1 - \cos\omega\zeta)]\sin\omega\zeta \, d\zeta$.

The integral I_4 may be separated to give

$$I_4 = (C + D\varepsilon_o)\int_0^t [1 - \cos\omega(t -\zeta)]^2 \sin\omega\zeta \ln(t -\zeta) \, d\zeta$$

$$- \frac{D\varepsilon_o}{2} \int_0^t [1 - \cos\omega(t -\zeta)]^2 \sin 2\omega\zeta \ln(t - \zeta) \, d\zeta \qquad 5.22$$

where the trigonometric identity $2 \sin\omega\zeta \cos\omega\zeta = \sin 2\omega\zeta$ has been employed. The change of variables $x = t - \zeta$ may be employed to write Equation 5.22 as

$$I_4 = (C + D\varepsilon_o)\int_0^t [1 - \cos\omega x]^2 \sin\omega(t - x) \ln x \, dx$$

$$- \frac{D\varepsilon_o}{2} \int_0^t [1 - \cos\omega x]^2 \sin 2\omega(t - x) \ln x \, dx \quad . \qquad 5.23$$

Using the trigonometric identity

$$\sin(\alpha - \beta) = \sin\alpha \cos\beta - \cos\alpha \sin\beta \quad ,$$

$$I_4 = (C + D\varepsilon_o)\sin\omega t \int_0^t [1 - \cos\omega x]^2 \cos\omega x \ln x \, dx$$

$$- (C + D\varepsilon_o)\cos\omega t \int_0^t [1 - \cos\omega x]^2 \sin\omega x \ln x \, dx$$

$$- \frac{D\omega_o}{2} \sin 2\omega t \int_0^t [1 - \cos\omega x]^2 \cos 2\omega x \ln x \, dx$$

$$+ \frac{D\omega_o}{2} \cos 2\omega t \int_0^t [1 - \cos\omega x]^2 \sin 2\omega x \ln x \, dx \quad . \qquad 5.24$$

In order to write Equation 5.24 in terms of simple integrals, the square term in the integrand must be expanded to yield

$$I_4 = (C + D\varepsilon_o)\sin\omega t \left[\int_0^t \cos\omega x \ln x dx - 2\int_0^t \cos^2\omega x \ln x dx + \int_0^t \cos^3\omega x \ln x dx\right]$$

$$- (C + D\varepsilon_o)\cos\omega t \left[\int_0^t \sin\omega x \ln x dx - \int_0^t \sin 2\omega x \ln x dx + \int_0^t \cos^2\omega x \sin\omega x \ln x dx\right]$$

$$- \frac{D\varepsilon_o}{2} \sin 2\omega t \left[\int_0^t \cos 2\omega x \ln x dx - 2\int_0^t \cos\omega x \cos 2\omega x \ln x dx + \int_0^t \cos^2\omega x \cos 2\omega x \ln x dx\right]$$

$$+ \frac{D\varepsilon_o}{2} \cos 2\omega t \left[\int_0^t \sin 2\omega x \ln x dx - 2\int_0^t \cos\omega x \sin 2\omega x \ln x dx + \int_0^t \cos^2\omega x \sin 2\omega x \ln x dx\right]. \qquad 5.25$$

Equation 5.25 appears to contain twelve different integrals. However, trigonometric identities reduce these twelve integrals to only two distinct ones. The resulting integrals involve sine and cosine integrals. The derivation of these integrals and the trigonometric identities used to obtain them are considered in Appendix A. Only the results of these integrations are listed in this derivation. Using the results of Appendix A, Equation 5.25 becomes

$$I_4 = (C + D\varepsilon_0)\frac{\sin\omega t}{\omega}\{\sin\omega t\,\ln t - Si(\omega t) - \frac{1}{2}[2\omega t(\ln t - 1) + \sin 2\omega t\,\ln t$$

$$- \sin(2\omega t)] + \frac{1}{4}[3\sin\omega t\,\ln t - 3Si(\omega t) + \frac{\sin 3\omega t}{3}\ln t$$

$$- \frac{Si(3\omega t)}{3}]\}$$

$$- (C + D\varepsilon_0)\frac{\cos\omega t}{\omega}\{Ci(\omega t) - \cos\omega t\,\ln t - \gamma - \frac{1}{2}[\,Ci(2\omega t) - \cos 2\omega t\,\ln t - \gamma]$$

$$- \frac{\cos^3\omega t}{3}\ln t + \frac{Ci(\omega t)}{4} + \frac{Ci(3\omega t)}{12} - \frac{\gamma}{3}\}$$

$$-\frac{D\varepsilon_0}{2\omega}\sin 2\omega t\,\{\frac{1}{2}[\sin 2\omega t\ln t - Si(2\omega t)] - \sin\omega t\ln t + \frac{\sin 2\omega t\ln t}{3} - Si(\omega t)$$

$$- \frac{Si(3\omega t)}{3} + \frac{1}{4}[\omega t(\ln t - 1) + \sin 2\omega t\ln t + \frac{\sin 4\omega t\ln t}{4}$$

$$- \frac{Si(4\omega t)}{4} - Si(2\omega t)]\}$$

$$+ \frac{D\varepsilon_0}{2\omega}\cos 2\omega t\{\frac{1}{2}[Ci(2\omega t) - \cos 2\omega t\ln t - \gamma] - \frac{4}{3}[\,-\cos^3\omega t\ln t - \gamma$$

$$+ \frac{Ci(3\omega t)}{4} + \frac{3}{4}Ci(\omega t)] + \frac{1}{2}[\,-\cos^4\omega t\ln t + \frac{3}{8}\ln t$$

$$- \frac{5}{8}\gamma + \frac{Ci(2\omega t)}{2} + \frac{Ci(4\omega t)}{8}]\}\,, \qquad 5.26$$

where $Ci(\alpha)$ and $Si(\alpha)$ are the cosine and sine integrals respectively of the argument α as defined in Abramowitz and Stegun (47). The substitution of Equation 5.26 into equation yields

$$\sigma(t) = C\varepsilon + D\varepsilon^2 +$$

$$\frac{\mu\varepsilon_o^3}{8}(C + D\varepsilon_o)\Big[\sin\omega t\{\omega t[1 - \ln t] + [\frac{7}{4}\sin\omega t - \frac{\sin 2\omega t}{2} + \frac{\sin 3\omega t}{12}]\ln t$$

$$- [\frac{7}{4}Si(\omega t) - \frac{Si(2\omega t)}{2} + \frac{Si(3\omega t)}{12}]\}$$

$$+ \cos\omega t\{\frac{5\gamma}{6} + [\frac{5}{4}\cos\omega t - \frac{\cos 2\omega t}{2} + \frac{\cos 3\omega t}{12}]\ln t$$

$$- [\frac{5}{4}Ci(\omega t) - \frac{Ci(2\omega t)}{2} + \frac{Ci(3\omega t)}{12}]\}\Big]$$

$$- \frac{\mu\varepsilon_o^4 D}{16}\Big[\sin 2\omega t\{\frac{\omega t}{4}[\ln t - 1] + [-\sin\omega t + \frac{3}{4}\sin 2\omega t - \frac{\sin\omega t}{3} + \frac{\sin 4\omega t}{16}]\ln t$$

$$-[-Si(\omega t) + \frac{3}{4}Si(2\omega t) - \frac{Si(3\omega t)}{3} + \frac{Si(4\omega t)}{16}]\}$$

$$- \cos 2\omega t\{ + \frac{25\gamma}{48} + [\cos\omega t - \frac{3}{4}\cos 2\omega t + \frac{\cos 3\omega t}{3} - \frac{\cos 4\omega t}{16}]\ln t$$

$$-[Ci(\omega t) - \frac{3}{4}Ci(2\omega t) + \frac{Ci(3\omega t)}{3} - \frac{Ci(4\omega t)}{16}]\}\Big]$$

5.27

which is the total response to a sinusoidal input as prescribed.

In order to render Equation 5.27 suitable for computation it is reasonable to read the sinusoidal response only at peak strain. That is, when

$$\varepsilon = \frac{\varepsilon_o}{2}(1 - \cos\omega t) = \varepsilon_o$$

or when

$$\cos\omega t = -1$$

which implies

$$\omega t = (2n - 1)\pi$$

thus

$$\cos 2\omega t = 1$$

$$\cos 3\omega t = 1$$

$$\cos 4\omega t = 1$$

$$\sin(n\omega t) = 0 \quad .$$

With these simplifications, Equation 5.27 simplifies to

$$\sigma(t)_p = C\varepsilon_o + D\varepsilon_o^2 + \frac{D\varepsilon_o^3}{8}(C + D\varepsilon_o)\left[-\frac{5\gamma}{6} + \frac{11}{6}\ln t + \frac{5}{4}Ci(\omega t) - \frac{Ci(2\omega t)}{2} + \frac{Ci(4\omega t)}{16}\right]$$

$$+ \mu'^4_o D\left[\frac{25\gamma}{16} - \frac{103}{48}\ln t - Ci(\omega t) + \frac{3}{4}Ci(2\omega t) - \frac{Ci(3\omega t)}{3} + \frac{Ci(4\omega t)}{16}\right] \qquad 5.28$$

which is the response to peak strain in cyclic sinusoidal strain input.

VI. PRESENTATION OF RESULTS

6.1 Experimental and Theoretical Results

Ligamentum nuchae specimens from four different animals were tested. The general constitutive equation formulation developed in Chapter 5 was used to describe the mechanical characteristics of the test pieces from all four animals. The three parameter constants specified in Chapter 5 were somewhat different from one specimen to another to describe the difference in mechanical character of those specimens.

The results of a number of relaxation tests at various strains, strain rates, and temperatures are listed in Tables 1 - 5. It was observed that stress decayed as a linear function of the logarithm of time for any given relaxation test. However, the magnitude of decay was strongly strain dependent. As shown in Tables 1 - 4, there is a strain level in each specimen at which test pieces display no relaxation or at least an undetectable amount. To account for the strain dependence of the coefficient of the logarithm of time in the "modified" relaxation function, and to account for the negligible relaxation of test pieces at lower strains, the power term in strain has been incorporated into the "modified" relaxation function. The slight curvature noted in the loading curves for relaxation tests suggested that the "elastic" stress be described as in Equation 5.5. Thus the response to stress relaxation from Equation 5.9 is written as

$$\sigma(t) = (C\varepsilon_o + D\varepsilon_o^2)\ (1 + \mu\varepsilon_o^2 \ln t)$$

where μ, C, and D are constants for a given ligamentum nuchae specimen and dependent only upon temperature. As may be observed from Tables 1 - 4, the constant μ varies considerably among the various pieces tested at a given temperature. The tests in which no relaxation was observed ($\mu = 0$) were not included in the averaging of μ. The time-dependent characteristics of test pieces at low strains were approximated by the determination of μ from higher strains and from the incorporation of strain into the "modified" relaxation function. It may be observed from Tables 1 - 3 that an increase in the temperature of the testing environment reduces μ in each case. Table 4 implies that heating pieces to 58°C and testing them in the same testing environment as untreated pieces seems to reduce μ also. The boiled test pieces from Specimen 4 showed a very slight stress relaxation in two cases but the relaxation was not logarithmic and μ could not be determined. The formic acid-treated pieces showed no relaxation even at strains at which untreated pieces from the same specimen (Specimen 4) showed a definite amount of stress relaxation and μ was measurable. Thus, increased temperature, in the testing environment or by previous treatment, does seem to reduce the time dependent character of the average test piece in all four cases tested.

The determination of the constant C and D appearing in the relaxation response expression was made from an analysis of the average loading curve for all test pieces at all strain rates for a given specimen at a given temperature. These constants were determined by

curve fitting the expression

$$\sigma = C\varepsilon + D\varepsilon^2$$

to the average stress-strain curve at low strains where time-dependent effects were assumed negligible as evidenced by negligible stress relaxation at the maximum strain in this curve fitting strain range. The experimental data from the average stress relaxation loading curve was fitted by a finite difference approximation as a first estimate of the constants C and D. Finer adjustments in the values of C and D were made to obtain the best possible curve fit as was determined by minimizing the standard deviation of the fitted curve from the average experimental loading curve. By adjustments of C and D it was always possible to fit the "elastic" curve to the average experimental loading curve within a standard deviation of less than one percent of the stress of the experimental curve at the maximum strain under consideration.

The constants C and D for all testing situations are listed in Table 5. The curves which they represent are shown in Figures 6.1 - 5. Table 5 shows that the increased temperature of the testing environment affects both C and D but in different ways. Thus, a single purely temperature-dependent parameter is very difficult to define. The average stress-strain ratios indicated in Table 5 serve to show that increasing temperature makes the average test piece more resistant to straining in all three cases. The average moduli were increased by 1.07%/°C, .1%/°C, and .64%/°C in Specimens 1, 2, and 3 respectively. Temperature variation tests at low strains were employed on single pieces

from each of the three specimens in order to verify the data in Table 5. These tests showed the average moduli were increased by .93%/°C, .61%/°C, and .69%/°C in Specimens 1, 2, and 3 respectively. The single piece temperature variation tests verified the information in Table 5 except for Specimen 2.

The theoretical stress-strain plots were determined from Equation 5.13 as

$$\sigma(t) = C\varepsilon + D\varepsilon^2 + \frac{\mu\varepsilon^3}{3}\left[(C + \frac{D\varepsilon}{2}) \ln \frac{\varepsilon}{\beta} - \frac{1}{3}(C + \frac{7}{8} D\varepsilon)\right] .$$

Typical comparisons of the theoretical and experimental stress-strain plots are shown graphically in Figures 6.7 - 11. The constants C, D, and μ determined from the stress relaxation tests for each specimen at each temperature were used to make the theoretical loading plots.

A further check upon the validity of the herditary integral is depicted in Figures 6.12 - 17. The equation for the loading curve of the hysteresis loops is the same as for a simple constant strain rate loading plot in Equation 5.13. The unloading cycle is described by Equation 5.19 as

$$\sigma(t) = C\varepsilon + D\varepsilon^2 + \frac{\mu\beta^3 t^3}{3}\left[(C + \frac{D\beta t}{2}) \ln t - \frac{1}{3}(C + \frac{7}{8} D\beta t)\right]$$

$$- 2\mu\beta^3\bar{t}\left\{\left[C(2t_1^2 - t_1\bar{t} + \frac{\bar{t}^2}{3}) + 4D\beta t_1 (2t_1^2 - t_1 t + \frac{\bar{t}^2}{3})\right] \ln \bar{t}\right.$$

$$\left. - \left[C(2t_1^2 - \frac{t_1\bar{t}}{2} + \bar{t}^2) + 4D\beta t_1 (2t_1^2 - t_1 t + \frac{7}{36}\bar{t}^2)\right]\right\}$$

$$t \geq t_1$$

where $\bar{t} = t - t_1$ and t_1 is the time of strain rate reverseal. The hysteresis loops depicted graphically were performed at strain levels much higher than those used to determine the parameter constants C and D. It may be noted from Figures 6.12 - 17 that the theoretical hysteresis loop is somewhat shifted and open relative to the experimental loop. That is to say, if the theoretical loop and experimental loop are of the same height at a strain about half way to the peak strain in the cycle, the theoretical loop will have a smaller height than the experimental loop at strains close to the peak strain and a greater height than the experimental at very low strain. The theoretical unloading cycle always predicts a residual strain of some low magnitude. The experimental loops usually show residual strain but not to the extent that the theory predicts it.

The final attempt to verify the hereditary integral was made through cyclic tests of sinusoidal strain input at different strain levels, frequencies, and at different temperatures. These tests were performed only on Specimens 2 and 3. The results of these tests are listed in Tables 6 and 7. The peak stresses at the peak strains at the end of the first and final cycles are noted there. From these tables it may be observed that the theory is able to predict the peak stress at the end of the first cycle fairly accurately in most cases. This is because the constants C and D which were evaluated by curve fit at low strains still apply at high strains to a test piece which has only weak time dependence in loading. However, the peak stress decay predicted by the theory is much too weak to even approximate the stress decay realized experimentally. The theoretical response to a sinusoidal input at peak strain is given by Equation 5.28 as

$$\sigma(t)_p = C\varepsilon_o + D\varepsilon_o^2 + \frac{\mu\varepsilon_o^3}{8}(C + D\varepsilon_o)\left[-\frac{5\gamma}{6} + \frac{11}{6}\ln t + \frac{5}{4}Ci(\omega t) - \frac{Ci(\omega t)}{2} + \frac{Ci(3\omega t)}{2}\right]$$

$$+ \frac{\mu\varepsilon_o^4 D}{16}\left[\frac{25\gamma}{48} - \frac{103}{48}\ln t - Ci(\omega t) + \frac{3}{4}Ci(2\omega t) - \frac{Ci(3\omega t)}{3} + \frac{Ci(4\omega t)}{16}\right]$$

where γ is Euler's constant and Ci(x) is the cosine integral of x. In Appendix B, some of the significant cosine integrals are evaluated to show that after only a few cycles of sinusoidal strain input they can all be neglected. The resulting equation for the theoretical peak stress indicates a stress decay in the logarithm of time considerably less than that which would be realized by a stress relaxation test at the same strain level for the same period of time. This theoretical implication is not realized in any of the twenty-nine cyclic sinusoidal tests run.

The stress decay predicted by the hereditary integral is very small and would appear as an almost horizontal line on graphs such as Figures 6.17 - 24. In order to accurately describe the experimental results an auxiliary model was attempted. The form of this model was motivated by two factors. One, is that the hereditary integral was reasonably accurate in predicting peak stresses at the end of the first cycle. Secondly, the stress decay with time over a large number of cycles was similar in form to although larger in

magnitude than stress relaxation under similar conditions. Thus an auxiliary model designed to fit the experimental data was of the form

$$\sigma(t) = \sigma_1 \, (1 + \alpha(\varepsilon) \, \ln n) \quad . \qquad 6.1$$

In Equation 6.1, the term σ_1 is the peak stress at the end of the first cycle, n is the cycle number, and $\alpha(\varepsilon)$ was judged to be a constant for a cyclic sinusoidal test at a given strain level, temperature, and on a given specimen.

Since the experimental and theoretical peak stresses at the end of the first cycle compared relatively well in most cases, σ_1 was taken to be the "elastic" stress associated with a given specimen at a given temperature. Thus, the experimental constants C and D already determined were applicable to this auxiliary model. The function $\alpha(\varepsilon)$ was observed to have a strong strain dependence so the use of a power term in strain was used in the same way and for the same reason it was used in the stress relaxation tests. With these considerations, the auxiliary model for stress decay at peak strain in the cyclic sinusoidal tests may be written as

$$\sigma_p = (C\varepsilon_o + D\varepsilon_o^2) \, (1 + \alpha\varepsilon_o^2 \, \ln n) \quad . \qquad 6.2$$

The α in Equation 6.2 is analogous to the μ in relaxation tests and the cycle number argument of the logarithm, n, is analagous to time in the relaxation tests. Equation 6.2 describes the stress decay for any given test very accurately up to as many as 350 cycles. However, the constant α varies somewhat among the test pieces of a given

specimen at a given temperature.

The auxiliary model of Equation 6.2 introduces a new constant parameter and uses two parameters used before. The α for eact test is recorded in Tables 6 and 7 with an average α computed below each table. Although the two temperatures at which stress relaxation and cyclic tests were conducted were not exactly the same for either specimen, the constants C and D determined for the higher and lower temperature at stress relaxation were used for the higher and lower temperature cyclic tests of the same specimen. The analogy between the μ and α for a given specimen seems all the more consistent when one compares their values at different temperatures. For Specimen 2, the average μ decreases in magnitude 2.1%/°C while the average α decreases 3.3%/°C. For Specimen 3, the average μ decreases 5.0%/°C while the average α decreases 5.1%/°C. It may also be observed from Tables 2,3, 6, and 7 that at the low temperature the average α is 2.85 times average μ for Specimen 2 and average α is 3.01 times average μ for Specimen 3. Thus temperature affects both α and μ in about the same way. Figures 6.18 - 24 compare the experimental results with those predicted by the auxiliary model of Equation 6.2. The α used in Equation 6.2 was the average α for a given specimen at a given temperature .

Table 1. Results of Stress Relaxation Tests for Specimen 1.

Temp	Strain Rate	Strain	$\mu\epsilon_o^2$	μ
°C	%/min.	%	$(\text{in min.})^{-1}$	$(\text{in min.})^{-1}$
	22.7	20.0	0	0
	3.1	21.1	0	0
	46.9	22.3	0	0
30	45.9	30.2	-.0055	-.0601
	45.8	40.8	-.0092	-.0553
	22.1	53.2	-.0141	-.0497
	46.7	55.7	-.0109	-.0353
	2.3	19.1	0	0
	42.8	20.0	0	0
	24.7	22.2	0	0
	43.4	30.0	-.0050	-.0552
40	25.7	32.1	-.0055	-.0536
	42.9	40.0	-.0053	-.0332
	26.4	44.0	-.0094	-.0473
	2.1	45.0	-.0092	-.0455
	43.5	50.0	-.0134	-.0536
	23.3	58.3	-.0110	-.0323

At 30°C , $C = 40 \times 10^5$ dynes/cm^2 , $D = 32 \times 10^5$ dynes/cm^2 , and $\mu = -.501$.

At 40°C , $C = 46 \times 10^5$ dynes/cm^2 , $D = 30 \times 10^5$ dynes/cm^2 , and $\mu = -.0455$.

Table 2. Results of Stress Relaxation Tests for Specimen 2.

Temp	Strain Rate	Strain	$\mu\varepsilon_o^2$	μ
°C	% /min.	%	$(\ln \text{min.})^{-1}$	$(\ln \text{ min.})^{-1}$
	32.6	60.0	-.0025	-.0070
	29.2	60.0	-.0040	-.0110
	3.0	62.5	0	0
	51.6	70.0	-.0047	-.0096
35.0	53.2	70.0	-.0052	-.0107
	32.5	70.0	-.0056	-.0114
	28.2	80.0	-.0056	-.0088
	3.1	80.0	-.0058	-.0090
	54.7	80.0	-.0071	-.0111
	54.0	80.0	-.0083	-.0129
	33.0	83.7	-.0077	-.0110
	3.1	90.0	-.0078	-.0096
	66.7	60.0	0	0
	35.0	60.0	-.0025	-.0068
	12.7	64.6	0	0
	39.3	70.0	-.0038	-.0077
40.4	13.0	70.0	-.0049	-.0099
	67.6	80.0	-.0045	-.0070
	36.1	80.0	-.0045	-.0071
	15.3	86.7	-.0090	-.0120
	66.1	94.7	-.0116	-.0130
	13.5	103.8	-.0107	-.0099

At 35.0°C , $C = 32 \times 10^5$ dynes/cm^2 , $D = 16.5 \times 10^5$ dynes/cm^2 , and $\mu = -.0102$.

At 40.0°C , $C = 30 \times 10^5$ dynes/cm^2 , $D = 22 \times 10^5$ dynes/cm^2 , and $\mu = -.0092$.

Table 3. Results of Stress Relaxation Tests for Specimen 3.

Temp	Strain Rate	Strain	$\mu\varepsilon_o^2$	μ
°C	%/min.	%	$(\ln \text{ min.})^{-1}$	$(\ln \text{ min.})^{-1}$
	60.0	40.0	0	0
	3.1	50.0	0	0
	47.2	50.0	0	0
	19.2	50.0	-.0031	-.0123
	47.1	60.0	-.0063	-.0176
	2.7	65.0	-.0066	-.0157
	19.4	67.4	-.0121	-.0266
34.7	3.1	69.4	-.0049	-.0102
	3.0	70.0	-.0085	-.0174
	3.0	70.0	-.0127	-.0260
	56.3	71.3	-.0129	-.0254
	49.8	73.8	-.0164	-.0312
	9.5	76.1	-.0197	-.0341
	54.5	76.6	-.0214	-.0365
	54.7	79.8	-.0193	-.0303
	28.1	81.4	-.0150	-.0226
	63.6	39.1	0	0
	61.9	41.8	0	0
	3.1	50.0	0	0
	20.0	50.8	0	0
	19.6	53.8	-.0038	-.0133
41.9	3.1	60.0	-.0058	-.0160
	62.6	61.8	-.0043	-.0114
	2.5	68.8	-.0105	-.0222
	64.3	68.9	-.0100	-.0211
	20.0	70.2	-.0104	-.0212
	65.4	71.4	-.0101	-.0198
	19.4	74.3	-.0150	-.0272

At 34.7°C , $C = 44 \times 10^5$ dynes/cm^2 , $D = 14 \times 10^5$ dynes/cm^2 , and $\mu = -.0255$.

At 41.9°C , $C = 47 \times 10^5$ dynes/cm^2 , $D = 11 \times 10^5$ dynes/cm^2 , and $\mu = -.0188$.

Table 4. Results of Stress Relaxation Tests for Specimen 4 at 35.0°C.

Piece Type	Strain Rate	Strain	$\mu\varepsilon_o^2$	μ
	%/min.	%	$(\ln \text{ min.})^{-1}$	$(\ln \text{ min.})^{-1}$
	3.1	39.9	-.0024	-.0153
	2.9	40.0	-.0042	-.0263
Untreated	3.5	40.0	-.0028	-.0177
	11.3	40.0	-.0056	-.0350
Pieces	12.3	43.0	-.0073	-.0396
	51.4	43.7	-.0074	-.0386
	10.5	79.9	-.0153	-.0240
	10.2	84.2	-.0087	-.0123
	55.1	87.7	-.0164	-.0213
	62.3	105.9	-.0191	-.0173
	19.5	29.0	0	0
	12.3	40.0	-.0032	-.0198
Heated	19.8	40.0	-.0056	-.0347
	12.5	40.0	-.0164	-.1024
Pieces	10.2	73.1	-.0095	-.0177
	11.4	87.1	-.0146	-.0193
	20.4	102.6	-.0132	-.0125

For Untreated Pieces:

$C = 23 \times 10^5 \text{dynes/cm}^2$, $D = 18 \times 10^5 \text{dynes/cm}^2$, and $\mu = -.0247$.

For Heated Pieces:

$C = 32.5 \times 10^5 \text{dynes/cm}^2$, $D = 20 \times 10^5 \text{dynes/cm}^2$, and $\mu = -.0208$.

For Boiled Pieces:

$C = 38.86 \times 10^5 \text{dynes/cm}^2$, $D = 0$, and μ is undetermined .

For Formic Acid-Treated Pieces:

$C = 27.95 \times 10^5 \text{dynes/cm}^2$, $D = 0$, and $\mu = 0$.

The value of μ of the heated piece at 40% strain and 12.5% strain/min. has been disregarded.

Table 5. A Listing of Constants for All Specimens.

(Specimen)	C	D	μ	Ave. σ/ε *
Type Pieces	10^5dynes/cm^2	10^5dynes/cm^2	(ln min.)$^{-1}$	10^6dynes/cm^2
1) At 30.0°C	40.0	32.0	-.0501	4.74
1) At 40.0°C	46.0	30.0	-.0455	5.25
2) At 35.0°C	32.0	16.5	-.0102	3.81
2) At 40.0°C	30.0	22.0	-.0092	3.83
3) At 34.7°C	44.0	14.0	-.0247	4.90
3) At 41.9°C	47.0	11.0	-.0188	5.13
4) Untreated	23.0	18.5	-.0247	2.85
4) Heated	32.5	20.0	-.0208	3.81
4) Boiled	38.86	0	UND	3.63
4) Acid Treated	27.95	0	0	2.72

* The stress over strain ratio is computed over 50% strain in all 10 cases above for standardization. Over higher strain ranges, this ratio will invariably be higher.

Table 6. Results of Sinusoidal Tests for Specimen 2.

Temp	Strain	Frequency	Experimental Peak Stress	Theoretical Peak Stress	α
°C	%	Rad./min.	10^5 dynes/cm^2	10^5 dynes/cm^2	$(\ln n)^{-1}$
	63.1	3.6	24.55/24.01	26.60/26.51	-.0232
	76.3	29.0	28.64/24.70	34.07/33.88	-.0378
	76.5	13.0	33.63/32.05	34.20/34.08	-.0267
34.9	77.4	3.3	35.39/33.22	34.67/34.47	-.0240
	78.7	49.6	35.75/30.62	35.40/35.15	-.0353
	81.8	28.6	40.82/35.18	37.38/37.18	-.0780
	83.5	3.7	36.10/32.87	38.19/37.98	-.0353
	90.0	66.2	44.60/38.58	42.39/41.96	-.0285
	91.1	3.3	44.79/42.28	42.92/42.64	-.0211
	63.3	3.7	27.83/27.26	29.56/29.42	-.0194
	67.0	34.6	31.33/30.43	30.07/29.98	-.0209
40.9	81.0	12.0	35.36/34.15	38.82/38.71	-.0242
	82.4	50.6	38.22/36.58	39.79/39.62	-.0214
	84.5	23.5	38.55/35.10	40.56/40.34	-.0322
	89.5	3.0	42.00/38.75	44.67/44.41	-.0232
	92.4	66.1	52.03/47.51	46.51/46.25	-.0272

Average α For 34.9°C is -.0290.

Average α For 40.9°C is -.0241.

The value of α at 34.9°C and 81.8% strain has been disregarded.

Table 7. Results of Sinusoidal Tests for Specimen 3.

Temp	Strain	Frequency	Experimental Peak Stress	Theoretical Peak Stress	α
°C	%	Rad./min.	10^5dynes/cm^2	10^5 dynes/cm^2	$(\ln n)^{-1}$
	61.0	76.6	30.29/26.73	32.21/31.86	-.0587
	71.5	76.2	42.40/35.00	38.89/38.44	-.0806
	77.7	75.4	42.39/35.00	42.75/42.06	-.0802
35	77.9	3.2	42.69/36.39	42.77/42.38	-.0548
	80.8	3.3	44.01/39.61	44.71/44.36	-.0734
	90.1	76.2	50.50/39.97	51.61/51.04	-.0950
	90.0	3.0	50.98/42.30	51.61/51.20	-.0944
	64.3	2.9	33.23/28.01	34.74/34.62	-.1728
	68.5	3.1	28.27/27.16	37.37/37.22	-.0341
40	68.8	76.4	30.60/27.67	37.72/37.40	-.0554
	73.5	3.7	41.83/32.92	40.49/40.29	-.1054
	74.0	77.8	39.41/35.24	41.04/40.74	-.0465
	78.1	76.3	43.7 /36.32	43.66/43.24	-.0594

Average α For 35°C is -.0767.

Average α For 40°C is -.0602.

The value of α at 40°C and 64.3% strain has been disregarded.

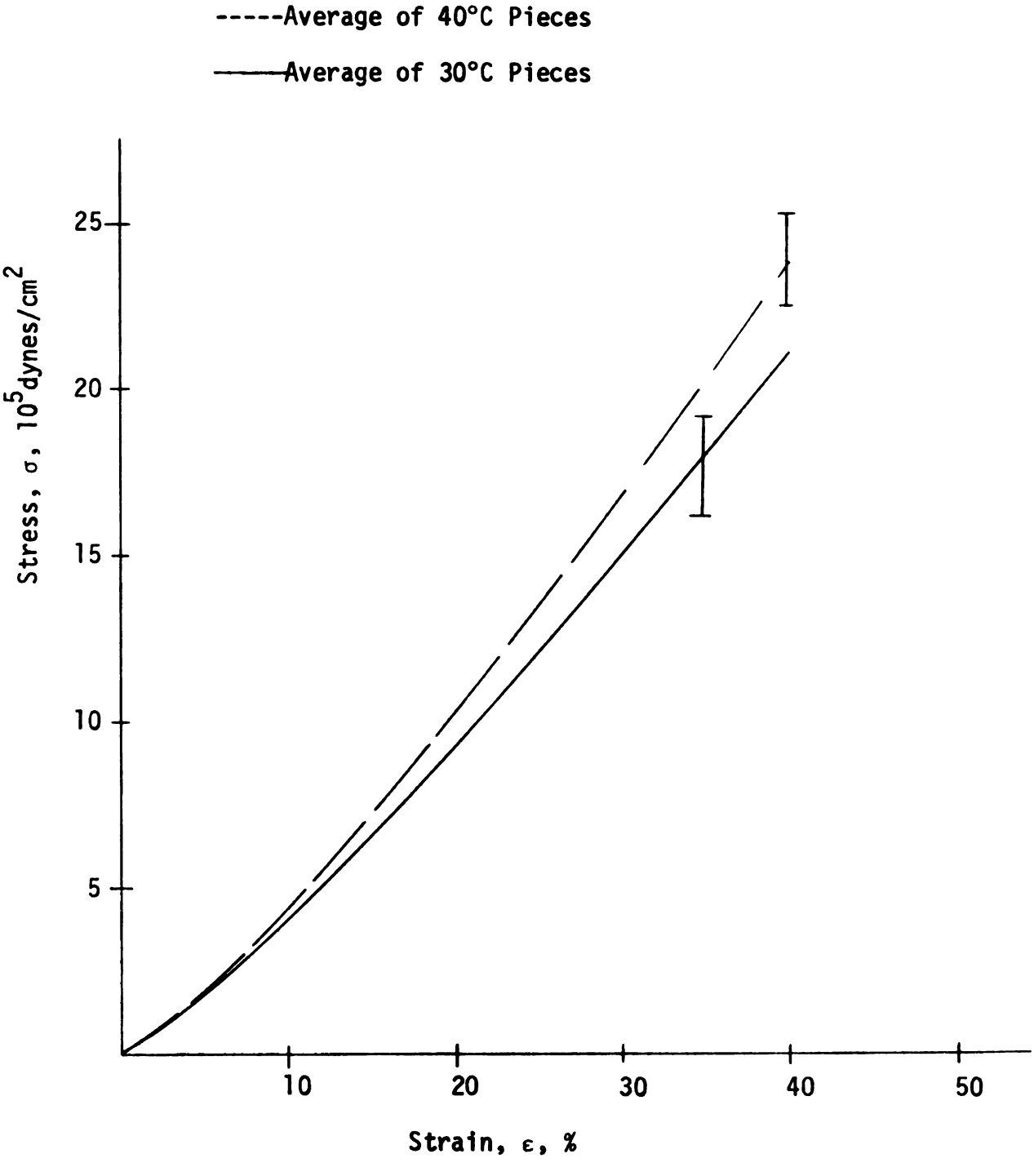

Fig. 6.1 Stress Strain Plot for Specimen 1.

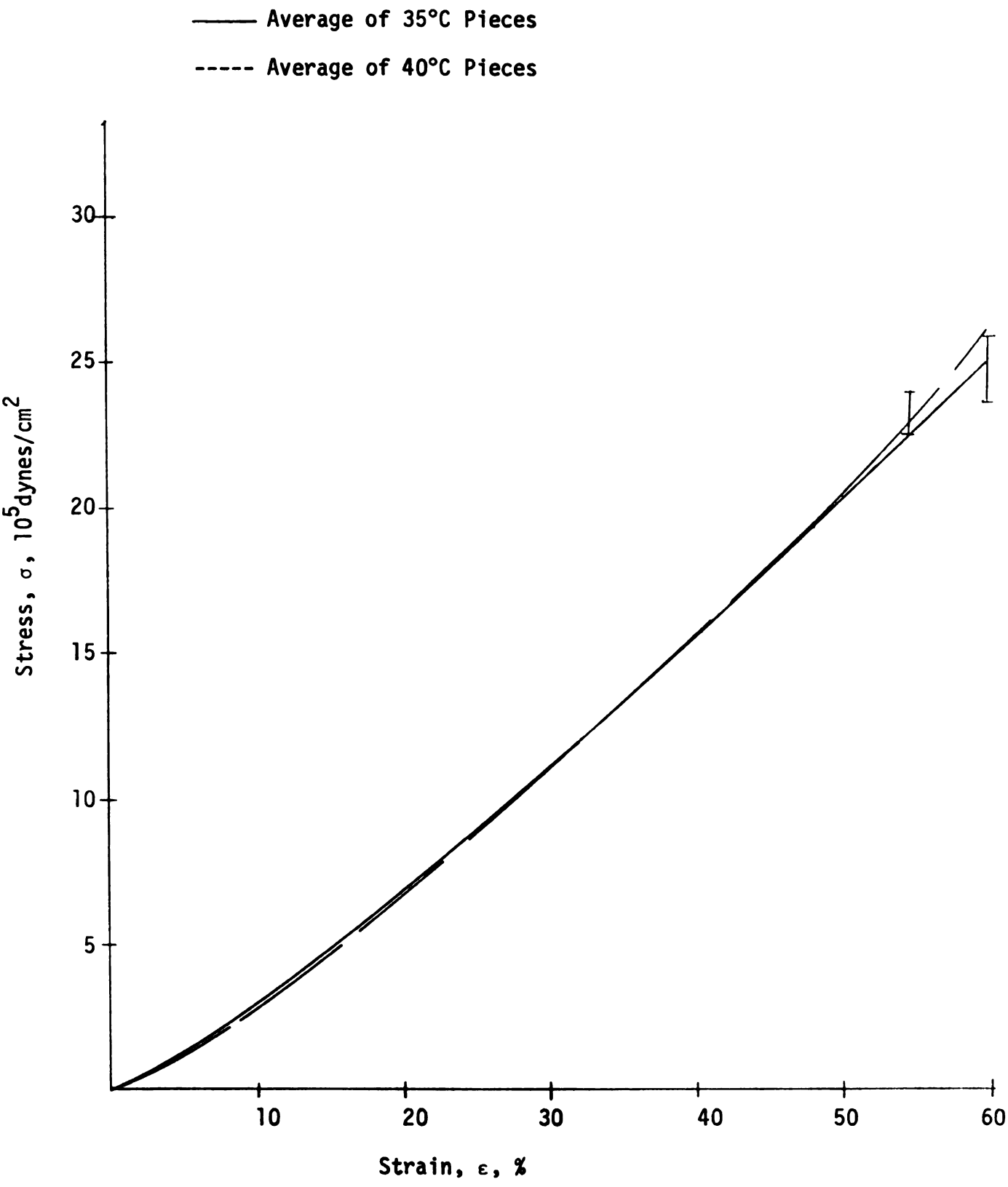

Fig. 6.2 Stress-Strain Plot for Specimen 2.

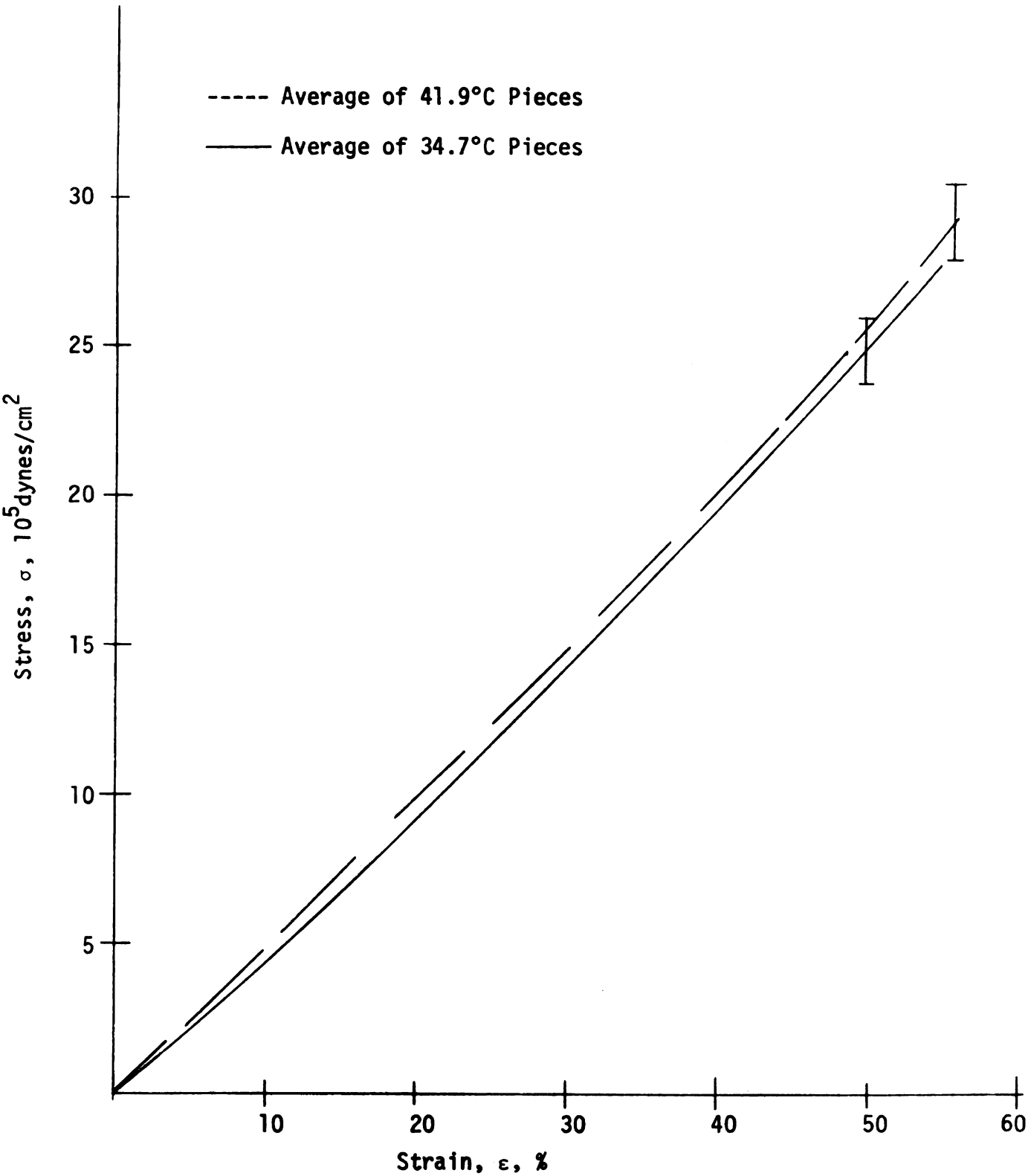

Fig. 6.3 Stress-Strain Plot for Specimen 3.

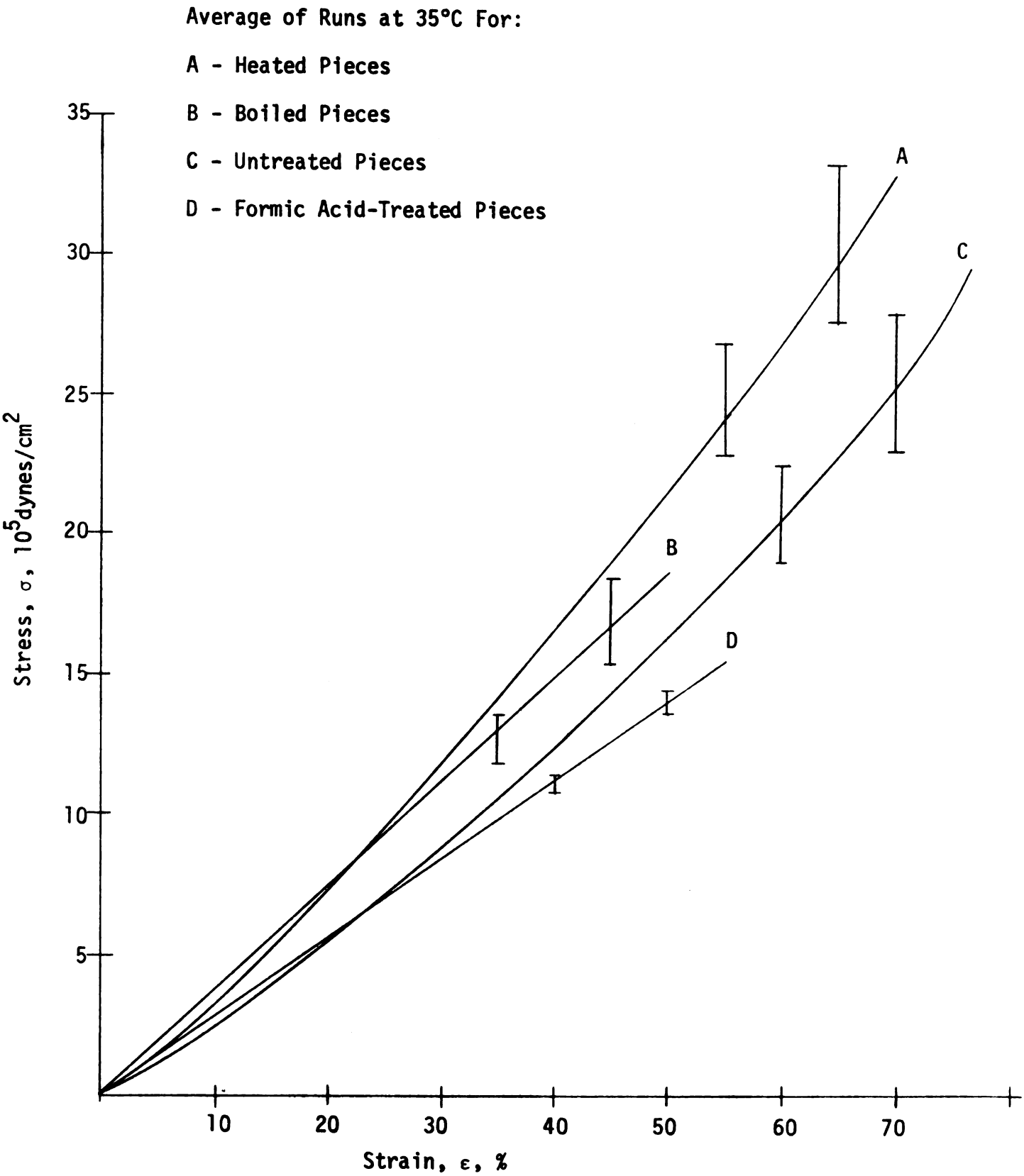

Fig. 6.4 Stress-Strain Plot for Specimen 4.

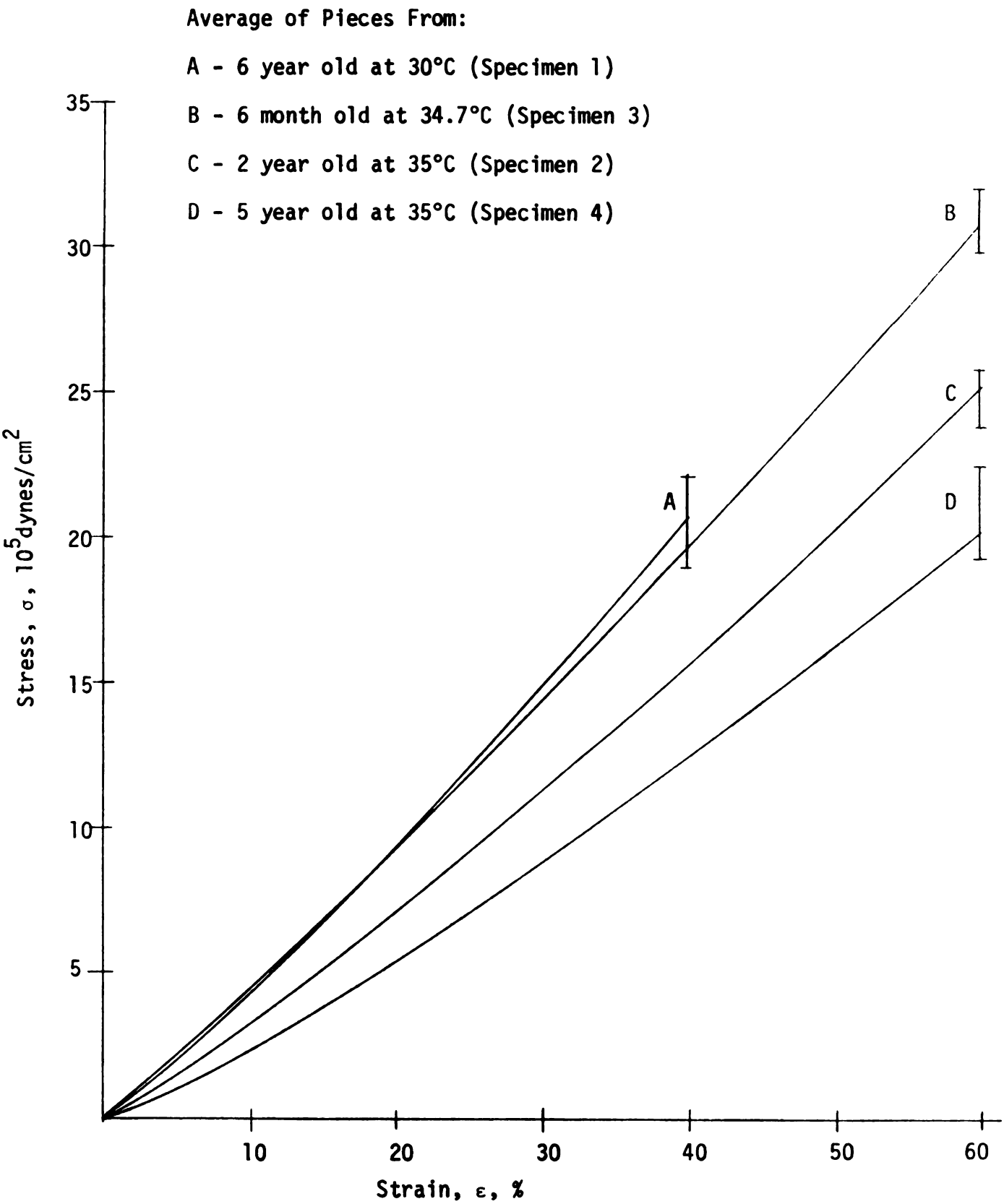

Fig. 6.5 Stress-Strain Plot of all Specimens .

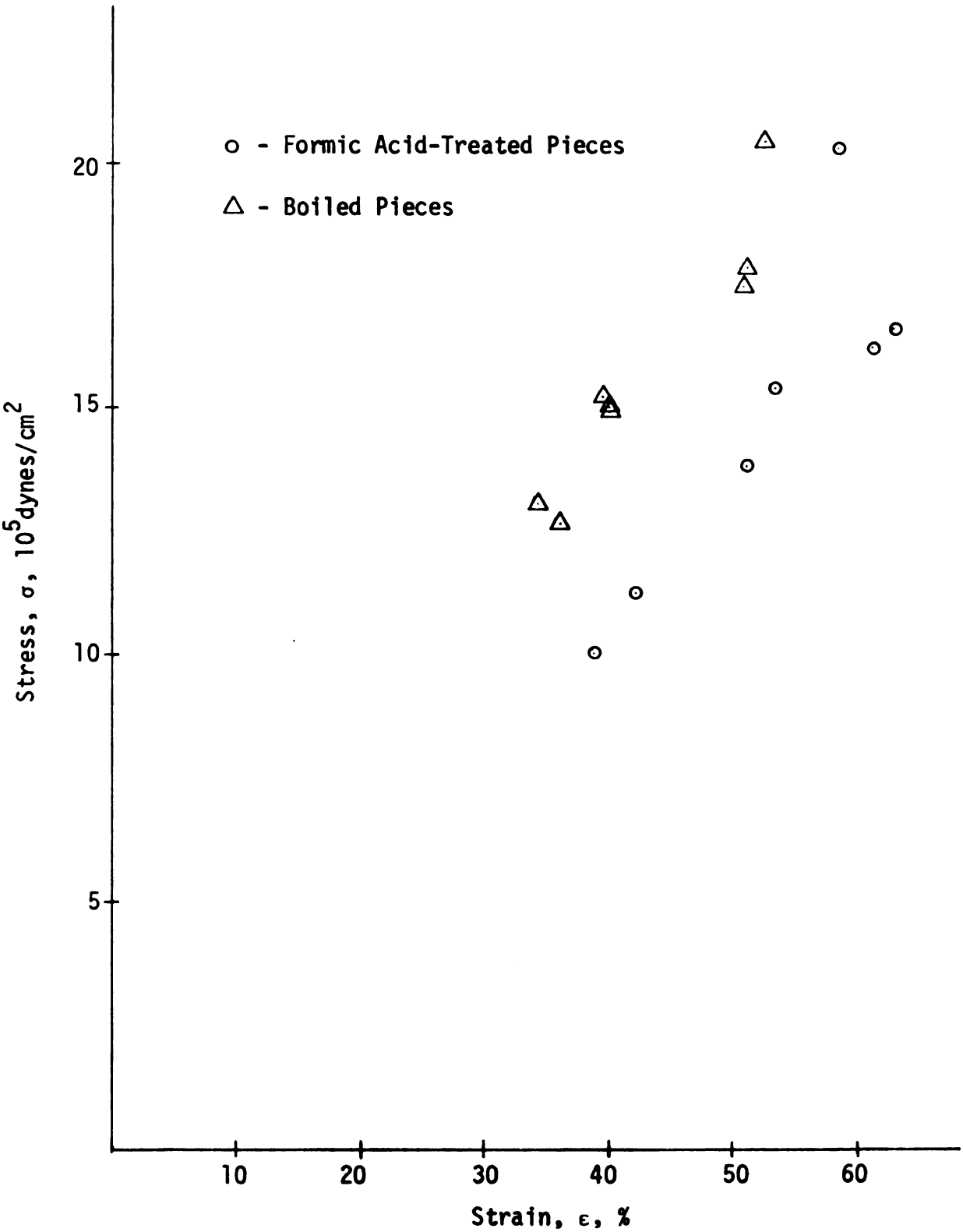

Fig. 6.6 Breakage Points of Pieces from Specimen 4 .

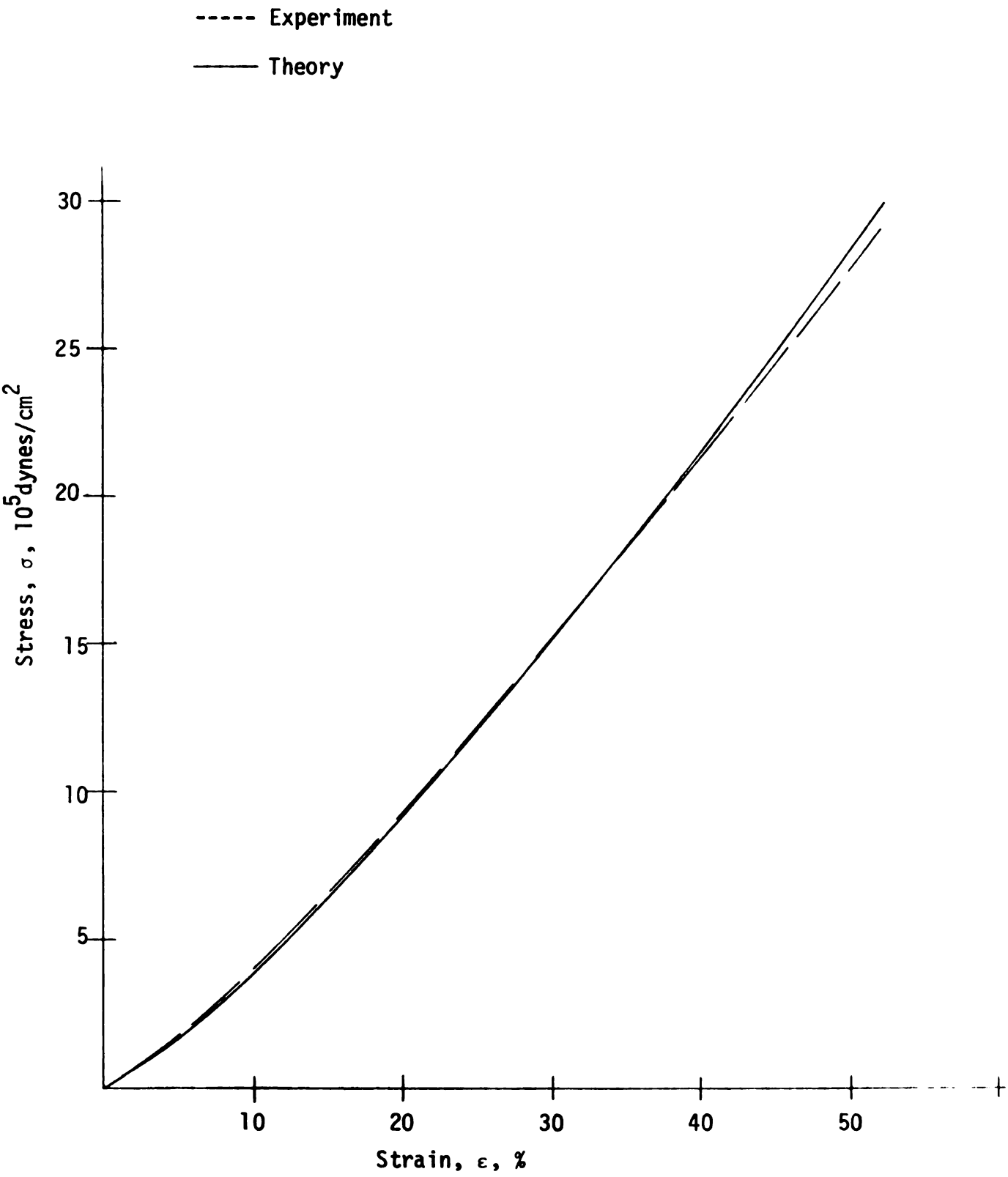

Fig. 6.7 Stress-Strain Plot for Specimen 1 at 43.4% Strain/min. and 30°C.

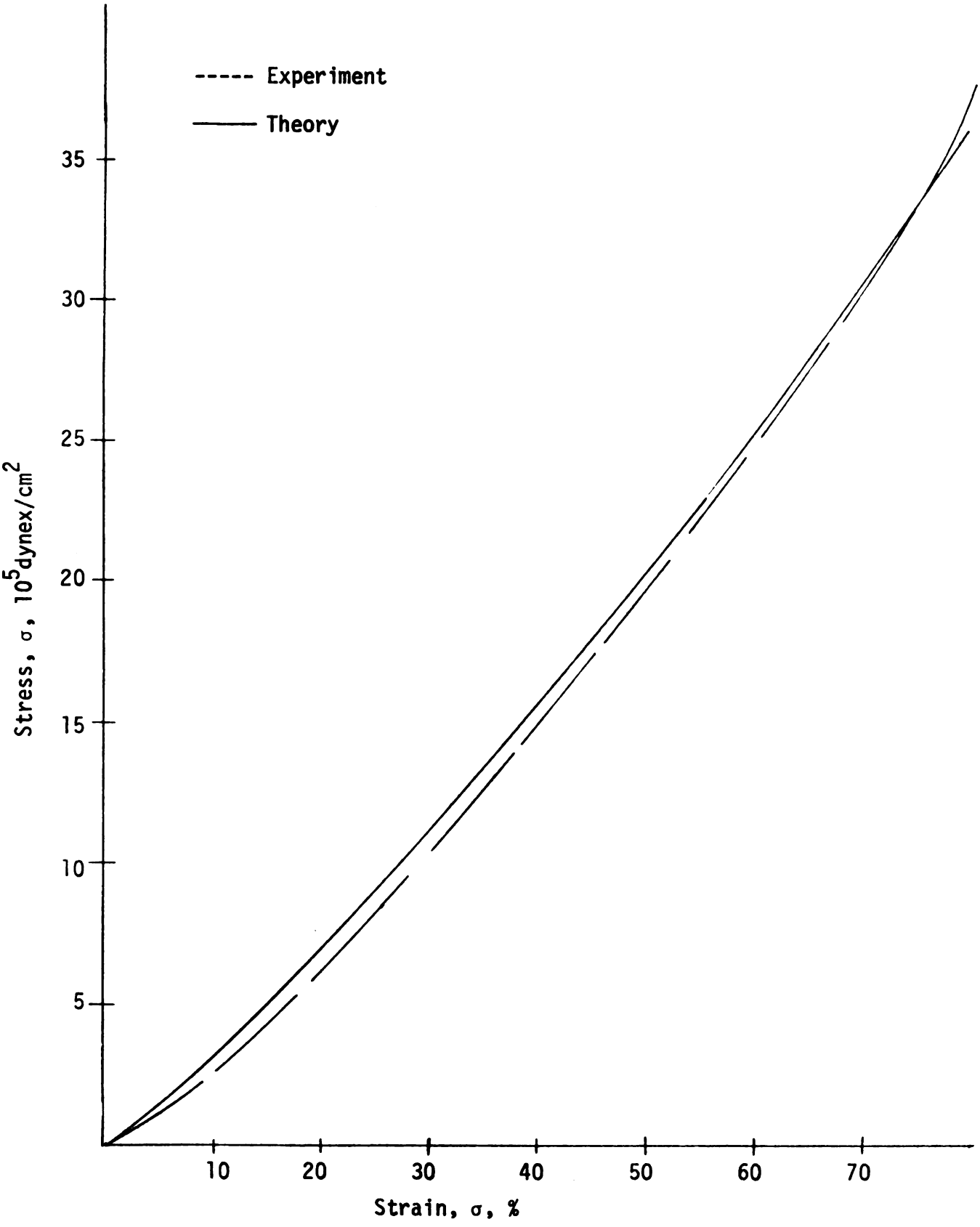

Fig. 6.8 Stress-Strain Plot for Specimen 2 at 28.4% Strain/min. and 35°C.

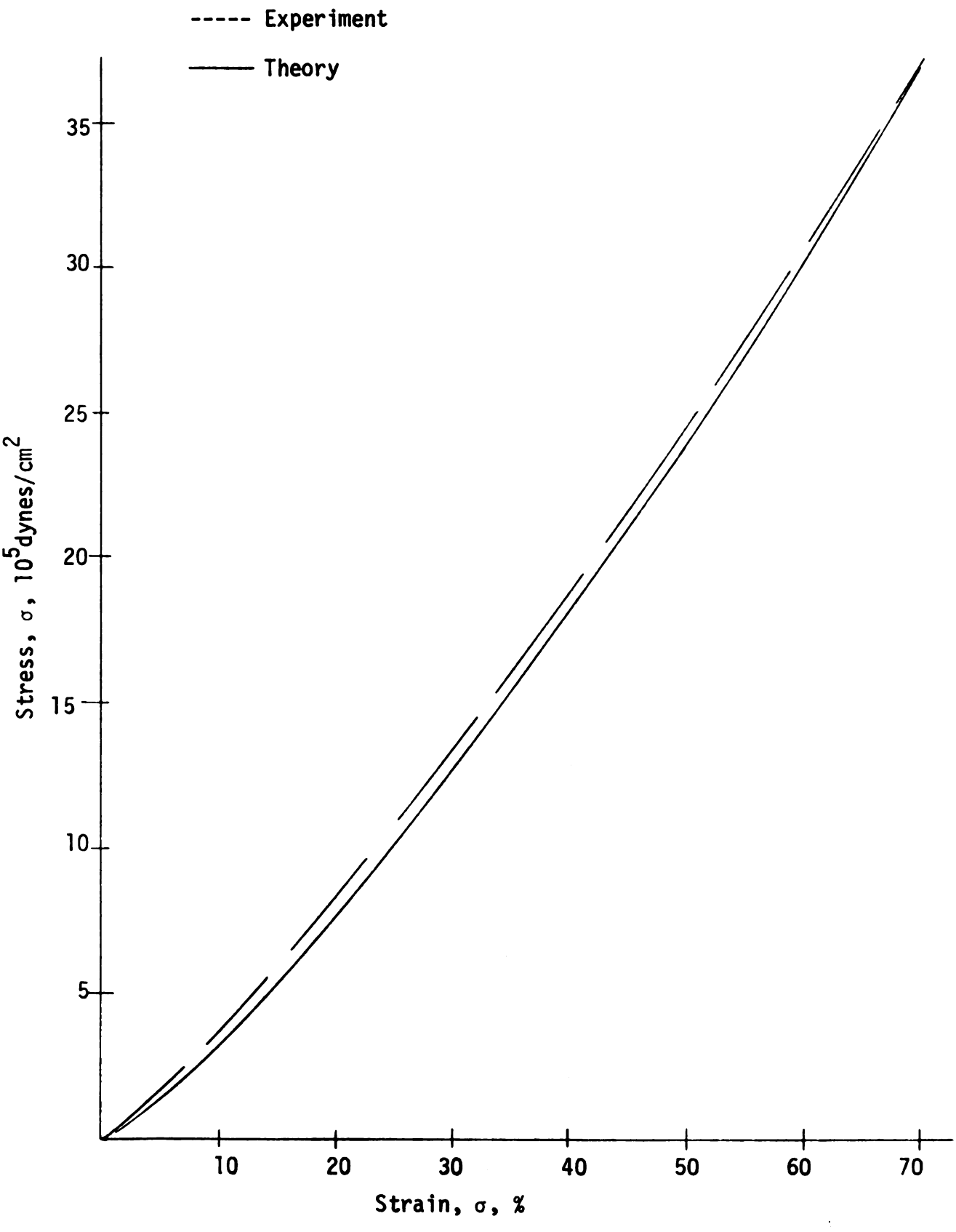

Fig. 6.9 Stress-Strain Plot for Specimen 2 at 73% Strain/min. and 40°C.

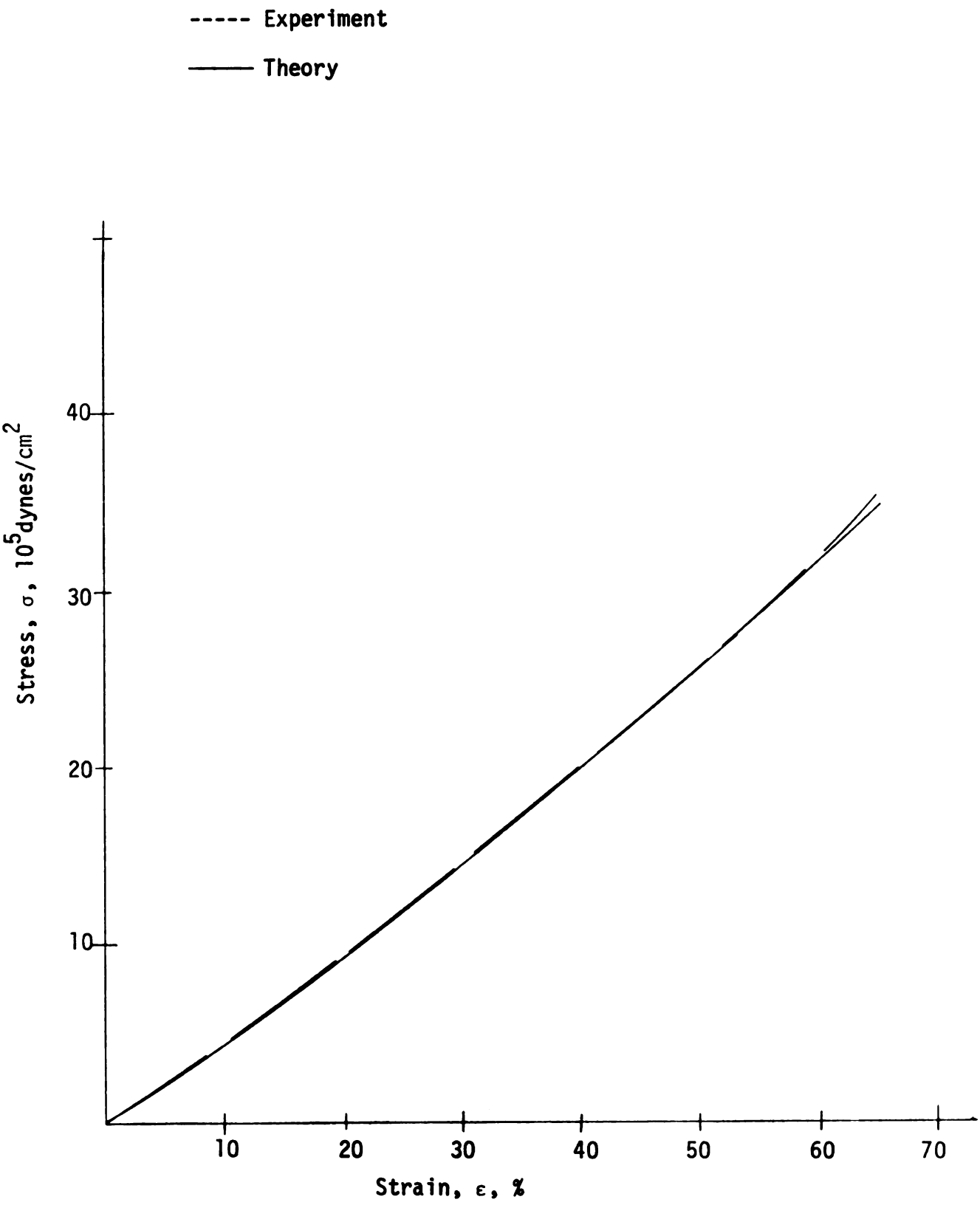

Fig. 6.10 Stress-Strain Plot for Specimen 3 at 46% Strain/min. and 34.7°C.

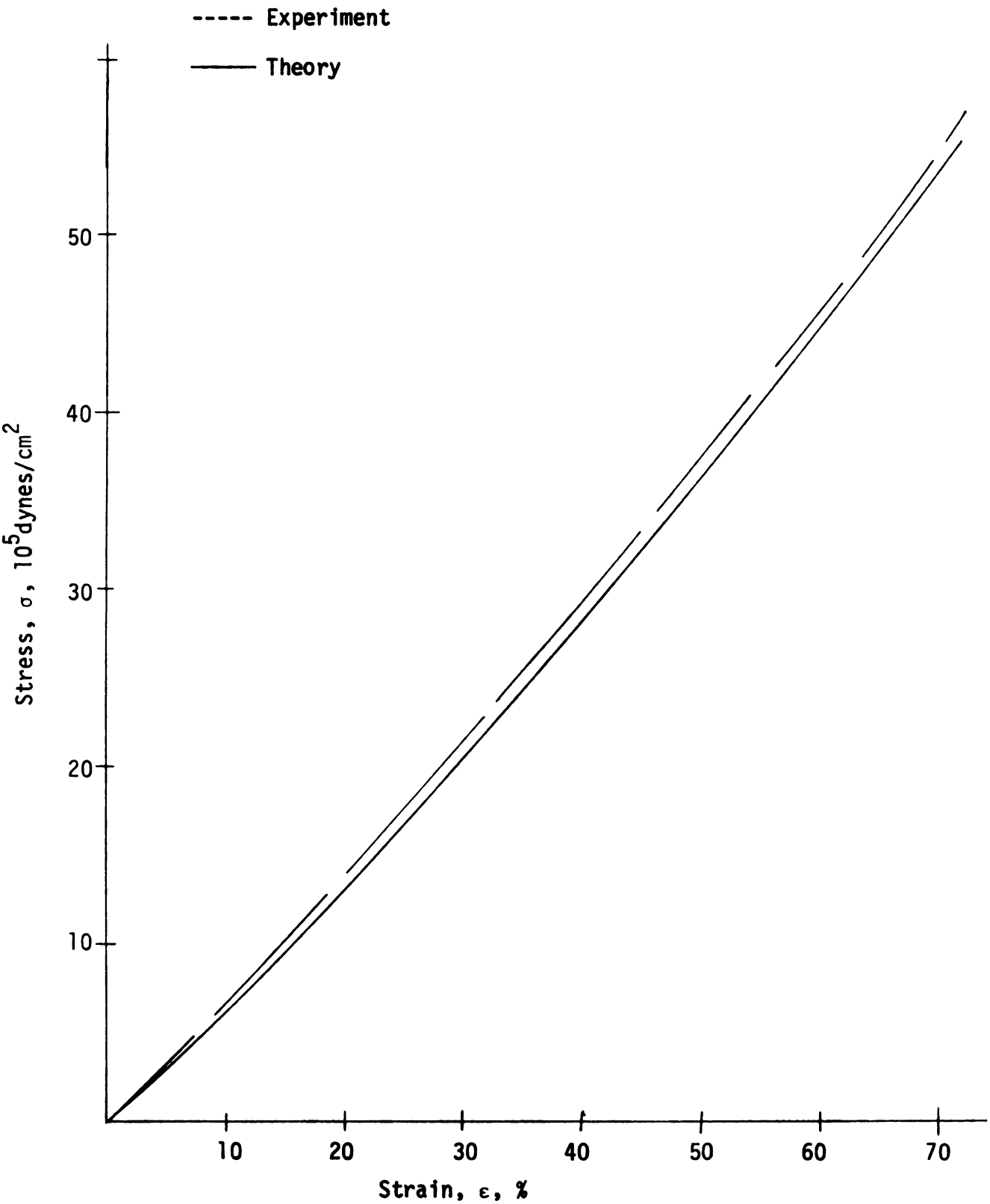

Fig. 6.11 Stress-Strain Plot for Specimen 3 at 59.3% Strain/min. and 41.9°C.

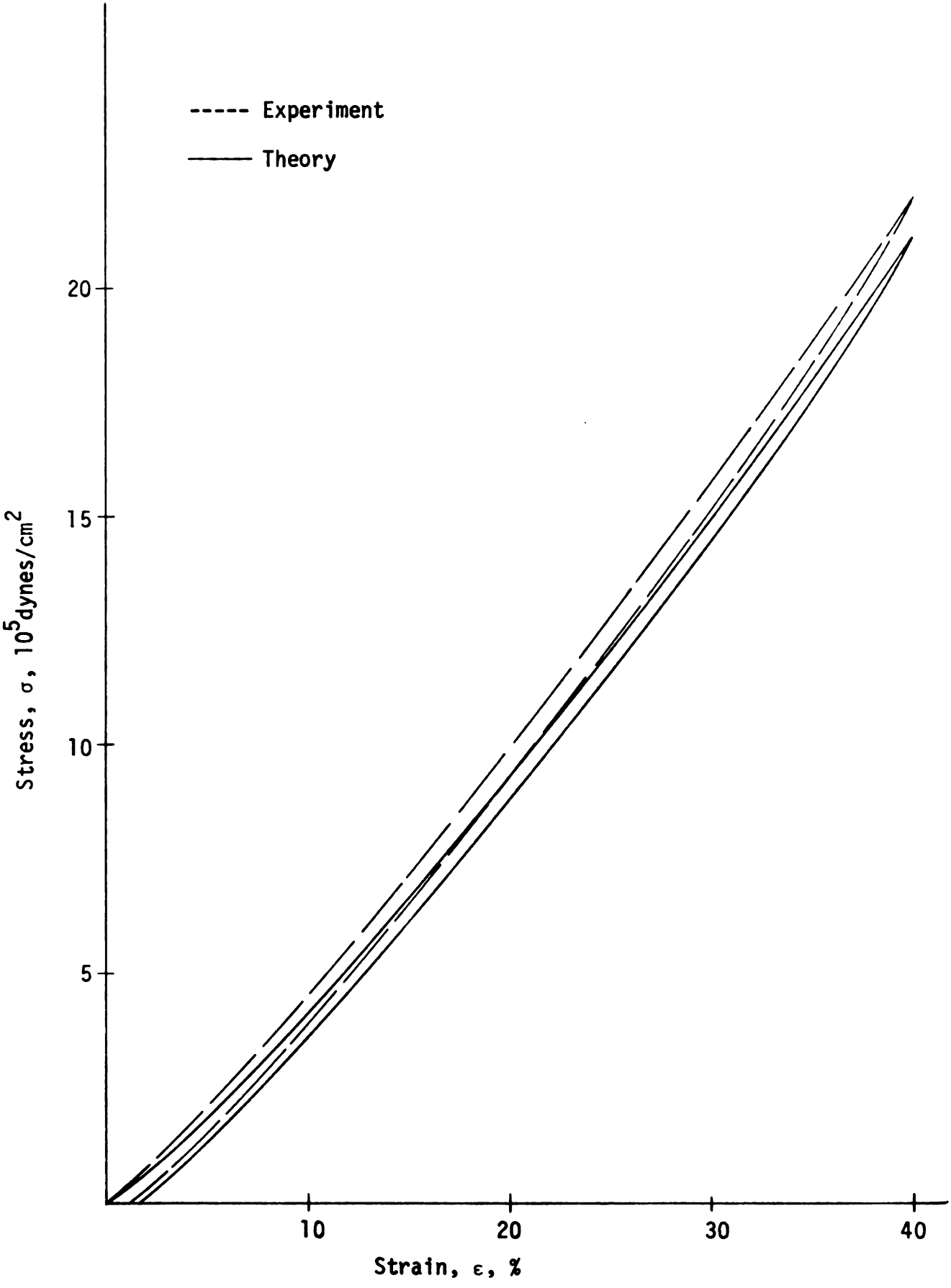

Fig. 6.12 Hysteresis Loop for Specimen 1 at 47.8% Strain/min., 40% Strain, and 30°C.

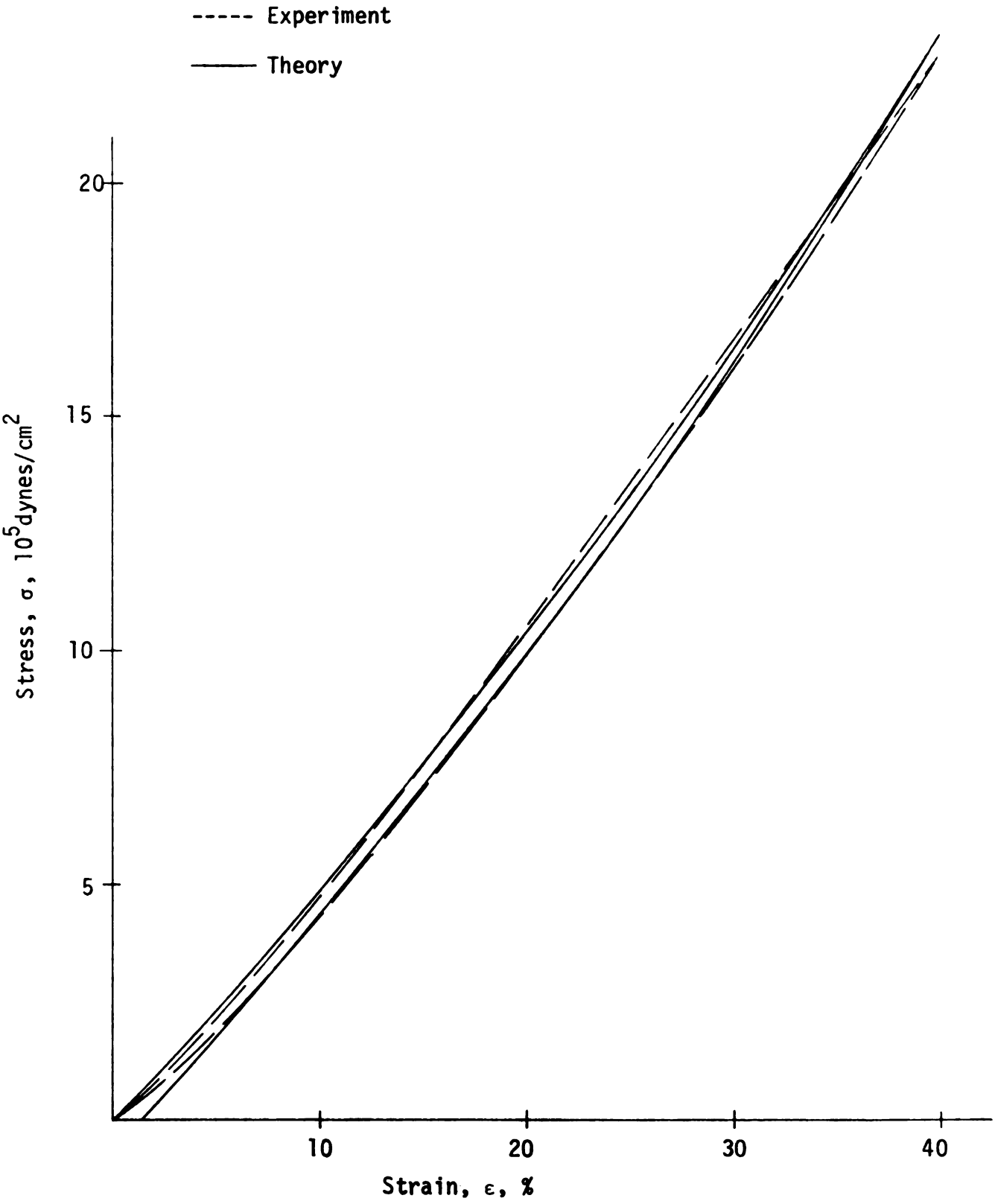

Fig. 6.13 Hysteresis Loop for Specimen 1 at 22.6% Strain/min., 40% Strain, and 40°C.

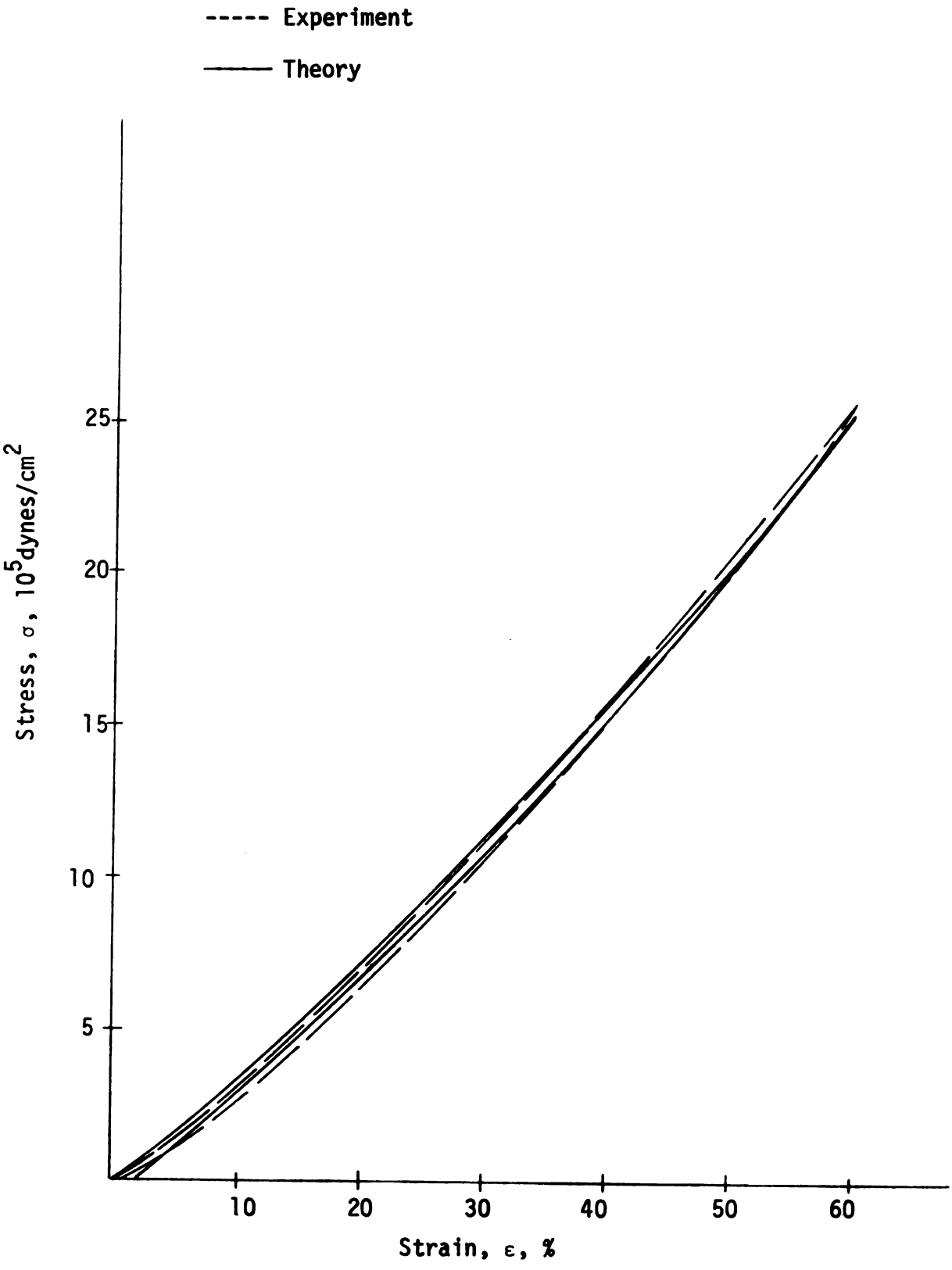

Fig. 6.14 Hysteresis Loop for Specimen 2 at 55.8% Strain/min., 60% Strain, and 35°C.

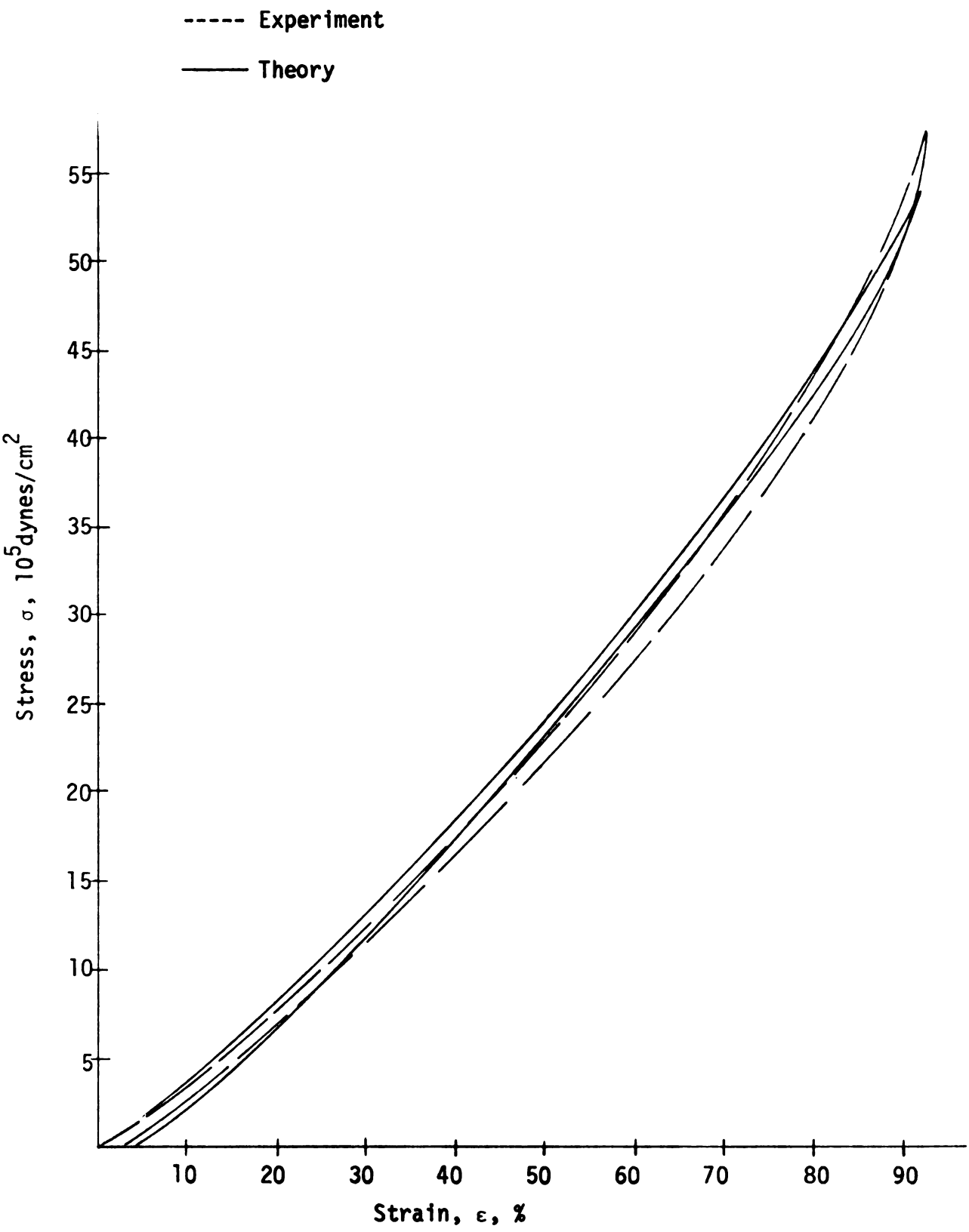

Fig. 6.15 Hysteresis Loop for Specimen 2 at 15.2% Strain/min., 92.4% Strain, and 40°C.

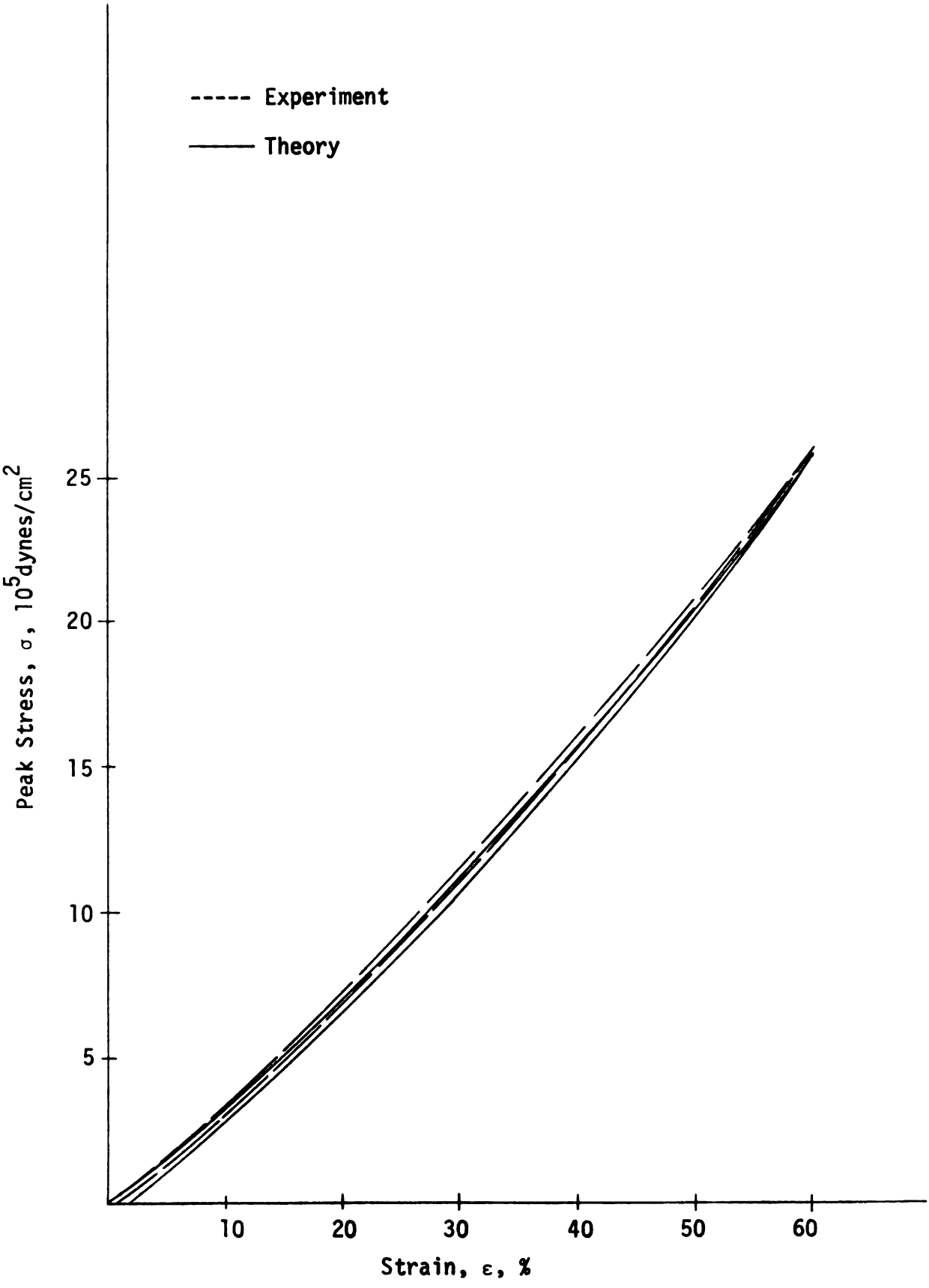

Fig. 6.16 Hysteresis Loop for Specimen 2 at 60% Strain/min., 60% Strain, and 40°C.

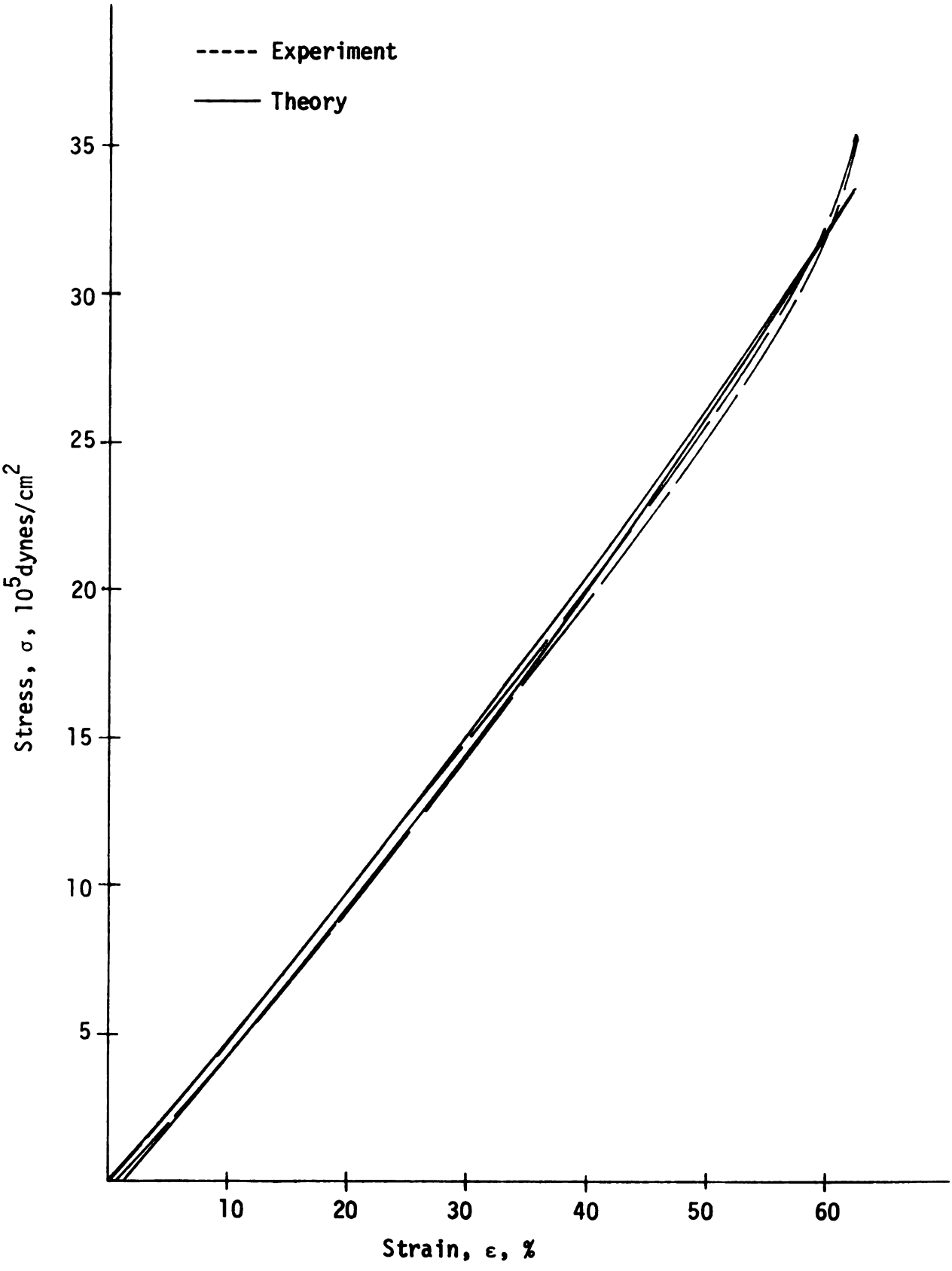

Fig. 6.17 Hysteresis Loop for Specimen 3 at 2.81% Strain/min., 62.6% Strain, and 41.9°C.

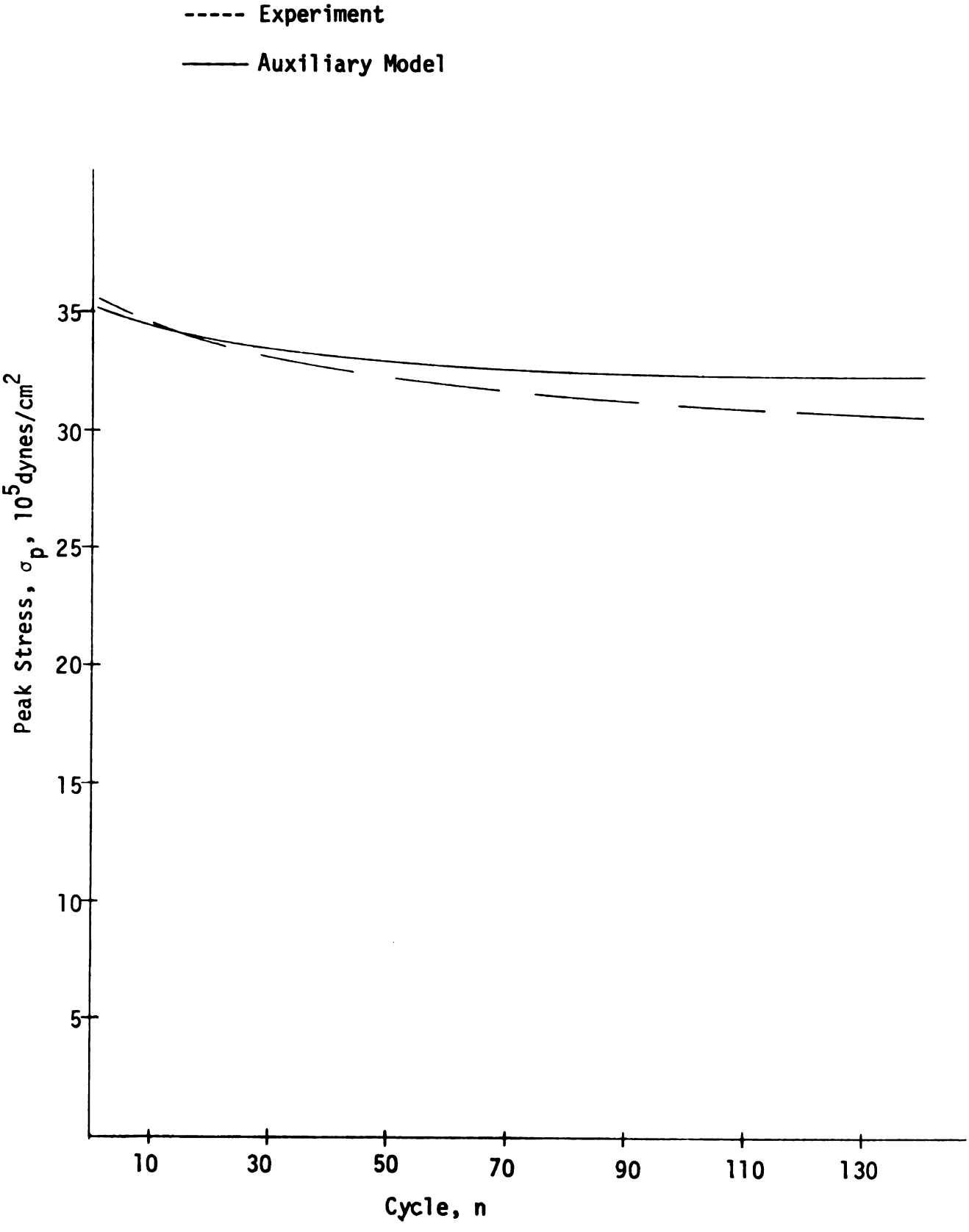

Fig. 6.18 Peak Stress-Cycle Number Plot for Specimen 2 at 49.6 Rad./min., 90% Strain, and 34.9°C.

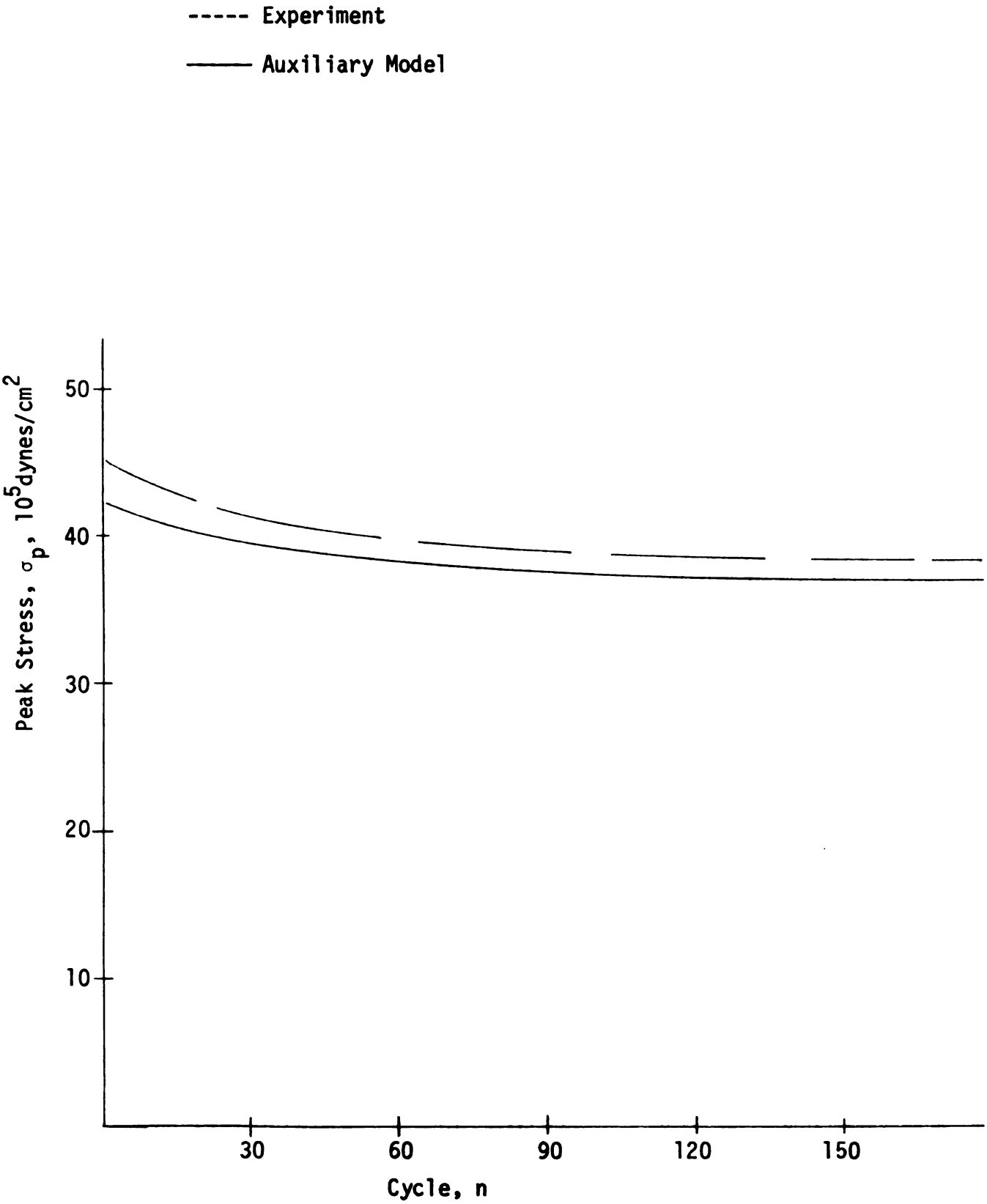

Fig. 6.19 Peak Stress-Cycle Number Plot for Specimen 2 at 66.2 Rad./min., 90% Strain, and 34.9°C.

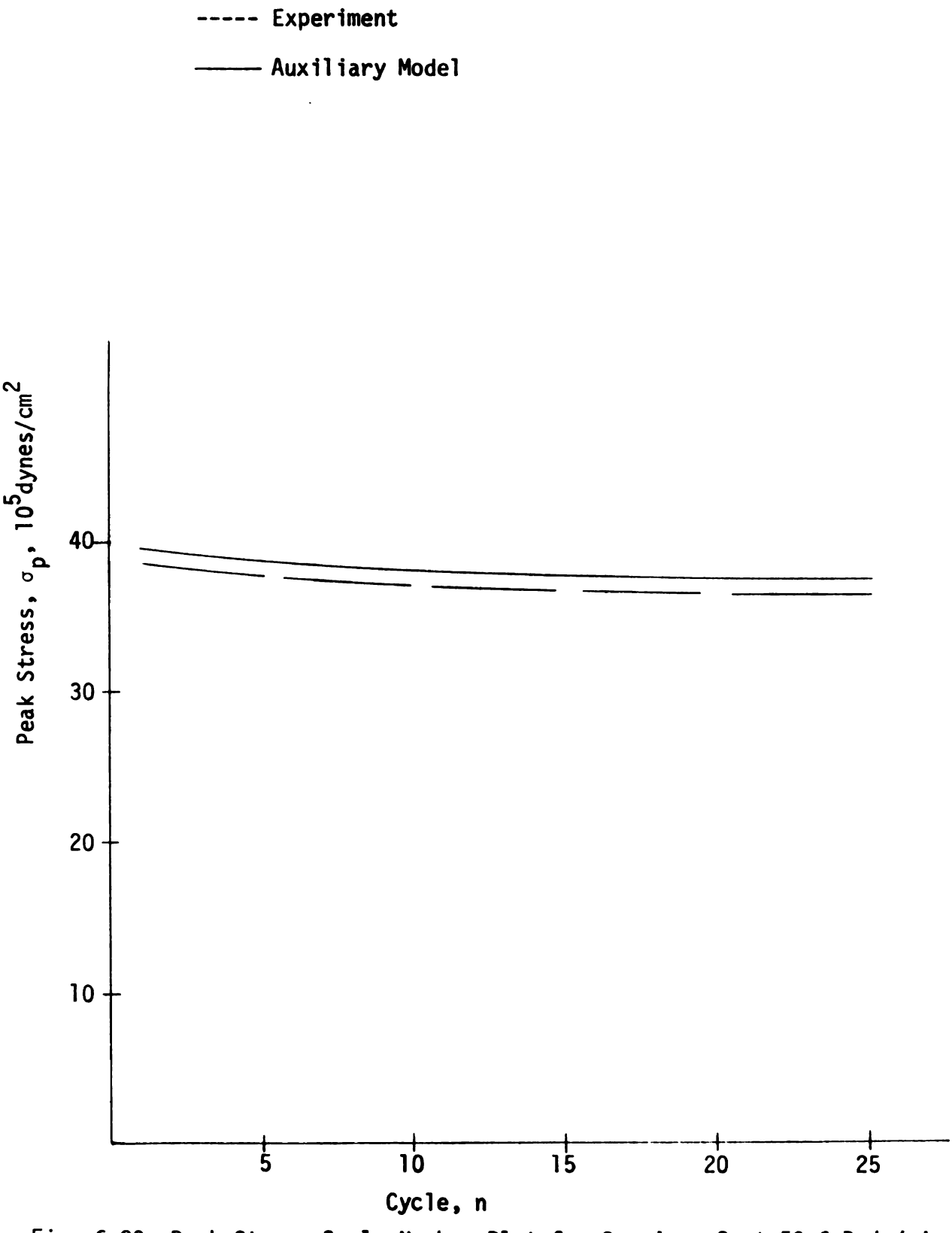

Fig. 6.20 Peak Stress-Cycle Number Plot for Specimen 2 at 50.6 Rad./min., 82.4% Strain, and 40.9°C.

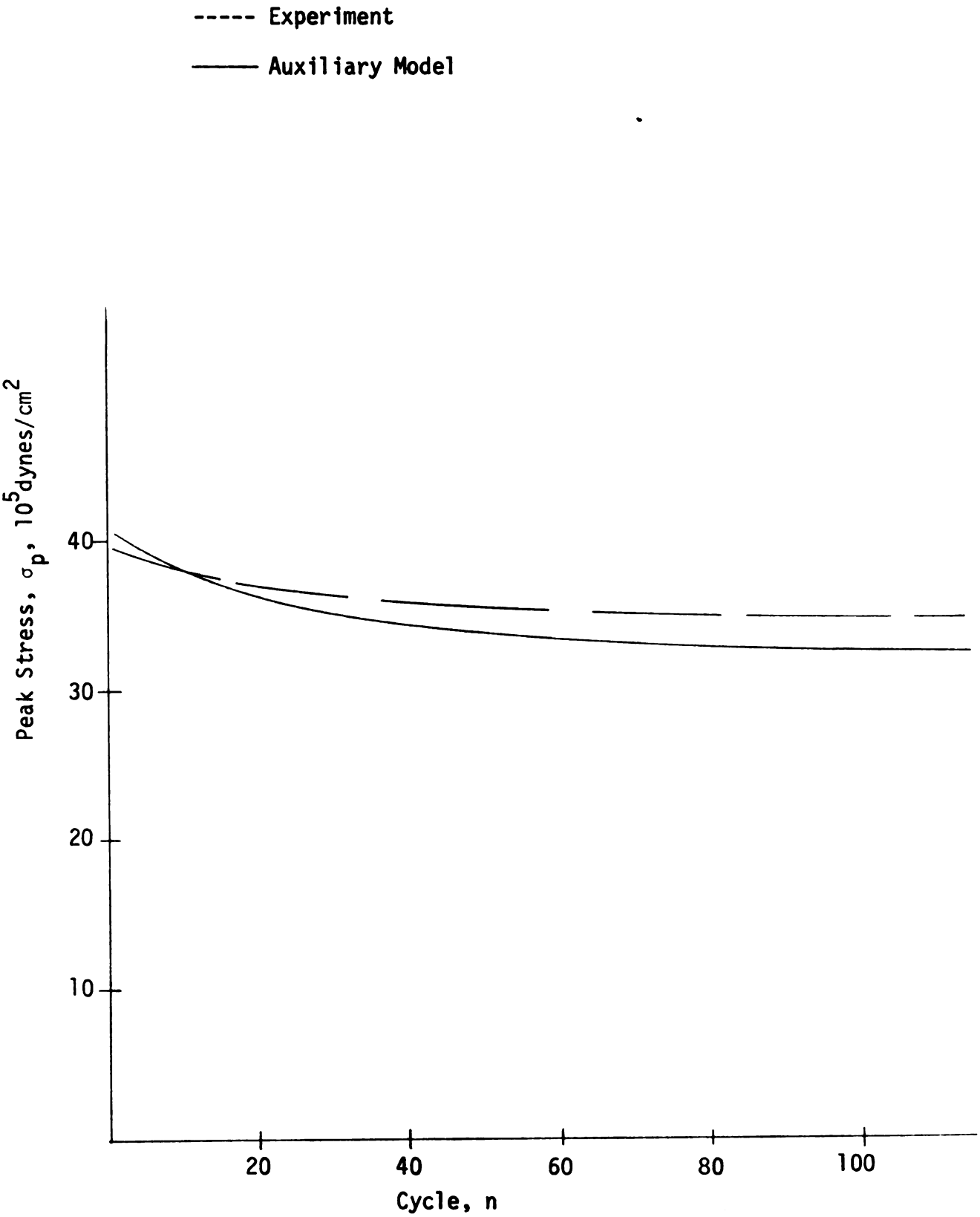

Fig. 6.21 Peak Stress-Cycle Number Plot for Specimen 3 at 77.8 Rad./min., 74.0% Strain, and 40°C.

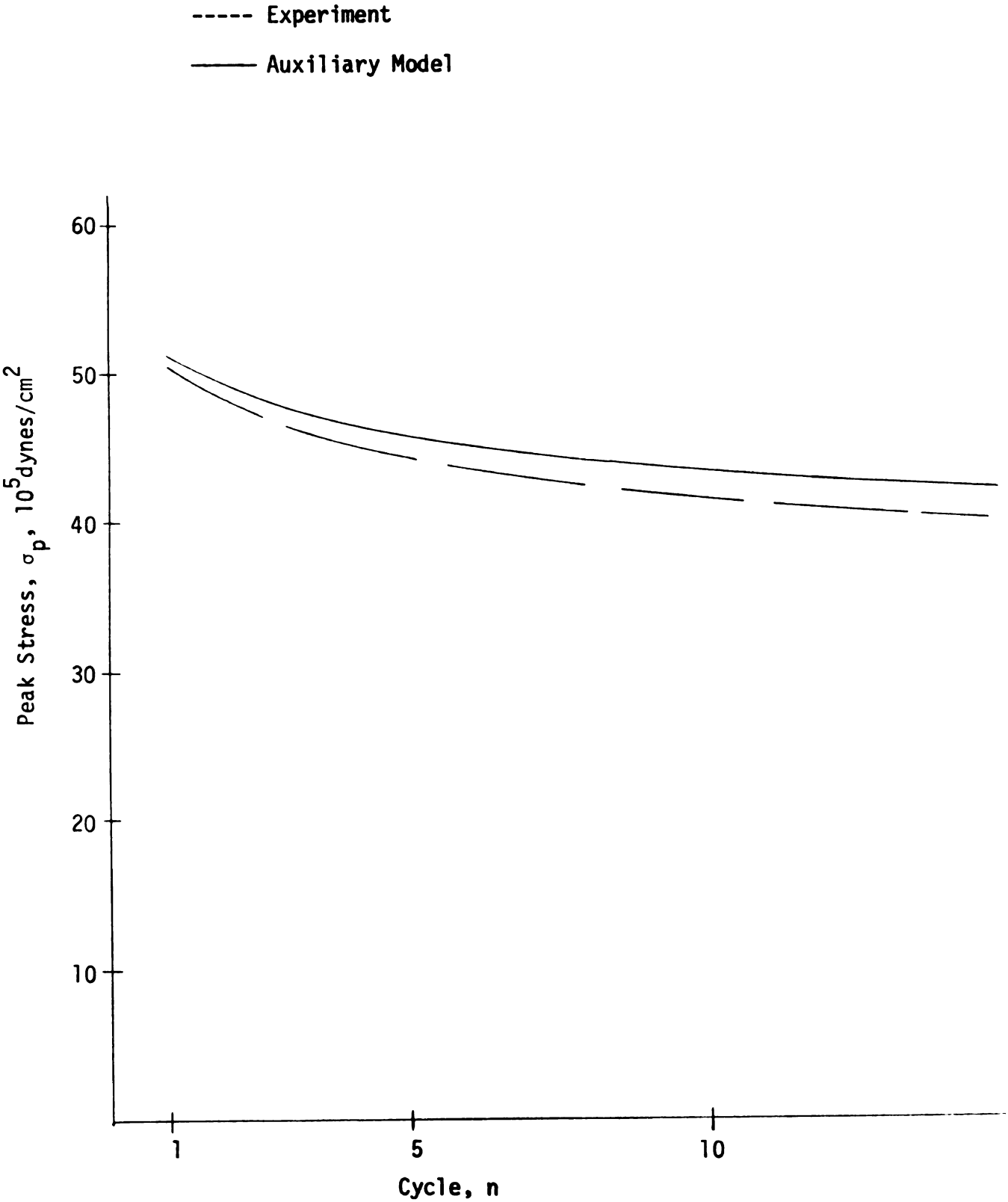

Fig. 6.22 Peak Stress-Cycle Number Plot for Specimen 3 at 76.2 Rad./min., 90.1% Strain, and 34.7°C.

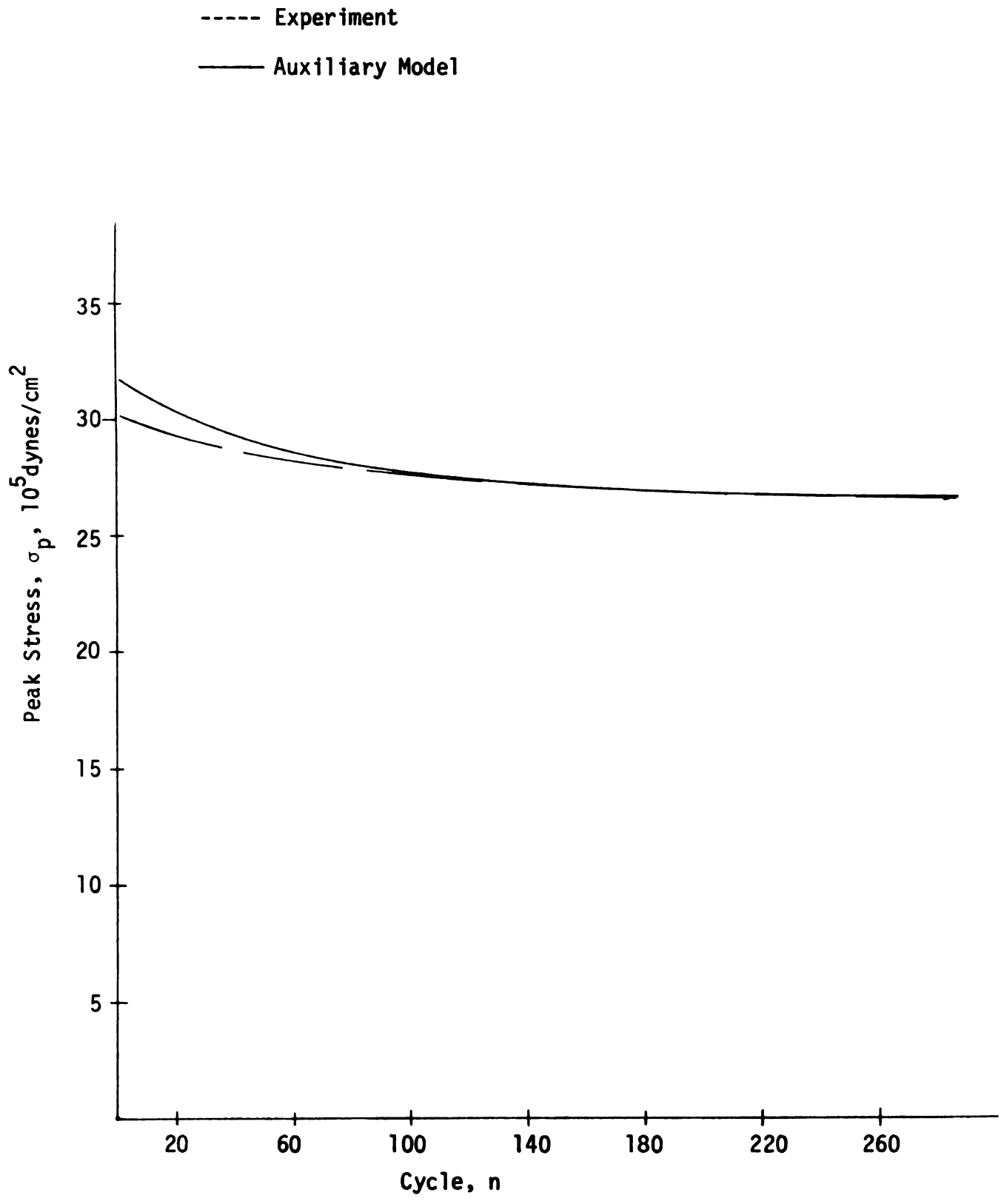

Fig. 6.23 Peak Stress-Cycle Number Plot for Specimen 3 at 76.6 Rad./min., 60% Strain, and 34.7°C.

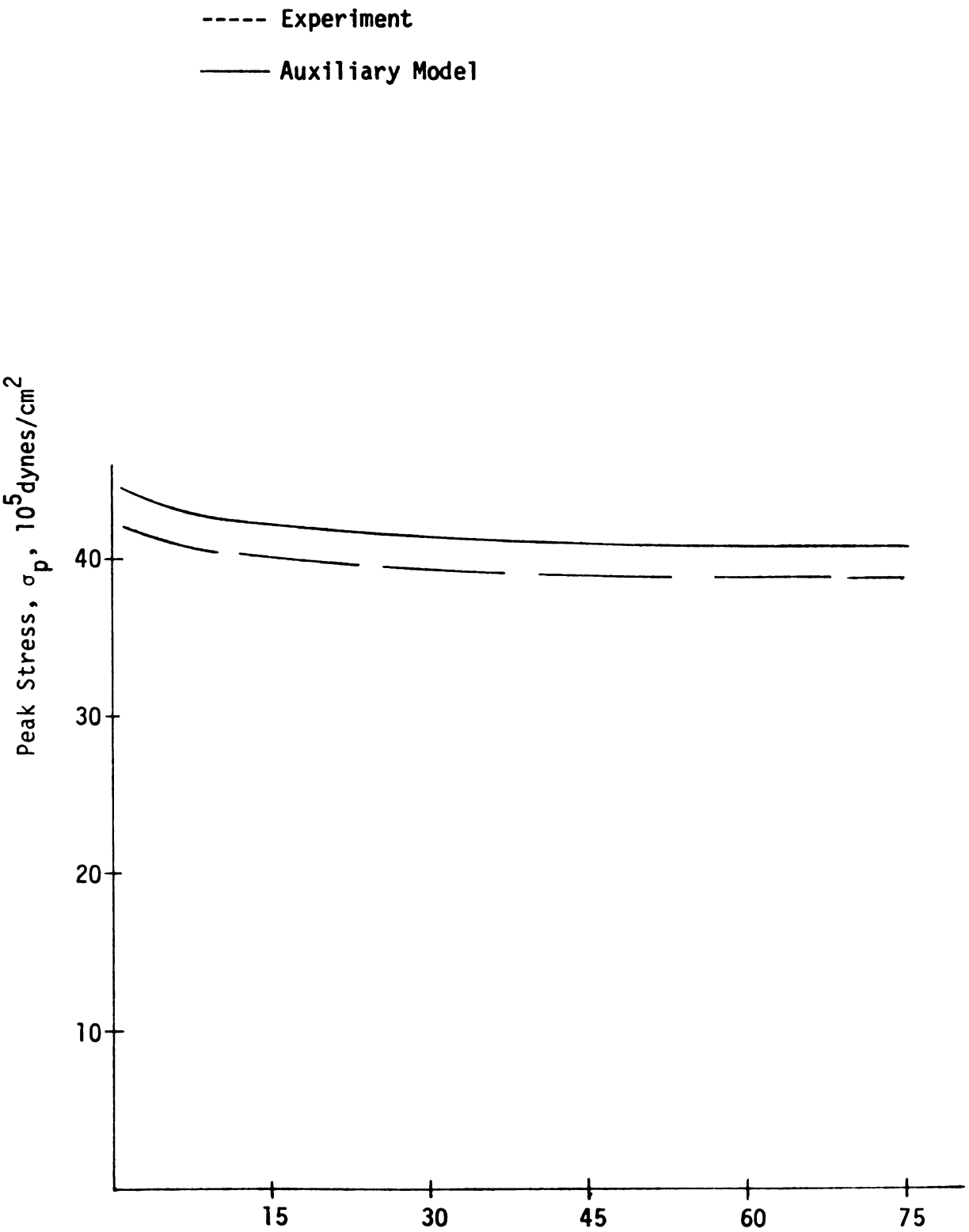

Fig. 6.24 Peak Stress-Cycle Number Plot for Specimen 3 at 66.1 Rad./min., 89.5% Strain, and 40.9°C.

6.2 Histologic Interpretation

Three specimens were tested in order to determine certain parameter constants and to illustrate the validity of the hereditary integral in using these constants to predict the response of ligamentum nuchae test pieces to other loadings. Experiments with Specimen 4 were designed to achieve a different objective. In Specimen 4, the same parameter constants were determined but no indication of their validity was attempted. Experiments on Specimen 4 were designed to determine the variations in the parameter constants as effected by chemical treatments which alter the elastic-collagen fiber balance in the native ligamentum nuchae test pieces. Only stress relaxation tests were conducted on this final specimen.

The parameters C, D, and μ for the four types of pieces run on Specimen 4 are listed in Tables 4 and 5. Graphical portrayal of these results is displayed in Figures 6.4 and 6.6. The radical difference in the mechanical properties of the four types of tests pieces suggests that a histological analysis might offer some insight into the interrelationship of components in the composite ligamentum nuchae. In order to facilitate such an analysis, three types of specimen sections were stained in three different ways as has been described.

Gomori's stain was the best of the three stains in differentiating the components of the ligamentum nuchae. Light microscopy of 100 magnification reveals many deep purple cell nuclei dispersed between fiber components. It is assumed that the cells are fibroblasts. Elastic fibers from the ligamentum nuchae were stained a rich red by Gomori's stain. They occur in compact bundles which have a generally parallel arrangement with one another. These long fiber bundles show

a slight waviness as they traverse the longitudinal dimension of the tissue. The collagen fibers from the ligamentum nuchae are stained green by Gomori's stain. A loose and rather irregular arrangement of collagen fibers is discernible in untreated sections. In untreated sections, individual collagen fibers may be seen clearly to display a large amount of waviness so as to simulate loops. These loops were so large that if individual collagen fiber networks could be separated from the ligamentum nuchae and stretched until they were straight, the straightened fiber network would probably be half again as long as the strip from which that fiber network was taken. This latter phenomenon seems to lend credence to the suggestion made by others (14,21) that collagen fibers contribute to the stress-strain character of tensile specimens only at some finite strain level estimated to be from 50% to 70%. However, the experimental and theoretical results of this work seem to imply that the entrance of the tensile characteristics of the collagen fiber into the stress-strain curve at a non-zero strain level does not break the continuity or smoothness of the curve. Neither does the tensile character of collagen preclude the curve fit of "elastic" stress at low strain from applying to high strains as well. This latter fact seems to confirm the assertion made by Wood that collagen from the ligamentum nuchae is of a highly extensible nature.

The examination of a cross-section of untreated ligamentum nuchae section showed that many groups of collagen fibers surrounded all elastic fiber bundles. By employing one of the most basic methods of stereology as described by Elias and Pauly (48) and Elias et al (49) it was possible to estimate the volume ratio of elastic to collagen fibers.

The grid point method employed resulted in the approximation that collagen fibers occupy 30.4% and elastic fibers 67.8% of the volume of the specimen under consideration (Appendix C).

Large specimen sections and test pieces which were boiled for 7.5 hours were also investigated microscopically. The elastic fiber bundles from boiled sections seemed to look the same as those of untreated sections. Cells were still present in boiled sections. However, the collagen fiber networks so evident in untreated sections were dispersed. Traces of collagen fibers were attached to the elastic fiber bundles but no collagen was observed in the gaps between fiber bundles. Cross-sections of boiled strips stained with Verhoeff's stain showed large black areas (elastic fiber bundles) surrounded closely by a reddish tint (collagen fibers) with empty spaces in between the elastic fiber bundles where collagen fibers had been observed in untreated sections.

Stained sections of formic acid-treated strips revealed no apparent alteration in the elastic fiber bundles, no cells, and almost no collagen. Cross-sections of formic acid-treated sections revealed empty gaps where collagen had been but no reddish tint with Verhoeff's stain as was observed in boiled sections. The gaps were much larger than those which collagen fibers occupied in the native ligament. This seems to imply that collagen fibers are capable of binding elastic fiber bundles together laterally or that reticular fibers which bind these bundles are dispersed by the same treatment which disperses collagen fibers.

Observation of large boiled ligamentum nuchae sections with the naked eye showed noticeable differences from untreated sections.

Boiled sections were white in color while native sections were yellowish. Boiled sections were very dry and compact and resisted lateral loading much more than native sections. Formic acid-treated sections were a rich gold in color and were very moist and soft. These gross physical properties were unaltered by six months of formalin fixation. The apparent compactness of boiled specimens may have been due to the hydrothermal contraction of collagen fibers or perhaps some hydrothermal effect on elastic fibers. Specimens heated for 90 minutes at 58°C showed this same conpactness. It is suggested that this compactness is only apparent because stereological studies (Appendix C) indicate that boiled specimens are no more compact than untreated ones and boiled specimens do have gaps in between elastic fiber bundles.

An examination of Table 4 and Figures 6.4 and 6.6 reveals that the untreated test pieces from Specimen 4 yielded the stress-strain curve of the lowest modulus of the four specimens. This average stress-strain curve showed the greatest curvature or the lowest C/D ratio of the four specimens. Heated pieces yielded a curve of similar form but of much higher modulus than that of the untreated pieces. The large increase in modulus of heated pieces is probably attributable to the thermal contraction of collagen fibers and to some degree to the increase in modulus of elastic fibers with temperature elevation. If this is true, thermal changes must be irreversible to a large extent since all testing was done in the same testing environment. The loading curves for formic acid-treated and boiled pieces were linear. Many pieces from both these latter types were broken at various strain levels as indicated in Figure 6.6. No untreated or heated piece was broken in any of the four specimens. Formic acid-treated pieces were

shown histologically to contain negligible amounts of collagen fibers and several stress relaxation experiments on such pieces revealed no stress relaxation at all. Boiled pieces showed traces of collagen fibers histologically and stress relaxation experiments showed very slight relaxation in two cases. Untreated and heated pieces showed considerable amounts of collagen and stress relaxation tests showed relaxation in both types of pieces at strains greater than 40%.

The above considerations imply that collagen fibers are responsible for the nonlinearity in the ligamentum nuchae stress-strain curve. The nonlinearity may be inherent in the stress-strain character of the collagen fibers themselves or may result from the interaction of collagen and elastic fibers structurally during deformation. It may be seen that the stress-strain curve of test pieces with no collagen fiber networks (boiled and formic acid-treated) were linear over the entire strain range. The curves of test pieces with collagen fiber networks were nonlinear over the entire strain range. This implies a collagen fiber effect in the stress-strain curve of the ligamentum nuchae even at low strain. Table 4 and histologic examinations of the three types of tissue imply that collagen fibers are primarily responsible for the time dependent or dynamic effects of the ligamentum nuchae as evidenced by stress relaxation. The large difference in moduli between the boiled and formic acid-treated pieces indicates that elastic fibers respond strongly to temperature treatment and that such thermal effects are largely irreversible.

Fig. 6.25 Formic Acid-Treated Longitudinal Section.
The elastic fiber bundles are stained black with Verhoeff's stain.
The very few collagen fibers are stained lightly (x 100).

Fig. 6.26 Untreated Longitudinal Section.
Elastic fiber bundles are stained black and meshes of collagen fibers appear gray with Verhoeff's stain. Just to the right of center an artery traverses the section. Collagen fibers are very dense around arteries and tissue cells (x 100).

Fig. 6.27 Untreated Longitudinal Section With **Gomori's Stain.** Very little color contrast between elastic fiber bundles and collagen fibers is shown here. Oval cell nuclei are dark. Irregular meshes of collagen fibers around tissue cells break up the otherwise longitudinal orientation of the tissue section (x 100).

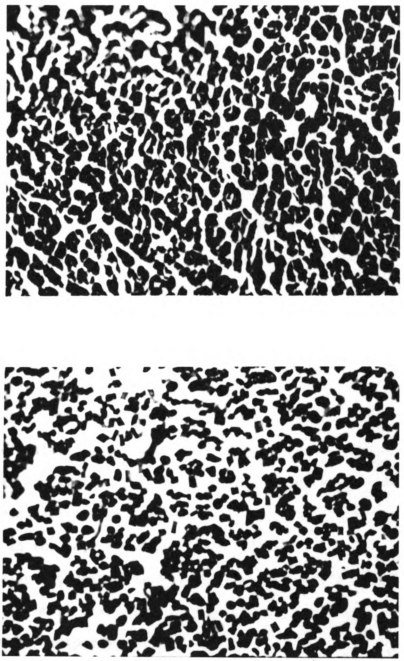

Fig. 6.28 Transverse Section of Treated Specimens.
Top: A boiled section with Verhoeff's stain showing the ends of elastic fiber bundles as black. Bottom: Formic acid-treated section. Note that the boiled section is more dense with elastic fiber bundles (x 100).

VII. CONCLUSIONS

An attempt has been made to develop a uniaxial constitutive equation for elastic fibers. A "quasi-linear" viscoelasticity law based upon a suggestion by Y. C. Fung has been developed. An adaptation of Fung's relaxation function has been employed to define an average loading curve and a "modified" relaxation function analagous to Fung's "elastic" curve and "reduced" relaxation function. The average stress-strain curve is depicted as the sum of a linear and a squared term in strain as was suggested by H. R. Elden (46) in his studies on skin. The "modified" relaxation function differs from the "reduced" relaxation function in that it possesses strain dependence. The "modified" relaxation function is logarithmic in form and introduces no irregularities or discontinuities in the process of integration due to the zero argument of the logarithm.

The bovine ligamentum nuchae was the souce of elastic fibers because it is the most elastic fiber-dominant tissue known. Collagen fibers and other components of the ligamentum nuchae were removed to varying degrees by chemical treatment. Such an isolation of elastic fibers was designed to interpret the mechanical properties of the composite tissue in terms of its basic fibrous components and their interaction in the process of deformation. Verification of the structural composition of the untreated and treated ligamentum was achieved by the histologic methods of fixation, sectioning, staining,

and light microscopy.

Three basic tests were performed on ligamentum nuchae test pieces from four different animal specimens. Stress relaxation tests were conducted at various strain levels and strain rates on each specimen to determine three parameter constants believed to be characteristic of the material at a given temperature. Variations of these parameters with temperature was discussed. Parameter evaluations determined from relaxation tests were used to predict hysteresis loops. The theoretical-experimetnal comparison of hysteresis loops was generally good. Theoretical computation predicted a slightly shifted and more open loop relative to experimental data. The theory predicted a slight compressive stress which implies the existence of an experimentally realizable residual strain. This experimental residual strain was usually observed but not to the degree to which an extrapolated theoretical unloading hysteresis loop curve predicted. Theoretically generated solutions of stress responses to sinusoidal loadings, as predicted from stress relaxation-determined parameters, were less satisfactory. For convenience, only stress response to peak strain was considered. In general, the theoretical and experimental comparison of peak stress at the end of the first sinusoidal cycle was good. However, the theory could not predict the large experimental stress decay with cycling. An auxiliary model to describe experimental stress decay with cycling was described. This auxiliary model suggested the existence of a fatigue factor in biological material. Cyclic stress relaxation tests were conducted upon some test pieces and the results showed that a fatigue factor must be included in the relaxation function in order for the hereditary integral to

adequately predict experimental cyclic test stress decay. Neither the experimental results of cyclic relaxation tests nor the attempt to incorporate a cyclic factor into the relaxation function are documented in this work.

Stress-strain ratio for all four tissues are listed. They are averaged only for 50% strain for standarization among the tissues. These ratios are listed in order to compare results for an average Young's modulus with the works of others. Although these average moduli vary considerably among the four specimens tested, they generally are higher than those described from the works of Krafka, Haas, and Hoeve and Flory. However, these same moduli are much lower than that determined from the data obtained from Clark et al. It is believed that such variation in moduli is the result of variation in the cross-sections of test specimens among the various works. In general, the larger the test specimen cross-section the lower the averaged Young's modulus for the test specimen. This cross-section problem was evident in test specimens in this work. Thus the need to define a certain size cross-section for uniformity among future tests and test data is obvious. In any work, specimen cross-sections and grip style should be stated explicity.

It is hoped that this work might suggest a basic method of analysis of biological material and especially of composite material. This method of collecting basic experimental results, mathematical modeling, and histologically interpreting test sections should be applicable to all biological material. Once control specimens are documented, the effect of age, fatigue, temperature, and testings environment upon the mechanical properties of elastic fibers need to

be clarified and defined in terms of some suitable parameters. From a more mathematical point of view, the mathematics of different forms of "elastic" stress equations and different "reduced" or "normalized" relaxation functions has yet to be worked out. A relaxation function which will describe a closed hysteresis loop is necessary as such loops exist in some biological materials (50).

BIBLIOGRAPHY

BIBLIOGRAPHY

1. Arey, J. B., Human Histology, W. B Saunders, 3rd Ed., Philadelphia, 1968, Chap. V.

2. Fullmer, H. M., "The Histochemistry of the Connective Tissues," International Review of Connective Tissue Research, Ed. by D. A. Hall, Vol. 3, 1965.

3. Gross, J., "Collagen," Sci. American, Vol. 204. No. 5, 1961, pp. 120-130.

4. Hass, G. M., "Elastic Tissue," Arch. Pathol., Vol. 27, pp. 334-365 and pp. 583-613.

5. Pearse, A. G. E., Histochemistry, Theoretical and Applied, Little, Brown Co., 2nd Ed., New York, 1961, Chap. V.

6. Gross. J., "Structure of Elastic Tissue as Studied by the Electron Microscope," J. Exper. Med., Vol. 89, 1949, pp. 699-707.

7. Gross, J., "Connective Tissue Fine Structure and Some Methods of its Analysis," J. Gerontol., Vol. 5, 1950, pp. 343-356.

8. Slack, H. G. B., "Some Notes on the Composition and Metabolism of Connective Tissue," Amer. J. Med., Vol. 26, 1959, pp. 113-124.

9. Porter, K. R., "Mesenchyma and Connective Tissue," In (R. O. Greep Ed.): Histology, McGraw Hill, 2nd Ed., New York, 1966, pp. 99-133.

10. Ham, A. W., Histology, J. B. Lippincott Co., 6th Ed., 1969.

11. Meyer, K. W., and C. Ferri, Arch. Ges. Physiol., Vol. 238, 1937, 78.

12. Jordan, L. D. and Garrod, Trans. Faraday Soc., Vol. 64, 1948, 441.

13. Partridge, S. M., Davis, H. F., and Adair, G. S., "The Chemistry of Connective Tissues: 2. Soluble Proteins Derived from Partial Hydrolysis of Elastin," Biochem. J., Vol. 61, 1955, pp. 11-21.

14. Ayer, J. P., "Elastic Tissue," Int. Rev. Connect. Tissue Res., Vol. 2, pp. 33-100.

15. Maximow, A. A., and W. Bloom, A Textbook of Histology, W. B. Saunders Co., Philadelphia, 1952.

16. Roy, C. S., "Elastic Properties of the Arterial Wall," J. of Physiol., Vol. 3, 1880, pp. 125-159.

17. Krafka, J., Jr. "Mechanical Factors in Arteriosclerosis," Arch. Path., Vol. 23, 1937, pp. 1-14.

18. Hass, G. M., "Elastic Tissue. II. A Study of the Elasticity and Tensile Strength of Elastic Tissue Isolated from the Human Aorta," Arch. Pathol., Vol. 34, pp. 971-981.

19. Hass, G. M., "Elastic Tissue, III. Relations Between the Structure of the Aging Aorta and the Properties of the Isolated Aortic Elastic Tissue," Arch. Pathol, Vol. 35, pp. 29-45.

20. Wood, G. C., "Some Tensile Properties of Elastic Tissues," Biochem. Biophys. Acta., Vol. 15, pp. 311-324.

21. Hoeve, C. A. J., and P. J. Flory, "The Elastic Properties of Elastin," J. Am. Chem. Soc., Vol. 80, 1958, pp. 6523-6526.

22. Burton, A. C., "Relation of Structure to Function of the Tissues of the Wall of Blood Vessels," Physiol. Rev., Vol. 34, 1954, pp. 619-642.

23. Carton, R. W., J. Dainauskas, and J. W. Clark, "Elastic Properties of Single Elastic Fibers," J. Appl. Physiol., Vol. 17, 1962, pp. 547-551.

24. Mead, J., Physical Rev., Vol. 21, 1961, 281.

25. Krafka, J., Jr "Comparative Study of the Histophysics of the Aorta," Am. J. Physiol., Vol. 125, 1939 pp. 1-14.

26. King, A. L., and R. W. Lawton, "Elasticity of Body Tissues," In Glasser, O. (Ed): Medical Physics, Year Book Pub. Inc., Chicago, Vol. II, pp. 303-316.

27. McCartney, J. E., Quart. J. Exp. Physiol., Vol. 7, 1914, 103.

28. Lennox, F. G., "Shrinkage of Collagen," Biochem. Et Biophys. Acta., Vol. 3, 1949, pp. 170-187.

29. Ayer, J. P., and L. Feldmanis, Federation Proc., Vol. 17, 1.

30. Verzar, F., "Aging of the Collagen Fiber," International Review of Connective Tissue Research, Vol. 2, 1964.

31. Fung, Y. C. B., "Stress-strain History Relations of Soft Tissues in Simple Elongation," in (Fung, Y. C. B., N. Perrowe, and M. Anclicer Eds.): Biomechanics: Its Foundations and Objectives, Prentice Hall, Englewood Cliffs, N. J., 1972 pp. 181-208.

32. Frisen, M., M. Magi, L. Sonnerup, and A. Viidik, "Rheological Analysis of Soft Collagenous Tissue," J. of Biomechanics, Vol. 2, 1969, pp. 13-28.

33. Crisp, J. D. C., "Properties of Tendon and Skin," In (Fung, Y.C., N. Perrone, and M. Anliker Eds.): Biomechanics: Its Foundations and Objectives, Prentice Hall, Englewood Cliffs, N. J., 1972. pp. 141-179.

34. Blatz, P. J., B. M. Chu, and H. Wayland, "On the Mechanical Behavior of Elastic Animal Tissue," Trans. Soc. Rheology, Vol. 13, 1969, pp. 83-102.

35. Fung, Y. C. B., "Elasticity of Soft Tissues in Simple Elongation," Am. J. Physiol., Vol. 213, No. 6, 1967, pp. 1532-1544.

36. Apter, J. T., "Correlation of Viscoelastic Properties with Microscopic Structure of Large Arteries," Circ. Res., Vol. 21, 1967. pp. 901-918.

37. Rigby, B., N. Hirai, J. Spikes, and H. Eyring, "The Mechanical Properties of Rat Tail Tendon," J. of General Physiology, Vol. 43, 1959, pp. 265-283.

38. Haut, R. C. and R. W. Little, "A Constitutive Equation for Collagen Fibers," Journal of Biomechanics, Vol. 5, 1972, pp. 423-430.

39. Abrahams, M., "Mechanical Behavior of Tendon in Vitro," Med. and Biol. Engring, Vol. 5, 1967, pp. 433-443.

40. Viidik, A., and T. Lewin, "Changes in the Tensile Strength Characteristics and Histology of Rabbit Ligaments Induced by Different Modes of Post Mortal Storage," Acta, Orthop. Scandav., Vol. 37, 1966, pp. 141-155.

41. Van Brocklin, J. D., and D. Ellis, "A Study of the Mechanical Behavior of the Extensor Tendons Under Applied Stress," Arch. of Physical Medicine and Rehabil., Vol. 46, 1965, pp. 369-373.

42. Partington, F. R. and G. C. Wood, "The Role of Non-Collagen Components in the Mechanical Behavior of Tendon Fibers," Biochem. et Biophys. Acta., Vol. 69, pp. 485-495.

43. Drury and Wallington Eds., Carleton's Histological Technique, Oxford University Press, 4th Ed., New York, 1967.

44. Luna, Lee G. Ed., Manual of Histologic and Special Staining Techniques, Armed Forces Institute of Pathology, Wash. D. C., 1957.

45. Fung, Y. C. B., "Biomechancis (Its Scope, History and Some Problems of Continuum Mechanics in Physiology)," Appl. Mech. Rev., Vol. 21, No. 1, 1968.

46. Elden, H. R., "Physical Properties of Collagen Fibers," International Review of Connective Tissue Research, Vol. 4, 1968.

47. Abramowitz, M. and I. A. Stegun, Handbook of Mathematical Functions, Nat. Bureau of Standards, 1964.

48. Elias, H. and J. Pauly, "The Elements of Stereology," In Human Microanatomy, 3rd Ed., F. A. Davis Co., Philadelphia.

49. Elias, H., A. Hennig, and D. E. Schwartz, "Stereology: Application to Biomedical Research," Physiological Reviews, Vol. 51, No. 1, Jan. 1971.

50. Millington, P. F., T. Gibson, J. H. Evans, and J. C. Barbenel, "Structural and Mechanical Aspects of Connective Tissue," In (Kenedi, R. M., Ed.), Advances in Biomedical Engineering, Academic Press, London and New York, Vol. 1, 1971.

APPENDIX

APPENDIX A

Trigonometric Identities and Integral Evaluations

The integral

$$\int_0^t \cos n\omega x \ln x dx = \left[\frac{\sin n\omega x \ln x}{n\omega}\right]_0^t - \frac{1}{n\omega}\int_0^t \frac{\sin n\omega x}{x}\, dx \qquad A.1$$

as is determined by a single integration by parts. Since $\lim_{x\to 0} \sin n\omega x \ln x = 0$ by a double application of L'Hospitals' rule, Equation A.1 may be written

$$\int_0^t \cos n\omega x \ln x dx = \frac{\sin n\omega t \ln t}{n\omega} - \frac{1}{n\omega}\int_0^t \frac{\sin n\omega x}{x}\, dx \quad . \qquad A.2$$

To integrate the expression on the right hand side of Equation A.2 one may employ the change of variables $y = n\omega x$. Thus

$$\int_0^t \frac{\sin n\omega x}{x}\, dx = \int_0^{n\omega t} \frac{\sin y}{y}\, dy$$

which is by Abramowitz and Stegun (47) simply $Si(n\omega t)$ where $Si(n\omega t)$ is the sine integral of the argument $n\omega t$.

Thus

$$\int_0^t \cos n\omega x \ln x dx = \frac{1}{n\omega}\left[\sin n\omega t \ln t - Si(n\omega t)\right] \qquad A.3$$

The integral

$$\int_0^t \sin n\omega x \ln x dx = \left[- \frac{\cos n\omega x \ln x}{n\omega}\right]_0^t + \frac{1}{n\omega} \int_0^t \frac{\cos n\omega x}{x} \, dx \qquad A.4$$

which is obtained by a simple integration by parts. The integral on the right hand side of Equation A.4 can by the change of variables $y = n\omega x$ be rewritten as

$$\int_0^t \frac{\cos n\omega x}{x} \, dx = \int_0^{n\omega t} \frac{\cos y}{y} \, dy \quad .$$

Substituting this into Equation A.4 yields

$$\int_0^t \sin n\omega x \ln x dx = \left[- \frac{\cos n\omega x \ln x}{n\omega}\right]_0^t + \frac{1}{n\omega} \int_0^{n\omega t} \frac{\cos y}{y} \, dy$$

$$= \left[- \frac{\cos n\omega x \ln x}{n\omega}\right]_0^t + \frac{\ln(n\omega t)}{n\omega} - \lim_{t \to 0} \frac{\ln(n\omega t)}{n\omega}$$

$$+ \frac{1}{n\omega} \int_0^{n\omega t} \frac{(\cos y - 1)}{y} \, dy$$

$$= - \frac{\cos n\omega t \ln t}{n\omega} + \left[\frac{\ln(n\omega t)}{n\omega} + \frac{1}{n\omega} \int_0^{n\omega t} (\cos y - 1) \, dy\right]. \qquad A.5$$

The quantity in the bracket is defined (47) as

$$\frac{Ci(n\omega t) - \gamma}{n\omega} \quad \text{since } Ci(\alpha) = \gamma + \ln\alpha + \int_0^{\alpha} \frac{\cos z}{z} \, dz$$

where $Ci(n\omega t)$ is the cosine integral and γ is Euler's constant.

Thus by Equation A.5 and the definitive of the cosine integral

$$\int_0^t \sin n\omega x \ln x dx = \frac{1}{n\omega}\left[-\cos n\omega t \ln t + Ci(n\omega t) - \gamma\right] \quad . \qquad A.6$$

Equations A.3 and A.6 along with the trigonometric identities A.7 through A.13 contain all the information necessary to perform all the integrations for Equation 5.25.

$$\sin^2\alpha = \frac{1}{2}(1 - \cos 2\alpha) \qquad A.7$$

$$\sin^3\alpha = \frac{1}{4}(3\sin\alpha - \sin 3\alpha) \qquad A.8$$

$$\sin^4\alpha = \frac{1}{8}(3 - 4\cos 2\alpha + \cos 4\alpha) \qquad A.9$$

$$\cos^2\alpha = \frac{1}{2}(1 + \cos 2\alpha) \qquad A.10$$

$$\cos^3\alpha = \frac{1}{4}(3\cos\alpha + \cos 3\alpha) \qquad A.11$$

$$\cos^4\alpha = \frac{1}{8}(3 + 4\cos 2\alpha + \cos 4\alpha) \qquad A.12$$

$$\sin 2\alpha = 2\sin\alpha \cos 2\alpha \qquad A.13$$

The integrals from Equation 5.25 are evaluated as follows:

1. $\int_0^t \cos\omega x \ln x dx = \frac{1}{}[\sin\omega t \ln t - Si(\omega t)]$ by A.3

2. $\int_0^t \cos^2\omega x \ln x dx = \frac{1}{2}\int_0^t \ln x dx + \int_0^t \frac{\cos 2\omega x \ln x dx}{2}$ by A.10

$$= \frac{t}{2}(\ln t - 1) + \frac{1}{4\omega}[\sin 2\omega t \ln t - Si(2\omega t)] \qquad \text{by A.3}$$

3. $\int_0^t \cos^3\omega x \ln x dx = \frac{3}{4}\int_0^t \cos\omega x \ln x dx + \frac{1}{4}\int_0^t \cos 3\omega x \ln x dx$ by A.11

$$= \frac{1}{4\omega}\left[3\sin\omega t \ln t + \frac{\sin 3\omega t \ln t}{3} - 3Si(\omega t) - \frac{Si(3\omega t)}{3}\right] \text{ by A.3}$$

4. $\int_0^t \sin\omega x \ln x dx = \frac{1}{\omega}[Ci(\omega t) - \gamma - \cos\omega t \ln t]$ by A.6

5. $\int_0^t \sin 2\omega x \ln x dx = \frac{1}{2\omega}[Ci(2\omega t) - \gamma - \cos 2\omega t \ln t]$ by A.6

6. $\int_0^t \cos^2\omega x \sin\omega x \ln x dx = \left[-\frac{\cos^3\omega x \ln x}{3\omega}\right]_0^t + \frac{1}{3\omega}\int_0^t \frac{\cos^3\omega x}{x} dx$ by integration by parts

$$= \frac{1}{3\omega}\{\left[-\cos^3\omega x \ln x\right]_0^t + \frac{3}{4}\int_0^t \frac{\cos\omega x}{x} dx + \frac{1}{4}\int_0^t \frac{\cos 3\omega x}{x} dx\} \text{ by A.11}$$

$$= \frac{1}{3\omega}\{-\cos^3\omega t \ln t + (\frac{3}{4}\lim_{x\to 0} \cos\omega x \ln x + \frac{3}{4}\int_0^t \frac{\cos\omega x}{x} dx) + (+\frac{1}{4}\lim_{x\to 0} \cos 3\omega x \ln x - \frac{1}{4}\int_0^t \frac{\cos 3\omega x}{x} dx)\}$$

$$= \frac{1}{3\omega}\{-\cos^3\omega t \ln t + \frac{3}{4}(Ci[\omega t] - \gamma) + \frac{1}{4}(Ci[3\omega t] - \gamma\}$$

by definition of cosine integral

7. $\int_0^t \cos 2\omega x \ln x = \frac{1}{2\omega}[\sin 2\omega t \ln t - Si(2\omega t)]$ by A.3

8. $\int_0^t \cos\omega x \cos 2\omega x \ln x dx = 2\int_0^t \cos^3\omega x \ln x dx - \int_0^t \cos\omega x \ln x dx$ by A.10

$= \frac{1}{2}[\int_0^t \cos\omega x \ln x dx + \int_0^t \cos 3\omega x \ln x dx]$ by A.11

$= \frac{1}{2\omega}[\sin\omega t \ln t + \frac{\sin 3\omega t \ln t}{3} - Si(\omega t) - \frac{Si(3t)}{3}]$

by A.3

9. $\int_0^t \cos^2\omega x \cos 2\omega x \ln x dx = 2\int_0^t \cos^4\omega x \ln x dx - \int_0^t \cos^2\omega x \ln x dx$

$= \frac{1}{4}\int_0^t \ln x dx + \frac{1}{2}\int_0^t \cos 2\omega x \ln x dx + \frac{1}{4}\int_0^t \cos 4\omega x \ln x dx$

by A.10 & A.12

$= \frac{1}{4\omega}[\omega t(\ln t - 1) + \sin 2\omega t \ln t + \frac{\sin 4\omega t}{4} \ln t$

$- Si(2\omega t) - \frac{Si(4\omega t)}{4}]$ by A.3

10. $\int_0^t \sin 2\omega x \ln x dx = \frac{1}{2}[Ci(2\omega t) - \cos 2\omega t \ln t - \gamma]$ by A.4

11. $\int_0^t \cos\omega x \sin 2\omega x \ln x dx = 2\int_0^t \cos^2\omega x \sin\omega x \ln x dx$ by A.13

$= \frac{2}{3\omega}\{[\cos^3\omega x \ln x]_0^t - \int_0^t \frac{\cos^3\omega x}{x} dx\}$ by integration by parts

$$= -\frac{2}{3\omega}\{\cos^3\omega t\ln t - \lim_{x\to 0}\frac{\cos 3\omega x\ln x}{4} - \lim_{x\to 0}\frac{3\cos\omega x\ln x}{4}$$

$$-\int_0^t \frac{\cos 3\omega x}{4x}dx - \int_0^t \frac{3\cos\omega x}{4x}dx\} \qquad \text{by A.11}$$

$$= -\frac{2}{3\omega}\{\cos^3\omega t\ln t + \gamma + [\frac{3Ci(\omega t) + Ci(3\omega t)}{4}]\} \qquad \text{by definition of cosine integral}$$

12. $\int_0^t \cos^2\omega x\sin 2\omega x\ln x dx = 2\int_0^t \cos^3\omega x\sin\omega x\ln x dx$ by A.13

$$= \frac{1}{2\omega}\{[-\cos^4\omega x\ln x]_0^t + \int_0^t \frac{\cos^4\omega x}{x}\,dx\} \qquad \text{by integration by parts}$$

$$= \frac{1}{16\omega}[-3\ln t - 4\cos 2\omega t\ln t - \cos 4\omega t\ln t$$

$$+ \lim_{x\to 0}(3\ln x + 4\cos 2\omega x\ln x + \cos 4\omega x\ln x)$$

$$+ \int_0^t \frac{3}{x}\,dx + \int_0^t \frac{4\cos 2\omega x}{x}\,dx + \int_0^t \frac{\cos 4\omega x}{x}\,dx]$$

$$= \frac{1}{16\omega}[-4\cos 2\omega t\ln t - \cos 4\omega t\ln t + 4Ci(2\omega t) + Ci(4\omega t) - 5\gamma]$$

by definition of the cosine integral

APPENDIX B

Cosine Integrals

Table B.1. Evaluation of Cosine Integrals

m	Ci(mπ)
1	+.07373
2	-.02257
3	+.01063
4	-.00607
5	+.00396
6	-.00277
7	+.00204
8	-.00157
9	+.00124
10	-.00103
11	+.00083
12	-.00070
13	+.00060
14	-.00052
15	+.00045

For $\alpha > 10$, $Ci(\alpha)$ may be approximated by

$$Ci(\alpha) = - \frac{Cos(\alpha)}{\alpha^2} \quad , \alpha = m\pi \quad .$$

In the cyclic sinusoidal strain input tests, $\omega t = (2n - 1)\pi$ where n is the cycle number. For n greater than 3, either the logarithmic

term or the term involving Euler's constant dominates all cosine integrals in the equation for the stress response to sinusoidal input. This is to say that the stress response as written in Equation 5.28 is dependent only upon strain and the logarithm of time after the first three cycles of sinusoidal strain input.

APPENDIX C

Methods of Quantitative Volume Measurements

In order to obtain some quantitative information concerning the relative proportion of elastic fibers and collagen fibers to the volume of a given test specimen, some very basic methods of stereology as described by Elias and Pauly (48) and Elias et al (49) were employed. Information acquired from these methods provides a means of determining the effect of boiling and formic acid upon the balance of components in test specimens.

Nine microscopic slides of ligamentum nuchae sections were employed. From these nine microscopic slides twenty color film slides were made. These film slides included cross-sections and longitudinal sections of the various tissues considered. A six by six square grid was constructed which defined 49 points of intersection between perpendicular lines. These points may be referred to as grid points. The projection of a film slide over the array of grid points showed elastic fiber bundles superposed on some grid points, collagen fibers on other grid points, and tissue cells and empty spaces on others. The grid points associated with elastic fibers, collagen fibers, and other tissue components were added up. A given film slide was reoriented somewhat 6 or 7 times and grid point counting was performed each time. By adding up all the grid points associated with the various tissue components, dividing by the total number of grid points,

and converting to a percentage one may determine the percentage of grid points associated with each component of the section of tissue shown on the film slide. It was then assumed that the grid point percentages closely approximate the percent composition each component has relative to the tissue section. Because the percentage composition of the components of the tissue seem consistent from slide to slide of a similar type tissue (untreated, boiled, or formic acid-treated) and because the results were the same for cross-sections and longitudinal tissue sections, it was determined that percentages determined by grid points approximate the percentages of their respective components in a three-dimensional test specimen. These percentages are listed in Table C.1.

Table C.1. Composition of Ligamentum Nuchae.

	Elastic Fibers	Collagen Fibers	Other Components
Untreated	67.8%	30.4%	1.8%
Boiled	63.5%	15.8%	20.7%
Formic Acid-Treated	45.4%	1.6%	53.0%

For untreated specimens, the designation "other components" refers mainly to connective tissue cells. However, in Verhoeff's stain, small blood vessels are also visible. The small reduction in the percentage of elastic fibers from the untreated specimens to boiled specimens may be too small to suggest any qualitative inference. However, there is a large reduction in collagen fiber percentage in boiled

pieces. The collagen fibers remaining in boiled specimens are on the periphery of the elastic fibers. Although collagen is present, the continuous collagen network linking elastic fiber bundles has been dispersed. The regions formerly occupied by collagen show only empty spaces. Some cells were still seen in boiled sections. There was almost no collagen fibers in formic acid-treated pieces. This fact is best shown by Verhoeff's stain. Elastic fiber bundles were very loosely packed.